

Electronic Supplementary Information for

14-electron Rh and Ir silylphosphine complexes and their catalytic activity in alkene functionalization with hydrosilanes

Niroshani S. Abeynayake,^a Julio Zamora-Moreno,^{a,b} Saidulu Gorla,^a Bruno Donnadieu,^a Miguel A. Muñoz-Hernández*^a and Virginia Montiel-Palma*^a

^a Department of Chemistry

Mississippi State University

Box 9573, Mississippi, 39762, United States

E-mails: mmunoz@chemistry.msstate.edu and vmontiel@chemistry.msstate.edu

^b Centro de Investigaciones Químicas- IICBA

Universidad Autónoma del Estado de Morelos

Cuernavaca, Morelos, 62209, Mexico

Table of Contents

1	Theoretical computations.....	5
1.1	General details.....	5
1.2	References Computational Part.....	5
1.3	Calculated cartesian coordinates of complexes Rh-1 to Rh-5	7
2	Experimental part	19
2.1	General experimental considerations.....	19
2.2	Synthesis of [RhBr{ κ^3 (P,Si,Si) PPh(o-C ₆ H ₄ CH ₂ Si ⁱ Pr ₂) ₂ }] (Rh-2).....	19
2.3	Synthesis of [RhI{ κ^3 (P,Si,Si) PPh(o-C ₆ H ₄ CH ₂ Si ⁱ Pr ₂) ₂ }] (Rh-3)	20
2.4	Synthesis of [Rh(OTf){ κ^3 (P,Si,Si) PPh(o-C ₆ H ₄ CH ₂ Si ⁱ Pr ₂) ₂ }] (Rh-4)	21
2.5	Synthesis of [Rh{ κ^3 (P,Si,Si) PPh(o-C ₆ H ₄ CH ₂ Si ⁱ Pr ₂) ₂ }Cl-GaCl ₃] (Rh-5)	22
3	Characterization of new complexes	23
3.1	Characterization of [RhBr{ κ^3 (P,Si,Si) PPh(o-C ₆ H ₄ CH ₂ Si ⁱ Pr ₂) ₂ }] (Rh-2).....	23
	NMR spectra of Rh-2	23
3.2	Characterization of [RhI{ κ^3 (P,Si,Si) PPh(o-C ₆ H ₄ CH ₂ Si ⁱ Pr ₂) ₂ }] (Rh-3)	26
	NMR spectra of Rh-3	26
3.3	Characterization of [RhOTf{ κ^3 (P,Si,Si) PPh(o-C ₆ H ₄ CH ₂ Si ⁱ Pr ₂) ₂ }] (Rh-4)	29
	NMR spectra of Rh-4	29
3.4	Synthesis of [RhCl{ κ^3 (P,Si,Si) PPh(o-C ₆ H ₄ CH ₂ Si ⁱ Pr ₂) ₂ } GaCl ₃] (Rh-5).....	33
	NMR spectra of Rh-5	33
3.5	Reaction of Rh-1 and styrene <i>in situ</i> in an NMR tube.....	36
3.6	Optimization of the catalytic dehydrogenative silylation conditions of styrene by Rhodium and Iridium complexes	38
3.7	General procedure for the catalytic dehydrogenative silylation of vinylarenes.....	40
3.8	Characterization of Silane Products.....	40
3.8.1	<i>E</i> -Triethyl(styryl)silane (a)	40
3.8.2	Triethyl(2-phenylethyl)silane (b)	40
3.9	Catalysis of aromatic and aliphatic alkenes under optimized conditions	41
4	A mechanistic proposal for styrene functionalization with Et ₃ SiH	42
5	Catalytic studies on the reaction of Et ₃ SiH and aliphatic alkenes.....	43
5.1	General procedure for the hydrogenative silylation of hexene isomers	43
5.2	Catalyzed functionalization of alkenes in toluene	43

5.2.1	Triethyl(hexyl)silane (c).....	44
5.3	Ir-1 catalysis of hexene isomers.....	44
5.3.1	Triethyl(hex-2-en-1-yl)silane (d)	45
5.3.2	General procedure for the hydrogenative silylation of other aliphatic alkenes	46
5.3.3	Triethyl(octyl)silane (e)	46
5.3.4	Triethyl(oct-2-en-1-yl)silane (f)	46
5.3.5	Triethyl(3,3-dimethylbutyl)silane (g)	47
5.3.6	Cinnamyltriethylsilane (h).....	47
5.3.7	Triethyl(3-phenylpropyl)silane (i)	47
6	Catalytic studies on the reactions of other silanes with styrene and 1-hexene	48
6.1	Characterization of silane products	49
6.1.1	Triethoxy(2-phenylethyl)silane (j).....	49
6.1.2	Triethoxy(hexyl)silane (k).....	49
6.1.3	Diethoxy(methyl)(2-phenylethyl)silane (l)	50
6.1.4	Diethoxy(hexyl)(methyl)silane (m)	50
6.1.5	1,1,1,3,5,5,5-heptamethyl-3-phenylethyltrisiloxane (n).....	50
6.1.6	3-hexyl-1,1,1,3,5,5,5-heptamethyltrisiloxane (o)	50
7	Mechanistic proposal for hydrosilylation/dehydrogenative silylation by Rh-1 with HSi(OEt) ₃	51
8	Hydrosilylation/dehydrogenative silylation of other substrates	52
8.1	General procedure for the catalytic reaction of 2,3-dimethyl-1,4-butadiene and Et ₃ SiH	52
8.1.1	(2,3-dimethylbut-2-en-1-yl)triethylsilane (p).....	52
8.1.2	(2,3-dimethylbut-3-en-1-yl)triethylsilane (q).....	52
9	NMR spectra	53
9.1	NMR spectra of a typical catalysis of styrene and Et ₃ SiH	53
9.2	NMR spectra of a typical hydrosilylation catalysis of 1-hexene with Et ₃ SiH.....	55
9.3	NMR spectra of a typical hydrosilylation catalysis of t-2-hexene with Et ₃ SiH.....	57
9.4	NMR spectra of a typical hydrosilylation catalysis of t-3-hexene with Et ₃ SiH	58
9.5	NMR spectra of a typical hydrosilylation catalysis of c-2-hexene with Et ₃ SiH	59
9.6	NMR spectra of a typical hydrosilylation catalysis of c-3-hexene with Et ₃ SiH	60
9.7	NMR spectra of the catalytic hydrosilylation of 1-octene with Et ₃ SiH.....	61
9.8	NMR spectra of the catalytic hydrosilylation of 3,3-dimethyl-1-butene with Et ₃ SiH	63
9.9	NMR spectra of the catalytic hydrosilylation of allylbenzene with Et ₃ SiH.....	64

9.10	NMR spectra of the catalytic hydrosilylation of styrene with (EtO) ₃ SiH.....	65
9.11	NMR spectra of the catalytic hydrosilylation of 1-hexene with (EtO) ₃ SiH.....	66
9.12	NMR spectra of the catalytic hydrosilylation of styrene with (EtO) ₂ MeSiH.....	67
9.13	NMR spectra of catalytic hydrosilylation of 1-hexene with (EtO) ₂ MeSiH.....	68
9.14	NMR spectra of catalytic hydrosilylation of styrene with (Me ₃ SiO) ₂ SiMeH.....	69
9.15	NMR spectra of catalytic hydrosilylation of 1-hexene with (Me ₃ SiO) ₂ SiMeH.....	70
9.16	NMR spectra of the catalysis of 2,3-dimethyl-1,4-butadiene with Et ₃ SiH.....	71
10	X-ray diffraction analysis data for the complexes.....	73
10.1	Crystal data of Rh-2.....	73
10.1.1	Crystal Structure Report for B_VM_040.....	73
10.1.2	Crystal's view.....	74
10.1.3	Asymmetric unit's view.....	75
10.2	Crystal data of Rh-3.....	83
10.2.1	Crystal Structure Report forA_VM_028.....	83
10.2.2	Asymmetric unit's view.....	84
10.3	Crystal data of Rh-4	99
10.3.1	Crystal Structure Report for CU_B_VM_020_Final.....	99
10.3.2	Asymmetric unit's view.....	101
10.4	Crystal data of Rh-5	109
10.4.1	Crystal Structure Report for A_VM_013_100K.....	109
10.4.2	Crystal's view.....	110
10.4.3	Asymmetric unit's view.....	112
11	References Experimental Section.....	122

1 Theoretical computations

1.1 General details

The DFT structures *in vacuo* of complexes **Rh-1**, **Rh-2**, **Rh-3**, **Rh-4**, and **Rh-5** were computed as implemented in the Gaussian16 suite of programs[1] with wb97XD method in conjunction with 6-31G(d) basis set for C, H, Cl, P, and Si atoms. Br, Ga, I, and Rh atoms were treated with their Stuttgart–Köln 7, 3, 7, and 17-active electrons relativistic effective core potentials (RECP) in combination with their adapted valence basis sets,[2] respectively. All the optimized structures have been confirmed to be minima through vibrational analysis by the absence of imaginary frequencies. Natural Bond Orbital (NBO) analyses[3] have been performed to gain insight into the electron distribution between donor atoms and Rh center.

Table S1. Computed HOMO and LUMO energy gap.

Complex	HOMO-LUMO Energy gap (eV)
Rh-1	8.20
Rh-2	8.04
Rh-3	7.73
Rh-4	8.54
Rh-5	7.58

Table S2. NBO natural charges on atoms Rh, Si1, Si2, P and X (**Rh-4** = O or **Rh-5** = Cl).

Complex	Rh	Si1	Si2	P	X
Rh-1	-0.72	1.78	1.77	1.28	-0.41
Rh-2	-0.78	1.78	1.77	1.29	-0.37
Rh-3	-0.88	1.77	1.77	1.29	-0.27
Rh-4	-0.53	1.74	1.74	1.29	-0.94, -0.96
Rh-5	-0.58	1.74	1.76	1.28	-0.38

1.2 References Computational Part

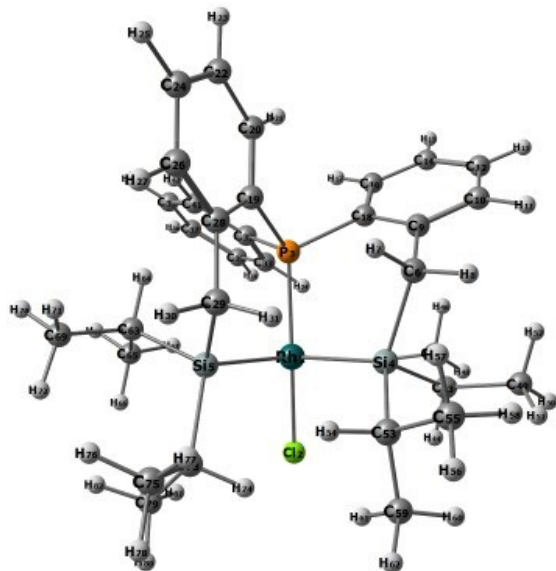
1. Gaussian 16, Revision C.01, M. J. Frisch, G. W. Trucks, H. B. Schlegel, G. E. Scuseria, M. A. Robb, J. R. Cheeseman, G. Scalmani, V. Barone, G. A. Petersson, H. Nakatsuji, X. Li, M. Caricato, A. V. Marenich, J. Bloino, B. G. Janesko, R. Gomperts, B. Mennucci, H. P. Hratchian, J. V. Ortiz, A. F. Izmaylov, J. L. Sonnenberg, D. Williams-Young, F. Ding, F. Lipparini, F. Egidi, J. Goings, B. Peng, A. Petrone, T. Henderson, D. Ranasinghe, V. G. Zakrzewski, J. Gao, N. Rega, G. Zheng, W. Liang, M. Hada, M. Ehara, K. Toyota, R. Fukuda, J. Hasegawa, M. Ishida, T. Nakajima, Y. Honda, O. Kitao, H. Nakai, T. Vreven, K. Throssell, J. A. Montgomery, Jr., J. E. Peralta, F. Ogliaro, M. J. Bearpark, J. J. Heyd, E. N. Brothers, K. N. Kudin, V. N. Staroverov, T. A. Keith, R. Kobayashi, J. Normand, K. Raghavachari, A. P. Rendell, J. C. Burant, S. S. Iyengar, J. Tomasi, M. Cossi, J. M. Millam, M. Klene, C. Adamo, R. Cammi, J. W. Ochterski, R. L. Martin, K. Morokuma, O. Farkas, J. B. Foresman, and D. J. Fox, Gaussian, Inc., Wallingford CT, 2019.

2. (a) A. Bergner, M. Dolg, W. Kuechle, H. Stoll, and H. Preuss, "Ab-initio energy-adjusted pseudopotentials for elements of groups 13-17," *Mol. Phys.*, **80** (1993) 1431-41. (b) U. Haeussermann, M. Dolg, H. Stoll, and H. Preuss, "Accuracy of energy-adjusted quasi-relativistic ab initio pseudopotentials – all-electron and pseudopotential benchmark calculations for HG, HGH and their cations," *Mol. Phys.*, **78** (1993) 1211-24. (c) G. Igel-Mann, H. Stoll, and H. Preuss, "Pseudopotentials for main group elements (IIIA through VIIA)," *Mol. Phys.*, **65** (1988) 1321-28. (d) U. Wedig, M. Dolg, H. Stoll, and H. Preuss, in *Quantum Chemistry: The Challenge of Transition Metals and Coordination Chemistry*, Ed. A. Veillard, Reidel, and Dordrecht (1986) 79.

3. Reed, A. E.; Weinstock, R. B.; Weinhold, F. *The Journal of Chemical Physics* **1985**, *83*, 735.

1.3 Calculated cartesian coordinates of complexes Rh-1 to Rh-5

Rh-1

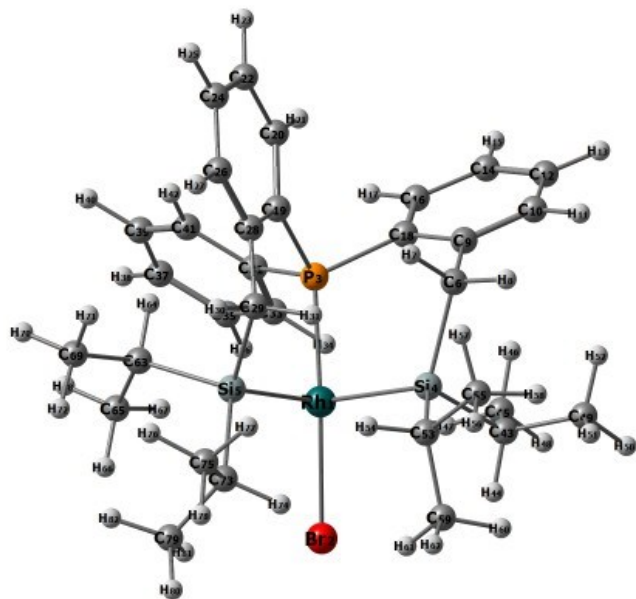


45	0.593650000	-0.261730000	-1.041889000
17	2.032354000	-0.962273000	-2.717133000
15	-1.143483000	0.586750000	0.088364000
14	2.016096000	1.035151000	0.226293000
14	0.455170000	-2.102902000	0.329423000
6	1.088628000	2.050191000	1.571830000
1	0.667535000	1.359787000	2.314874000
1	1.826886000	2.660968000	2.104462000
6	0.018457000	2.936156000	1.000068000
6	0.101967000	4.325199000	1.130110000
1	0.934215000	4.750785000	1.684939000
6	-0.847199000	5.167115000	0.560915000
1	-0.749742000	6.242901000	0.673041000
6	-1.918279000	4.631688000	-0.146894000
1	-2.665879000	5.281278000	-0.591316000
6	-2.028881000	3.251664000	-0.280448000
1	-2.865665000	2.833729000	-0.831652000
6	-1.070773000	2.403894000	0.279882000
6	-1.712103000	0.056420000	1.751081000
6	-2.866220000	0.690252000	2.236592000
1	-3.327536000	1.479119000	1.648191000
6	-3.437471000	0.326559000	3.445973000
1	-4.333465000	0.827014000	3.799281000
6	-2.844410000	-0.686381000	4.195158000
1	-3.278055000	-0.993365000	5.142394000

6	-1.684960000	-1.295441000	3.737938000
1	-1.215021000	-2.067265000	4.341841000
6	-1.079961000	-0.937035000	2.523929000
6	0.222704000	-1.603253000	2.155942000
1	0.341292000	-2.499076000	2.777049000
1	1.054757000	-0.943786000	2.439012000
6	-2.559141000	0.254246000	-1.031182000
6	-2.411539000	0.648753000	-2.369737000
1	-1.537880000	1.220726000	-2.675004000
6	-3.372455000	0.313668000	-3.316257000
1	-3.242979000	0.626325000	-4.347643000
6	-4.487293000	-0.433440000	-2.941874000
1	-5.232837000	-0.706529000	-3.682400000
6	-4.639522000	-0.832311000	-1.617970000
1	-5.504634000	-1.417287000	-1.320856000
6	-3.682993000	-0.489451000	-0.665348000
1	-3.813212000	-0.814092000	0.361696000
6	2.729519000	2.261393000	-1.056736000
1	3.420675000	1.650234000	-1.652823000
6	1.694813000	2.846655000	-2.031505000
1	0.947669000	3.461892000	-1.518638000
1	1.170108000	2.057336000	-2.584196000
1	2.191859000	3.482023000	-2.776608000
6	3.531171000	3.387914000	-0.387013000
1	3.999705000	4.030466000	-1.144194000
1	4.331096000	3.005066000	0.256585000
1	2.883929000	4.028616000	0.224369000
6	3.430295000	0.085529000	1.099024000
1	3.005555000	-0.873884000	1.419851000
6	3.951188000	0.780894000	2.366956000
1	4.762946000	0.194968000	2.817186000
1	3.167568000	0.894523000	3.124712000
1	4.352770000	1.778704000	2.153672000
6	4.578070000	-0.231678000	0.129561000
1	5.114653000	0.679985000	-0.160354000
1	4.218084000	-0.709101000	-0.788680000
1	5.306803000	-0.903736000	0.600995000
6	-1.153947000	-3.033666000	-0.125275000
1	-1.954386000	-2.367648000	0.225809000
6	-1.382356000	-3.248205000	-1.627081000
1	-0.617226000	-3.894134000	-2.069115000
1	-1.368561000	-2.300651000	-2.178985000
1	-2.359714000	-3.716377000	-1.805104000
6	-1.300577000	-4.341732000	0.668700000
1	-2.278501000	-4.802018000	0.474284000
1	-1.227821000	-4.172980000	1.749978000
1	-0.536120000	-5.076375000	0.393259000
6	2.029134000	-3.185128000	0.192797000

1	2.845983000	-2.484265000	-0.015974000
6	2.365839000	-3.920974000	1.499724000
1	1.558937000	-4.598280000	1.807114000
1	2.553470000	-3.227732000	2.327997000
1	3.269864000	-4.530233000	1.371408000
6	1.988367000	-4.163824000	-0.989804000
1	2.952689000	-4.679860000	-1.083903000
1	1.799396000	-3.643435000	-1.933017000
1	1.220605000	-4.934624000	-0.857112000

Rh-2

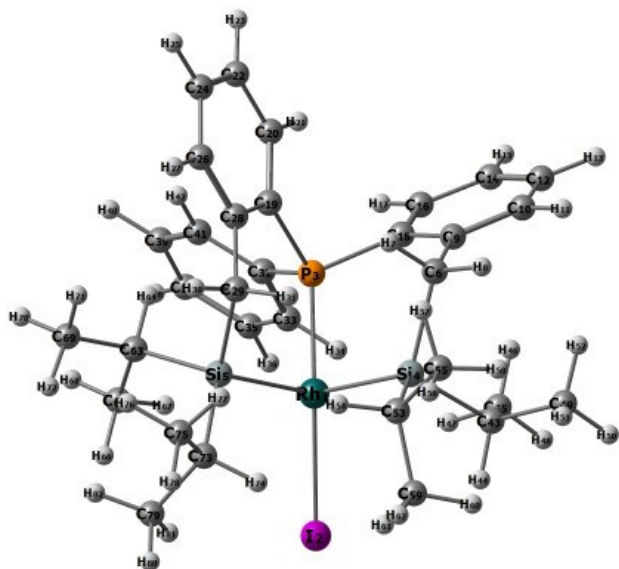


45	0.659937000	-0.082730000	-0.798221000
35	2.551434000	-0.404824000	-2.355519000
15	-1.399608000	0.245314000	0.006604000
14	1.424767000	1.619437000	0.560473000
14	0.850474000	-1.835285000	0.683738000
6	0.039926000	2.348335000	1.681367000
1	-0.276878000	1.586161000	2.405662000
1	0.474452000	3.166365000	2.267533000
6	-1.134248000	2.858510000	0.895512000
6	-1.481507000	4.211771000	0.932170000
1	-0.912331000	4.882180000	1.571019000
6	-2.527104000	4.714649000	0.165641000
1	-2.766940000	5.772903000	0.209576000
6	-3.263556000	3.864079000	-0.652540000
1	-4.083232000	4.247896000	-1.251792000
6	-2.944873000	2.510924000	-0.696373000
1	-3.520844000	1.846340000	-1.333022000

6	-1.888127000	2.005286000	0.063915000
6	-2.049842000	-0.380756000	1.603485000
6	-3.402506000	-0.112593000	1.863502000
1	-3.973453000	0.481378000	1.154539000
6	-4.029868000	-0.596569000	3.000876000
1	-5.078668000	-0.381669000	3.179428000
6	-3.294502000	-1.358598000	3.905146000
1	-3.766701000	-1.754307000	4.799541000
6	-1.948450000	-1.599799000	3.671783000
1	-1.376573000	-2.173622000	4.396273000
6	-1.287118000	-1.111137000	2.535229000
6	0.195149000	-1.360689000	2.412118000
1	0.473147000	-2.153012000	3.117066000
1	0.739297000	-0.468585000	2.751385000
6	-2.447407000	-0.532112000	-1.283292000
6	-2.194137000	-0.157106000	-2.611749000
1	-1.484171000	0.638568000	-2.827300000
6	-2.840849000	-0.796706000	-3.662591000
1	-2.632474000	-0.495906000	-4.684486000
6	-3.739067000	-1.829255000	-3.401606000
1	-4.236137000	-2.338019000	-4.221904000
6	-3.993473000	-2.209580000	-2.087844000
1	-4.690432000	-3.015438000	-1.878807000
6	-3.353599000	-1.564604000	-1.032235000
1	-3.556979000	-1.878088000	-0.013602000
6	1.941448000	2.975181000	-0.686825000
1	2.864261000	2.586127000	-1.138064000
6	0.945614000	3.211126000	-1.834068000
1	-0.012938000	3.599519000	-1.473458000
1	0.752399000	2.290337000	-2.398222000
1	1.352782000	3.941966000	-2.545252000
6	2.268403000	4.301570000	0.016697000
1	2.644472000	5.037642000	-0.706062000
1	3.033342000	4.185997000	0.792740000
1	1.375890000	4.735085000	0.484275000
6	2.895837000	1.161484000	1.697511000
1	2.732355000	0.123262000	2.011727000
6	2.965279000	2.002779000	2.982182000
1	3.828845000	1.701187000	3.588969000
1	2.069156000	1.882114000	3.601553000
1	3.078225000	3.072247000	2.768157000
6	4.231354000	1.197192000	0.940822000
1	4.505786000	2.223486000	0.668193000
1	4.195395000	0.608824000	0.017118000
1	5.039676000	0.797939000	1.567007000
6	-0.330031000	-3.218346000	0.087796000
1	-1.332931000	-2.800261000	0.251481000
6	-0.232873000	-3.565821000	-1.403219000

1	0.745569000	-3.981565000	-1.663821000
1	-0.392036000	-2.684669000	-2.036325000
1	-0.995433000	-4.307739000	-1.675682000
6	-0.234379000	-4.469131000	0.976509000
1	-0.990488000	-5.208736000	0.681138000
1	-0.404823000	-4.231927000	2.033633000
1	0.743537000	-4.956103000	0.896862000
6	2.671129000	-2.406415000	0.867442000
1	3.277771000	-1.510362000	0.689703000
6	2.994606000	-2.919009000	2.280358000
1	2.375918000	-3.783987000	2.551683000
1	2.845547000	-2.148447000	3.045658000
1	4.043000000	-3.238909000	2.337553000
6	3.097732000	-3.435060000	-0.190079000
1	4.172036000	-3.641537000	-0.100176000
1	2.917985000	-3.068934000	-1.204782000
1	2.573276000	-4.389476000	-0.067452000

Rh-3

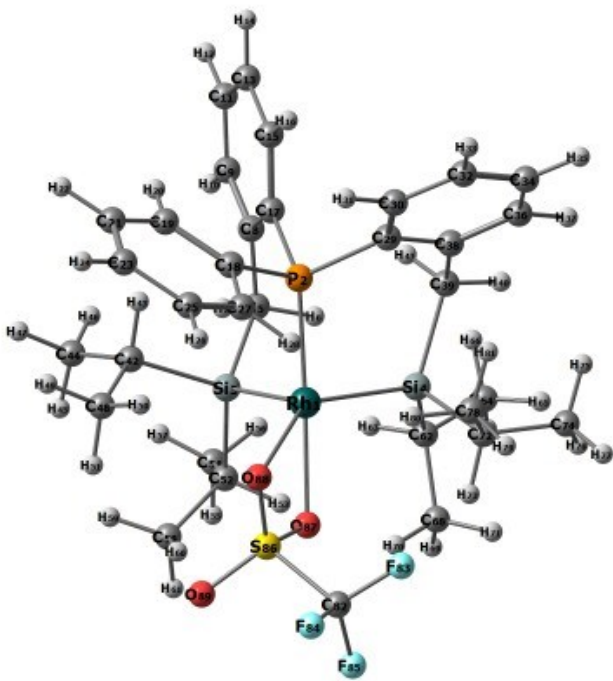


45	0.645598000	-0.023312000	-0.563788000
53	2.898395000	-0.224650000	-1.923912000
15	-1.546898000	0.119100000	-0.144339000
14	0.987971000	1.782291000	0.839709000
14	0.732571000	-1.707939000	1.010457000
6	-0.640430000	2.388854000	1.671518000
1	-1.007974000	1.614155000	2.357402000
1	-0.398216000	3.258100000	2.293781000
6	-1.698485000	2.762059000	0.672907000
6	-2.178883000	4.072351000	0.598244000

1	-1.803908000	4.809598000	1.303482000
6	-3.112648000	4.449912000	-0.360535000
1	-3.460216000	5.478076000	-0.398477000
6	-3.600115000	3.513287000	-1.266506000
1	-4.330805000	3.799656000	-2.016405000
6	-3.147261000	2.199788000	-1.203427000
1	-3.529598000	1.467382000	-1.907852000
6	-2.202094000	1.820716000	-0.247721000
6	-2.413585000	-0.532761000	1.334121000
6	-3.810774000	-0.403131000	1.335395000
1	-4.299028000	0.109343000	0.510526000
6	-4.583454000	-0.922572000	2.362343000
1	-5.663354000	-0.815891000	2.340919000
6	-3.952963000	-1.579396000	3.416074000
1	-4.538561000	-2.000628000	4.227935000
6	-2.569618000	-1.681992000	3.438335000
1	-2.085157000	-2.173535000	4.277917000
6	-1.764298000	-1.154273000	2.418174000
6	-0.267253000	-1.248264000	2.571180000
1	-0.044751000	-1.983363000	3.353300000
1	0.116167000	-0.293314000	2.955711000
6	-2.256329000	-0.791217000	-1.569739000
6	-1.798452000	-0.423317000	-2.844381000
1	-1.140885000	0.435466000	-2.960840000
6	-2.173624000	-1.151153000	-3.967405000
1	-1.808314000	-0.855185000	-4.945682000
6	-3.000691000	-2.263869000	-3.831113000
1	-3.285006000	-2.840535000	-4.705995000
6	-3.457037000	-2.637000000	-2.570883000
1	-4.099813000	-3.504814000	-2.458688000
6	-3.089403000	-1.905244000	-1.444528000
1	-3.446954000	-2.214007000	-0.467751000
6	1.585004000	3.174508000	-0.330455000
1	2.607185000	2.878006000	-0.602438000
6	0.790912000	3.310178000	-1.639655000
1	-0.246018000	3.613907000	-1.460964000
1	0.779684000	2.372026000	-2.207340000
1	1.251902000	4.069356000	-2.285206000
6	1.652394000	4.529690000	0.391434000
1	2.081835000	5.294813000	-0.268615000
1	2.271274000	4.493385000	1.294869000
1	0.653086000	4.877138000	0.680720000
6	2.263903000	1.495288000	2.240258000
1	2.156019000	0.447303000	2.544766000
6	2.000978000	2.344857000	3.494230000
1	2.761175000	2.140201000	4.259130000
1	1.021689000	2.131481000	3.937655000
1	2.039699000	3.419310000	3.279080000

6	3.707113000	1.672262000	1.748082000
1	3.917446000	2.719074000	1.497701000
1	3.912943000	1.071734000	0.855039000
1	4.419049000	1.373136000	2.528137000
6	-0.194919000	-3.217734000	0.286646000
1	-1.241090000	-2.885810000	0.237847000
6	0.206965000	-3.621797000	-1.137239000
1	1.246871000	-3.959488000	-1.189495000
1	0.099140000	-2.788116000	-1.841130000
1	-0.429260000	-4.441289000	-1.497533000
6	-0.170109000	-4.413712000	1.252637000
1	-0.792562000	-5.231473000	0.865712000
1	-0.560391000	-4.146638000	2.242084000
1	0.840632000	-4.813036000	1.388468000
6	2.532978000	-2.094191000	1.552332000
1	3.088188000	-1.159187000	1.408737000
6	2.637890000	-2.478071000	3.037522000
1	2.058323000	-3.381820000	3.265540000
1	2.285398000	-1.679177000	3.700081000
1	3.682346000	-2.686599000	3.302510000
6	3.224931000	-3.151117000	0.679220000
1	4.279088000	-3.245717000	0.969745000
1	3.201193000	-2.882871000	-0.380602000
1	2.766718000	-4.139728000	0.794417000

Rh-4

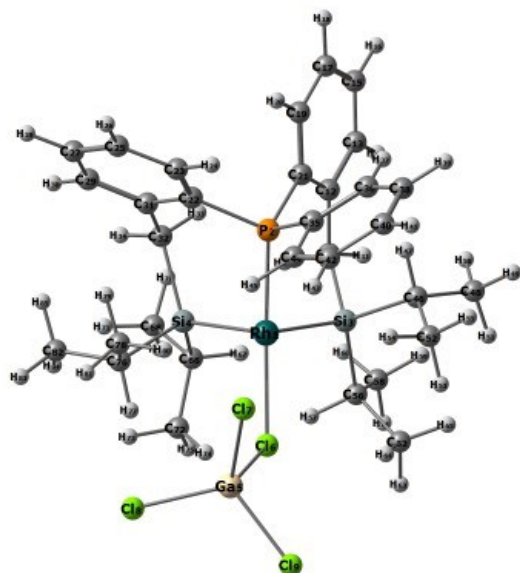


45	0.540705000	-0.080192000	0.020657000
----	-------------	--------------	-------------

15	-1.588264000	0.205547000	0.631485000
14	-0.193528000	-1.733346000	-1.398597000
14	0.315110000	1.675371000	-1.447717000
6	-1.733968000	-1.205589000	-2.384818000
1	-1.490760000	-0.293017000	-2.946370000
1	-1.934417000	-1.967255000	-3.147615000
6	-2.998430000	-0.973415000	-1.596301000
6	-4.212983000	-1.384369000	-2.165772000
1	-4.186982000	-1.893382000	-3.125646000
6	-5.435158000	-1.145917000	-1.555270000
1	-6.351920000	-1.479880000	-2.032139000
6	-5.481092000	-0.464743000	-0.341723000
1	-6.429740000	-0.251949000	0.140709000
6	-4.294103000	-0.059517000	0.247553000
1	-4.328829000	0.469444000	1.196178000
6	-3.050499000	-0.327185000	-0.346644000
6	-1.737839000	-0.678788000	2.229610000
6	-2.652553000	-1.709917000	2.459465000
1	-3.391638000	-1.965871000	1.707779000
6	-2.613940000	-2.428063000	3.651339000
1	-3.325176000	-3.231949000	3.814784000
6	-1.666868000	-2.123116000	4.624036000
1	-1.635320000	-2.690109000	5.549474000
6	-0.752038000	-1.096736000	4.403250000
1	0.001019000	-0.861731000	5.148340000
6	-0.782015000	-0.383550000	3.211232000
1	-0.039822000	0.390299000	3.037609000
6	-2.003326000	1.956324000	0.962092000
6	-2.379445000	2.400348000	2.231131000
1	-2.449775000	1.694068000	3.052423000
6	-2.657180000	3.744537000	2.457161000
1	-2.941987000	4.079553000	3.449566000
6	-2.569670000	4.648302000	1.403773000
1	-2.785368000	5.700051000	1.566875000
6	-2.205894000	4.206787000	0.136039000
1	-2.139863000	4.918938000	-0.682561000
6	-1.909199000	2.864314000	-0.113234000
6	-1.449658000	2.428893000	-1.477371000
1	-1.439988000	3.291251000	-2.154120000
1	-2.149480000	1.703959000	-1.913299000
6	-0.788128000	-3.188173000	-0.309560000
1	-1.706919000	-2.813280000	0.163120000
6	-1.204916000	-4.395503000	-1.165887000
1	-0.352285000	-4.839825000	-1.690558000
1	-1.956815000	-4.125368000	-1.917376000
1	-1.641346000	-5.179935000	-0.533641000
6	0.162544000	-3.591131000	0.825692000
1	-0.280155000	-4.396709000	1.426450000

1	0.366828000	-2.754977000	1.503818000
1	1.126607000	-3.949238000	0.450617000
6	1.193804000	-2.207868000	-2.629363000
1	1.775556000	-1.292489000	-2.786454000
6	0.640160000	-2.649062000	-3.994431000
1	1.463844000	-2.910021000	-4.671263000
1	0.054193000	-1.860360000	-4.480746000
1	-0.000863000	-3.535453000	-3.906748000
6	2.174974000	-3.254285000	-2.081019000
1	1.691240000	-4.224023000	-1.919155000
1	2.632239000	-2.940378000	-1.139807000
1	2.988266000	-3.415280000	-2.800501000
6	0.870849000	1.366365000	-3.250305000
1	0.526853000	0.357908000	-3.512074000
6	0.233702000	2.326809000	-4.266632000
1	0.477906000	3.374035000	-4.052263000
1	-0.858642000	2.238528000	-4.283495000
1	0.598109000	2.109604000	-5.278973000
6	2.403177000	1.364797000	-3.369553000
1	2.711962000	1.032404000	-4.368912000
1	2.872563000	0.704317000	-2.632442000
1	2.813490000	2.370665000	-3.219021000
6	1.490954000	2.928199000	-0.601700000
1	2.494446000	2.513727000	-0.769335000
6	1.428275000	4.313941000	-1.262438000
1	0.435985000	4.766092000	-1.141972000
1	1.653716000	4.276360000	-2.333755000
1	2.153309000	4.995725000	-0.798493000
6	1.304829000	3.062094000	0.920087000
1	2.105711000	3.678338000	1.347588000
1	1.341323000	2.093711000	1.436452000
1	0.351125000	3.535529000	1.172557000
6	4.467066000	0.317246000	1.423056000
9	3.964656000	1.552233000	1.458990000
9	4.971487000	0.026145000	2.616876000
9	5.434948000	0.277093000	0.513956000
16	3.150715000	-0.902709000	0.989324000
8	2.661639000	-0.392492000	-0.345193000
8	2.079992000	-0.707414000	1.988917000
8	3.817376000	-2.189220000	0.949076000

Rh-5



45	0.175852000	-0.204291000	0.148264000
15	-1.776701000	0.387278000	-0.781781000
14	-0.963348000	-1.922120000	1.197759000
14	-0.123700000	1.439169000	1.756029000
31	4.071038000	-0.164965000	-0.726387000
17	2.414522000	-0.885625000	0.803954000
17	2.953766000	0.159580000	-2.615152000
17	4.882262000	1.683974000	0.139716000
17	5.467687000	-1.845911000	-0.816578000
6	-2.602231000	-1.307123000	1.946561000
1	-3.009859000	-2.108247000	2.574212000
6	-3.674062000	-0.863366000	0.983425000
6	-5.003090000	-1.209043000	1.268338000
1	-5.203000000	-1.818784000	2.145398000
6	-6.062155000	-0.783255000	0.480064000
1	-7.076811000	-1.072213000	0.737183000
6	-5.821247000	0.025339000	-0.627749000
1	-6.640500000	0.382090000	-1.243559000
6	-4.515420000	0.371151000	-0.937531000
1	-4.324281000	0.999374000	-1.803447000
6	-3.436337000	-0.082419000	-0.162877000
6	-1.935120000	2.193480000	-0.989942000
6	-2.027915000	2.787611000	-2.250361000
1	-2.023070000	2.170615000	-3.143272000
6	-2.116378000	4.169950000	-2.373126000
1	-2.179874000	4.623307000	-3.357111000
6	-2.123568000	4.960492000	-1.228628000
1	-2.192353000	6.040885000	-1.312194000

6	-2.042692000	4.369734000	0.027757000
1	-2.050279000	4.994454000	0.917107000
6	-1.939800000	2.984444000	0.176597000
6	-1.786156000	2.372437000	1.540776000
1	-2.620554000	1.694275000	1.763808000
1	-1.821726000	3.160185000	2.302324000
6	-1.663749000	-0.329105000	-2.461332000
6	-2.583730000	-1.245152000	-2.978762000
1	-3.486595000	-1.488240000	-2.428283000
6	-2.340330000	-1.862061000	-4.202461000
1	-3.058664000	-2.575971000	-4.593656000
6	-1.181412000	-1.573078000	-4.917974000
1	-0.991988000	-2.064747000	-5.867194000
6	-0.262755000	-0.657239000	-4.412039000
1	0.650002000	-0.431638000	-4.953689000
6	-0.501818000	-0.040136000	-3.189665000
1	0.230414000	0.662833000	-2.801202000
6	-1.459164000	-3.160933000	-0.167442000
1	-2.219034000	-2.623798000	-0.750575000
6	-2.160154000	-4.400415000	0.411961000
1	-2.530079000	-5.043007000	-0.397569000
1	-3.022298000	-4.127658000	1.032562000
1	-1.485620000	-5.007726000	1.024493000
6	-0.334878000	-3.535030000	-1.142902000
1	0.477367000	-4.074846000	-0.646083000
1	0.101164000	-2.649382000	-1.622519000
1	-0.719750000	-4.177835000	-1.944993000
6	0.089913000	-2.694640000	2.601127000
1	0.729254000	-1.887425000	2.979928000
6	-0.772634000	-3.185885000	3.776240000
1	-1.485416000	-3.958878000	3.462237000
1	-1.342158000	-2.373672000	4.242055000
1	-0.136064000	-3.627326000	4.553276000
6	1.027307000	-3.815929000	2.125215000
1	1.675404000	-4.136916000	2.950176000
1	1.677333000	-3.495372000	1.306996000
1	0.468976000	-4.696729000	1.790318000
6	-0.003869000	0.865693000	3.577483000
1	-0.444037000	-0.138225000	3.626930000
6	-0.817551000	1.753796000	4.534068000
1	-0.709938000	1.397728000	5.566377000
1	-1.886556000	1.749128000	4.293316000
1	-0.476411000	2.795870000	4.514123000
6	1.452037000	0.746221000	4.052594000
1	1.941047000	1.726489000	4.092328000
1	2.052684000	0.108371000	3.396600000
1	1.490404000	0.320140000	5.063024000
6	1.305565000	2.615694000	1.303867000

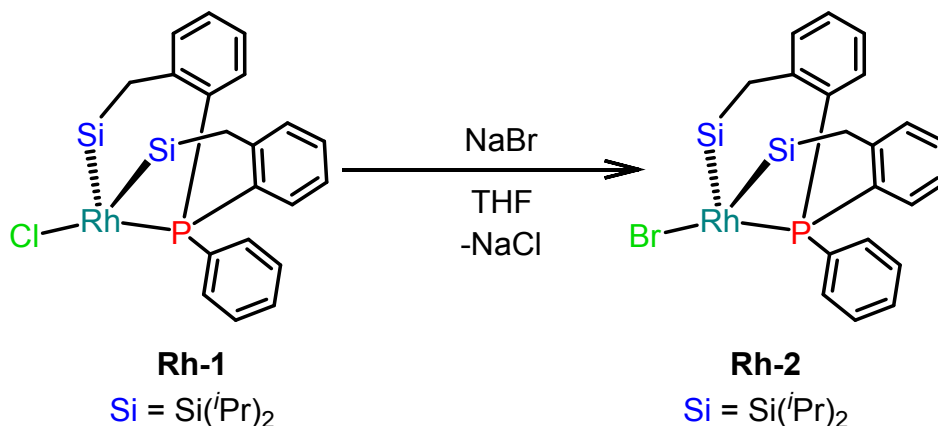
1	2.216147000	2.095850000	1.631469000
6	1.453013000	2.879852000	-0.203992000
1	0.613894000	3.460032000	-0.601249000
1	1.518124000	1.953144000	-0.792248000
1	2.377159000	3.433729000	-0.404528000
6	1.214811000	3.943751000	2.071750000
1	2.092201000	4.566503000	1.856792000
1	1.174451000	3.797982000	3.157241000
1	0.327514000	4.515722000	1.773866000
1	-2.379577000	-0.484239000	2.639816000

2 Experimental part

2.1 General experimental considerations

All experiments were performed under argon atmosphere using standard Schlenk methods or in MBraun glove boxes. THF, DCM, toluene, CH₃CN and pentane were dried and purified over MBraun column systems. Benzene-d₆ and CDCl₃ were passed through a Pasteur pipette containing molecular sieves and basic alumina and then degassed via three freeze–pump–thaw cycles and stored over molecular sieves. [MCl(COD)]₂ (M = Rh, Ir)^{1, 2} and [MCl{κ³(P,Si,Si)PPh(o-C₆H₄CH₂SiⁱPr₂)₂}] (M = Rh, **Rh-1** and M = Ir, **Ir-1**)^{31, 22, 3} were synthesized according to reported procedures. The other reagents were purchased from Sigma Aldrich and used as received. Nuclear magnetic resonance (NMR) experiments were performed on Bruker Avance 300, 500 and 600 MHz spectrometer operating with frequency, deuterated solvent and temperature indicated in parentheses. Chemical shifts (δ) are reported in parts per million (ppm). GC-MS analyses were performed on a GC MS-QP2010S instrument equipped with a Rtx-5MS column (30.0 m x 0.25 mm x 0.25 μm).

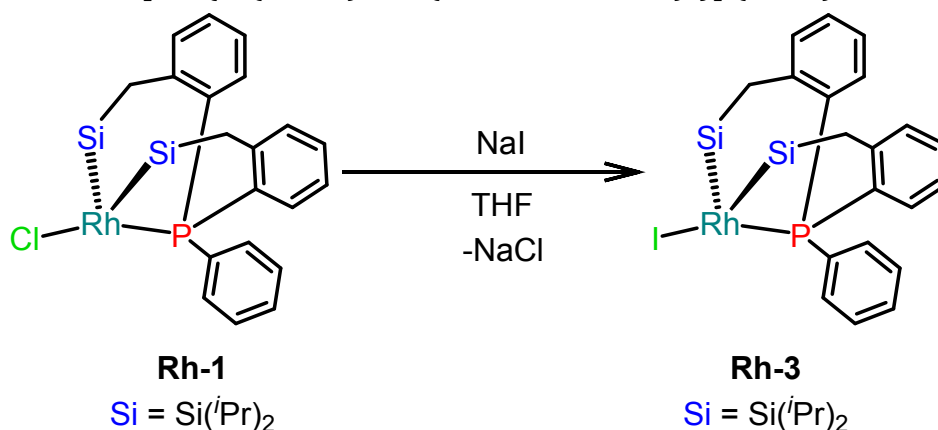
2.2 Synthesis of [RhBr{κ³(P,Si,Si) PPh(o-C₆H₄CH₂SiⁱPr₂)₂}] (**Rh-2**)



In a Schlenk flask, 30 mg (0.046 mmol) of **Rh-1** and 4.7 mg of NaBr (0.046 mmol) was dissolved in 2 mL of dry THF. The resulted yellow solution was left stirring for 24 hours. The solution was filter through celite and volatiles were removed under the vacuum, the crude was washed with 3 portions of 1 mL of dry pentane and dried in vacuum for 6 hours. Complex **Rh-2** was obtained as a yellow solid (30 mg, 93% yield). ¹H NMR (500 MHz, C₆D₆): δ 7.59 – 7.56 (m, 2H, CH_{arom}), 7.00 (q, J_{HH} 6.1 Hz, J_{HH} 4.8Hz, 5H, CH_{arom}), 6.94 – 6.89 (m, 4H, CH_{arom}), 6.74 (t, J_{HH} 7.4 Hz, 2H, CH_{arom}), 2.24

(dd, J_{HH} 14.7, J_{HH} 5.9, 2H, CH₂), 2.12 (d, J_{HH} 14.6 Hz, 2H, CH₂), 1.80 (sept, J_{HH} 7.5 Hz, 2H, CH-*i*Pr), 1.70 (sept, J_{HH} 7.3 Hz, 2H, CH-*i*Pr), 1.59 (d, J_{HH} 7.4 Hz, 6H, CH₃-*i*Pr), 1.16 (d, J_{HH} 7.6 Hz, 6H, CH₃-*i*Pr), 0.94 (dd, J_{HH} 10 Hz, J_{HH} 7.4 Hz, 12H, CH₃-*i*Pr) ppm. **¹³C{¹H} NMR (150.9 MHz, C₆D₆):** 146.69 (d, J_{CP} 14.2 Hz, C_{ipso}), 134.18 (d, J_{CP} 11.1 Hz, CH_{arom}), 132.45 (d, J_{CP} 5.0 Hz, CH_{arom}), 131.76 (d, J_{CP} 8.1 Hz, CH_{arom}), 131.19 (d, J_{CP} 2.3 Hz, CH_{arom}), 131.00 (d, J_{CP} 2.1 Hz, CH_{arom}), 130.53 (d, J_{CP} 49.3 Hz, C_{ipso}), 129.31 (d, J_{CP} 10.0 Hz, CH_{arom}), 126.84 (d, J_{CP} 55.2 Hz, C_{ipso}), 125.48 (d, J_{CP} 8.4 Hz, CH_{arom}), 23.40 (d, J_{CP} 17.7 Hz, CH₂), 21.65 (s, CH₃-*i*Pr), 21.63 (s, CH-*i*Pr), 20.74 (s, CH₃-*i*Pr), 20.10 (s, CH₃-*i*Pr), 18.94 (s, CH₃-*i*Pr), 18.88 (t, [J_{CP} + J_{CRh}] 1.5 Hz, CH-*i*Pr) ppm. **³¹P{¹H} NMR (202.46 MHz, C₆D₆):** 31.77 (d, J_{PRh} 148.6, J_{PSi} 13 Hz) ppm. **DEPT ²⁹Si{¹H} NMR (99.36 MHz, C₆D₆):** 75.58 (dd, $J_{\text{Si-Rh}}$ 38.3, $J_{\text{Si-P}}$ 13 Hz) ppm. **Anal. Calcd for C₃₂H₄₅RhBrPSi₂·0.67CH₂Cl₂:** C: 51.87%, H: 6.17%; Found: C:51.85%, H:6.43%.

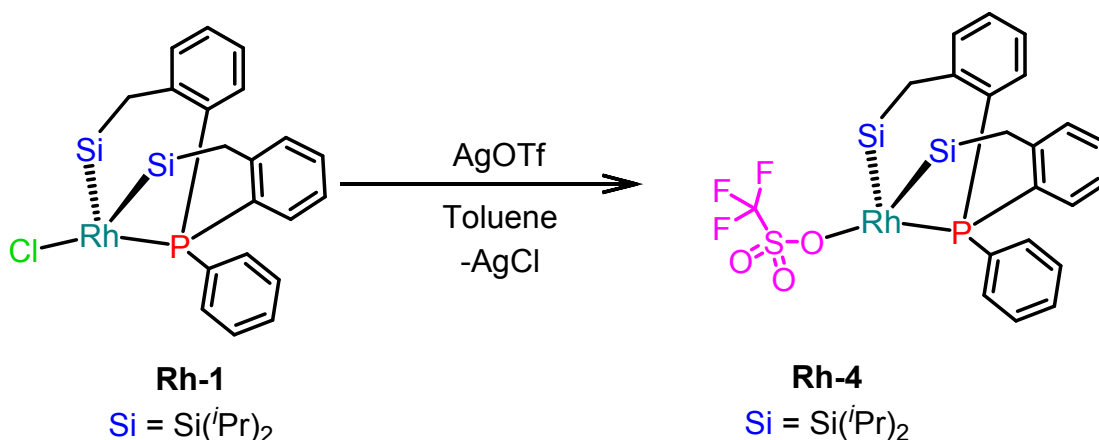
2.3 Synthesis of [RhI{κ³(P,Si,Si) PPh(o-C₆H₄CH₂Si^{*i*}Pr₂)₂}] (**Rh-3**)



In a Schlenk flask, 30 mg (0.046 mmol) of **Rh-1** and 6.9 mg of NaI (0.046 mmol) was dissolved in 2 mL of dry THF. The resulted yellow solution was left stirring for 24 hours. The solution was filter through celite and volatiles were removed under the vacuum, the crude was washed with 3 portions of 1 mL of dry pentane and dried in vacuum for 6 hours. Complex **Rh-3** was obtained as a pale-yellow solid (32 mg, 94% yield). **¹H NMR (500 MHz, C₆D₆):** δ 7.63 – 7.54 (m, 2H, CH_{arom}), 7.04 – 6.89 (m, 9H, CH_{arom}), 6.78 – 6.70 (m, 2H, CH_{arom}), 2.22 (ddd, J_{HH} 14.8, J_{HH} 6.9, J_{HP} 1.9 Hz, 2H, CH₂), 2.12 (d, J_{HH} 14.7 Hz, 2H, CH₂), 1.82 – 1.66 (m, 4H, CH-*i*Pr), 1.59 (d, J_{HH} 7.4 Hz, 6H, CH₃-*i*Pr), 1.21 (d, J_{HH} 7.7 Hz, 6H, CH₃-*i*Pr), 0.93 (d, J_{HH} 7.4 Hz, 6H, CH₃-*i*Pr), 0.87 (d, J_{HH} 7.5 Hz, 6H, CH₃-*i*Pr)

ppm. $^{13}\text{C}\{^1\text{H}\}$ NMR (150.9 MHz, C_6D_6): 146.77 (d, J_{CP} 14.4 Hz, C_{ipso}), 133.90 (d, J_{CP} 10.8 Hz, CH_{arom}), 132.66 (d, J_{CP} 4.9 Hz, CH_{arom}), 131.85 (d, J_{CP} 8.1 Hz, CH_{arom}), 131.18 (d, J_{CP} 2.5 Hz, CH_{arom}), 130.90 (d, J_{CP} 2.7 Hz, CH_{arom}), 129.82 (d, J_{CP} 48.8 Hz, C_{ipso}), 129.26 (d, J_{CP} 10.0 Hz, CH_{arom}), 126.47 (d, J_{CP} 55.1 Hz, C_{ipso}), 125.49 (d, J_{CP} 8.2 Hz, CH_{arom}), 23.54 (d, J_{CP} 18.4 Hz, CH_2), 22.41 (s, CH_3 - ^iPr), 21.20 (s, CH - ^iPr), 20.82 (s, CH_3 - ^iPr), 19.99 (s, CH_3 - ^iPr), 19.35 (t, [J_{CP} + J_{CRh}] 1.9 Hz, CH - ^iPr), 19.02 (s, CH_3 - ^iPr) ppm. $^{31}\text{P}\{^1\text{H}\}$ NMR (202.46 MHz, C_6D_6): 30.90 (d, J_{PRh} 147.4, J_{PSi} 12 Hz) ppm. DEPT $^{29}\text{Si}\{^1\text{H}\}$ NMR (99.36 MHz, C_6D_6): 75.77 (dd, $J_{\text{Si-Rh}}$ 37.0, $J_{\text{Si-P}}$ 12 Hz) ppm. Anal. Calcd for $\text{C}_{32}\text{H}_{45}\text{RhIPSi}_2$: C: 51.48%, H: 6.07%; Found: C: 51.79%, H: 6.22%.

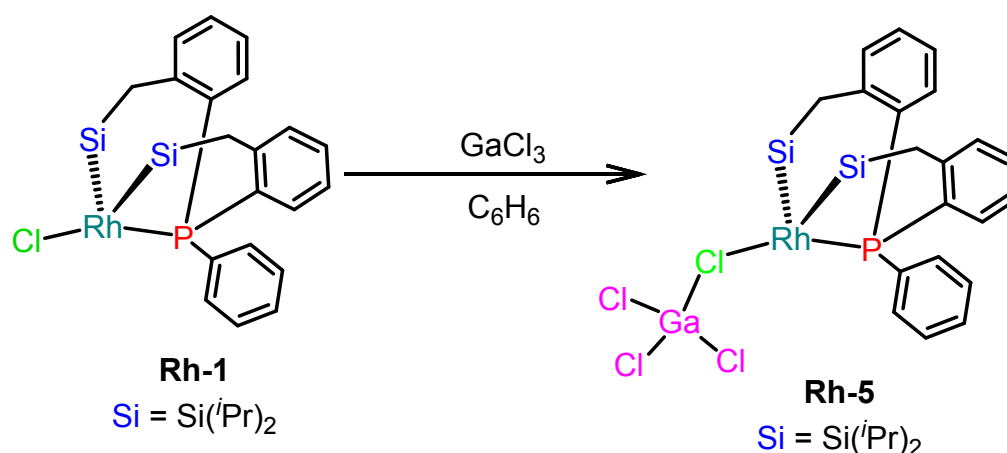
2.4 Synthesis of $[\text{Rh}(\text{OTf})\{\kappa^3(\text{P},\text{Si},\text{Si})\text{PPh}(\text{o}-\text{C}_6\text{H}_4\text{CH}_2\text{Si}^i\text{Pr}_2)_2\}]$ (**Rh-4**)



In a Schlenk flask, 30 mg (0.046 mmol) of **Rh-1** and 23.5 mg of AgOTf (0.092 mmol) was dissolved in 2 mL of dry Toluene. The resulted brown solution was left stirring for 24 hours in dark. The solution was filter through celite and volatiles were removed under the vacuum, the crude was washed with 3 portions of 1 mL of dry pentane and dried in vacuum for 6 hours. Complex **Rh-4** was obtained as a orange viscous compound (29 mg, 82% yield). ^1H NMR (500 MHz, C_6D_6): δ 7.64 (ddd, $J_{\text{HH}} = 11.3$ Hz, $J_{\text{HH}} = 7.9$ Hz, $J_{\text{HP}} = 1.6$ Hz 2H, CH_{arom}), 7.09 – 7.03 (m, 3H, CH_{arom}), 6.98 – 6.82 (m, 6H, CH_{arom}), 6.70 (tt, $J_{\text{HH}} = 7.4$ Hz, $J_{\text{HP}} = 1.6$ Hz 2H, CH_{arom}), 2.25 (ddd, $J_{\text{HH}} = 15.2$, $J_{\text{HH}} = 5.8$, $J_{\text{HP}} = 2.5$ 2H, CH_2), 2.05 (d, $J_{\text{HH}} = 15.2$ Hz, 2H, CH_2), 1.83(sept, $J_{\text{HH}} = 7.5$ Hz, 2H, CH - ^iPr), 1.65 (sept, J_{HH}

= 7.7 Hz, 2H, CH-*i*Pr), 1.45 (d, $J_{\text{HH}} = 7.5$ Hz, 6H, CH₃-*i*Pr), 1.08 (d, $J_{\text{HH}} = 7.3$ Hz, 6H, CH₃-*i*Pr), 0.94 (pseudo dd, $J_{\text{HH}} = 7.5$ Hz, $J_{\text{HH}} = 4.7$ Hz, 12H, CH₃-*i*Pr) ppm. **¹³C{¹H} NMR (125.76 MHz, C₆D₆):** 145.83 (d, $J_{\text{CP}} 13.5$ Hz, C_{ipso}), 134.44 (d, $J_{\text{CP}} 10.8$ Hz, CH_{arom}), 132.76 (d, $J_{\text{CP}} 5.9$ Hz, CH_{arom}), 131.99 (d, $J_{\text{CP}} 8.4$ Hz, CH_{arom}), 131.75 (dd, $J_{\text{CP}} 6.2, 2.6$ Hz, CH_{arom}), 129.61 (d, $J_{\text{CP}} = 10.6$ Hz, CH_{arom}), 126.17 (d, $J_{\text{CP}} 60.3$ Hz, C_{ipso}), 125.68 (d, $J_{\text{CP}} 2.1$ Hz, CH_{arom}), 21.83 (d, $J_{\text{CP}} 14.6$ Hz, CH₂), 21.57 (s, CH₃-*i*Pr), 20.73 (s, CH-*i*Pr), 19.09 (s, CH₃-*i*Pr), 18.67 (s, CH₃-*i*Pr), 18.18 (s, CH₃-*i*Pr), 17.00 (t, [$J_{\text{CP}} + J_{\text{CRh}}$] 1.5 Hz, CH-*i*Pr) ppm. **³¹P{¹H} NMR (202.46 MHz, C₆D₆):** 37.67 (d, $J_{\text{PRh}} 169.5, J_{\text{PSi}} 15$ Hz) ppm. **DEPT ²⁹Si{¹H} NMR (99.36 MHz, C₆D₆):** 73.82 (dd, $J_{\text{Si-Rh}} 38.4, J_{\text{Si-P}} 15$ Hz) ppm.

2.5 Synthesis of [Rh{κ³(*P,Si,Si*) PPh(o-C₆H₄CH₂Si^{*i*}Pr₂)₂}Cl·GaCl₃] (**Rh-5**)

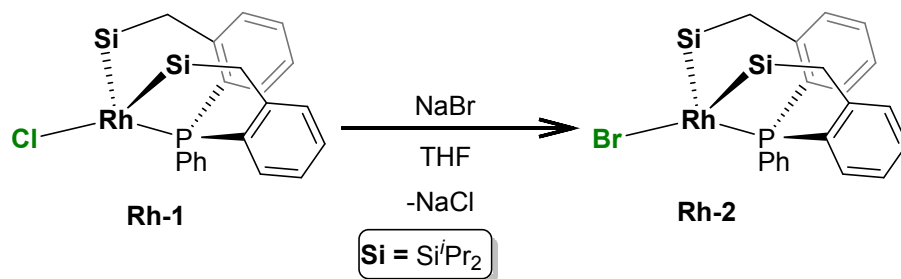


In a Schlenk flask, 30 mg (0.046 mmol) of **Rh-1** and 8.1 mg of GaCl₃ (0.046 mmol) was dissolved in 2 mL of dry benzene. The resulted yellow solution was left stirring for 24 hours. The volatiles were removed under the vacuum; the crude was washed with 3 portions of 1 mL of dry pentane and dried in vacuum for 6 hours. Complex **Rh-5** was obtained as a yellow-brown solid (29 mg, 75% yield). **¹H NMR (500 MHz, CDCl₃):** δ 7.50 – 7.36 (m, 4H, CH_{arom}), 7.33 (t, $J_{\text{HH}} 7.6$ Hz, 2H, CH_{arom}), 7.22 (t, $J_{\text{HH}} 6.4$ Hz, 2H, CH_{arom}), 7.15 (s, 1H, CH_{arom}), 7.05 (t, $J_{\text{HH}} 7.7$ Hz, 2H, CH_{arom}), 2.21 (dd, $J_{\text{HH}} 15.0, J_{\text{HH}} 4.7$, 2H, CH₂), 2.06 (d, $J_{\text{HH}} 14.8$ Hz, 2H, CH₂), 1.60 (sept, $J_{\text{HH}} 7.5$ Hz, 2H, CH-*i*Pr), 1.30 (sept, $J_{\text{HH}} 7.3$ Hz, 2H, CH-*i*Pr), 1.11 (d, $J_{\text{HH}} 7.3$ Hz, 6H, CH₃-*i*Pr), 0.92 (d, $J_{\text{HH}} 7.4$ Hz, 6H, CH₃-*i*Pr), 0.84 (d, $J_{\text{HH}} 7.2$ Hz, 6H, CH₃-*i*Pr), 0.67 (d, $J_{\text{HH}} 7.3$ Hz, 6H, CH₃-*i*Pr) ppm. **¹³C{¹H} NMR (125.758 MHz, CDCl₃):**

145.89 (d, J_{CP} 13.1 Hz, C_{ipso}), 134.65 (d, J_{CP} 10.9 Hz, CH_{arom}), 132.64 (d, J_{CP} = 5.8 Hz, CH_{arom}), 131.75 (d, J_{CP} 8.4 Hz, CH_{arom}), 129.65 (d, J_{CP} 10.7 Hz, CH_{arom}), 127.36 (d, J_{CP} 53.2 Hz, C_{ipso}), 125.89 (d, J_{CP} 9.3 Hz, CH_{arom}), 125.04 (d, J_{CP} 60.0 Hz, C_{ipso}), 21.95 (s, CH_3 - iPr), 21.88 (d, J_{CP} 12.4 Hz, CH_2), 20.75 (s, CH - iPr), 19.91 (s, CH_3 - iPr), 19.89 (s, CH_3 - iPr), 18.96 (s, CH_3 - iPr), 18.21 (t, [J_{CP} + J_{CRh}] 1.8 Hz, CH - iPr) ppm. $^{31}P\{^1H\}$ NMR (202.46 MHz, $CDCl_3$): 34.80 (d, J_{PRh} 177.6) ppm. DEPT $^{29}Si\{^1H\}$ NMR (99.36 MHz, $CDCl_3$): 78.42 (dd, J_{Si-Rh} 37.3, J_{Si-P} 12.6 Hz) ppm. **Anal. Calcd for $C_{32}H_{45}Cl_4GaRhPSi_2 \cdot 0.37CDCl_3$:** C: 44.39%, H: 5.26%; Found: C:44.45%, H:5.33%.

3 Characterization of new complexes

3.1 Characterization of $[RhBr\{\kappa^3(P,Si,Si)PPh(o-C_6H_4CH_2Si^iPr_2)_2\}]$ (Rh-2)



NMR spectra of Rh-2

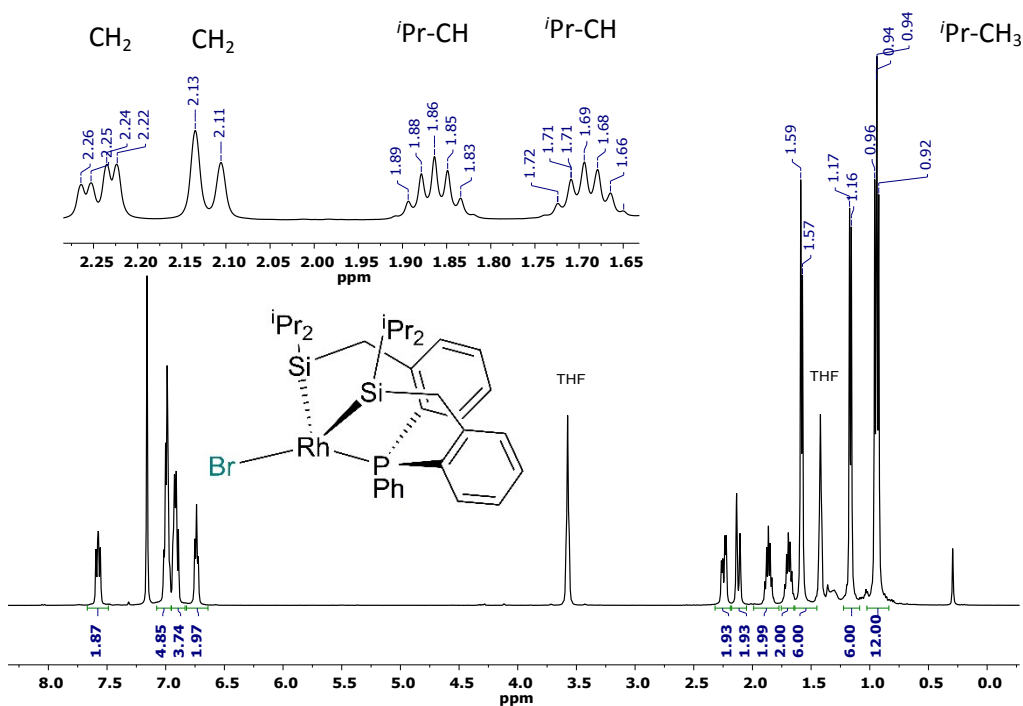


Figure S1. 1H NMR spectrum (500 MHz, C_6D_6 , 293 K) of Rh-2

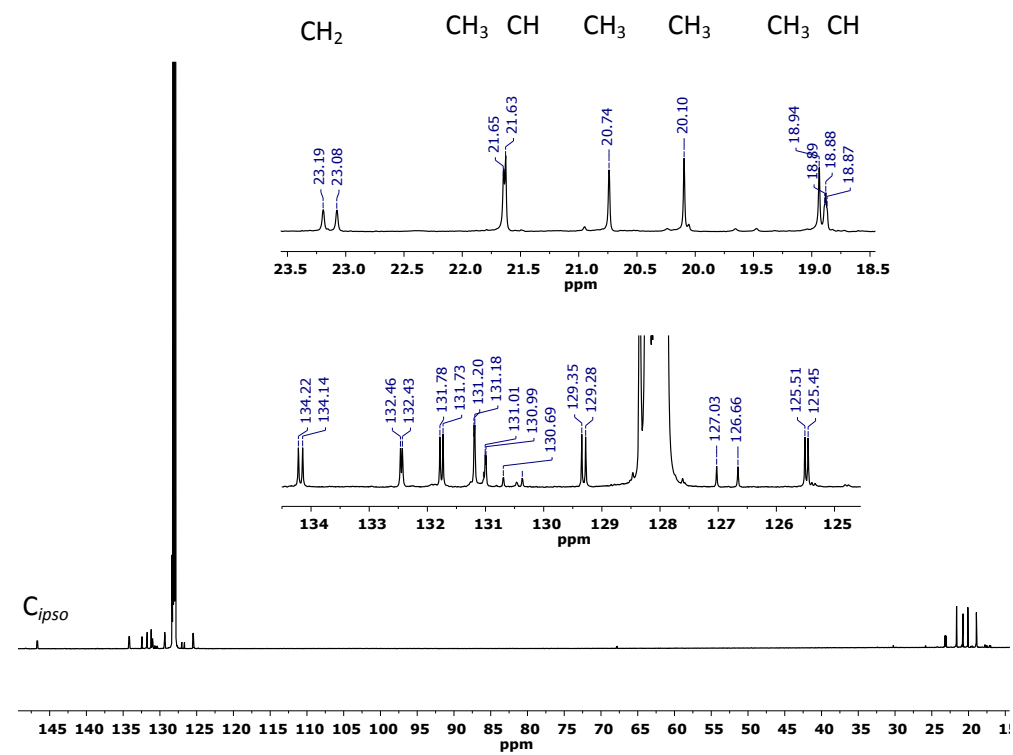


Figure S2. ¹³C{¹H} NMR spectrum (150.9 MHz, C₆D₆, 293 K) of Rh-2

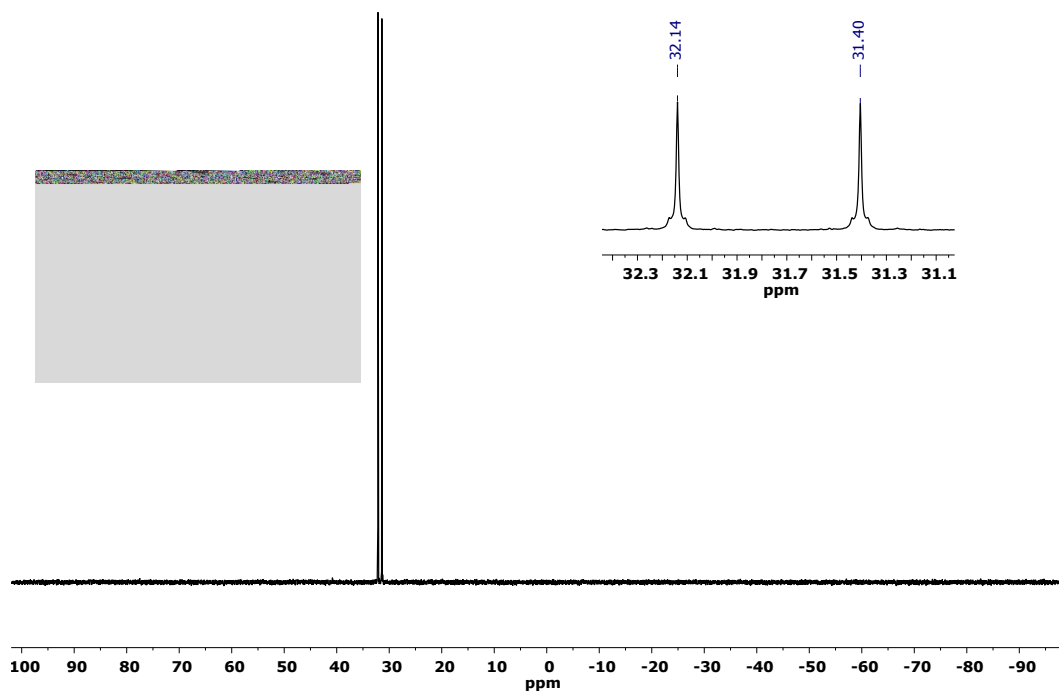


Figure S3. ³¹P{¹H} NMR spectrum (202.46 MHz, C₆D₆, 293 K) of Rh-2.

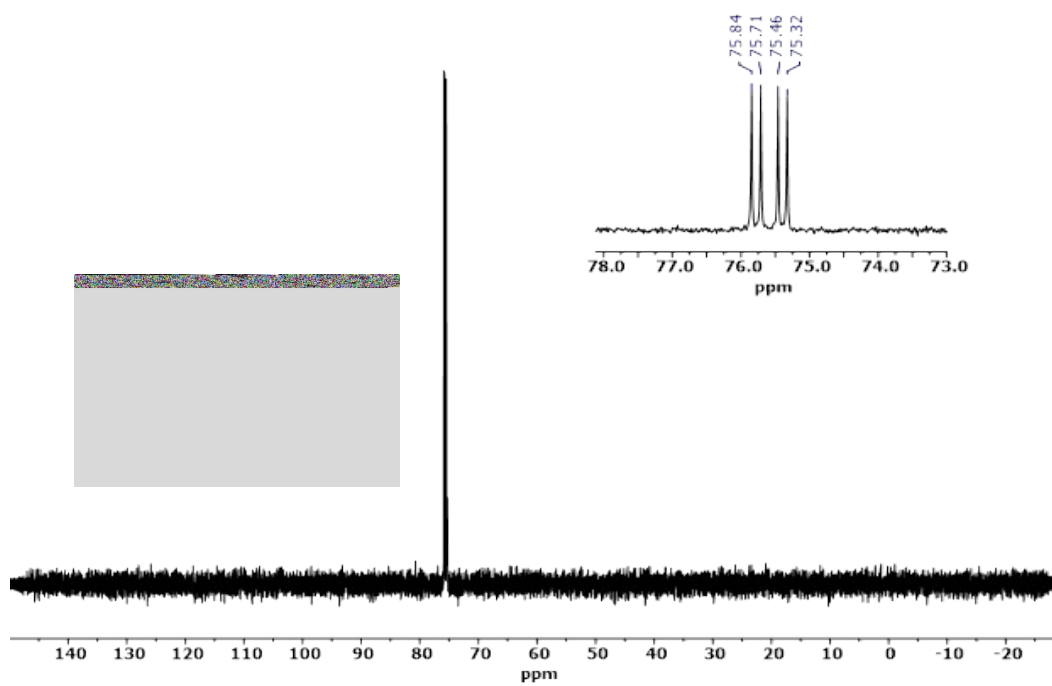
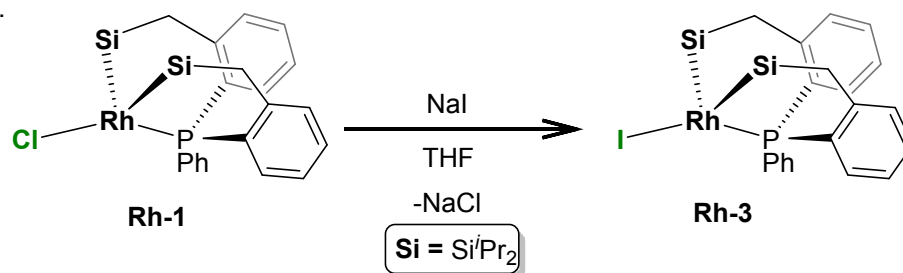


Figure S4. $^{29}\text{Si}\{^1\text{H}\}$ DEPT NMR spectrum (99.36 MHz, C_6D_6 , 293 K) of **Rh-2**.

3.2 Characterization of $[\text{RhI}\{\kappa^3(\text{P},\text{Si},\text{Si})\text{PPh}(\text{o}-\text{C}_6\text{H}_4\text{CH}_2\text{Si}^i\text{Pr}_2)_2\}]$ (**Rh-3**)



NMR spectra of **Rh-3**

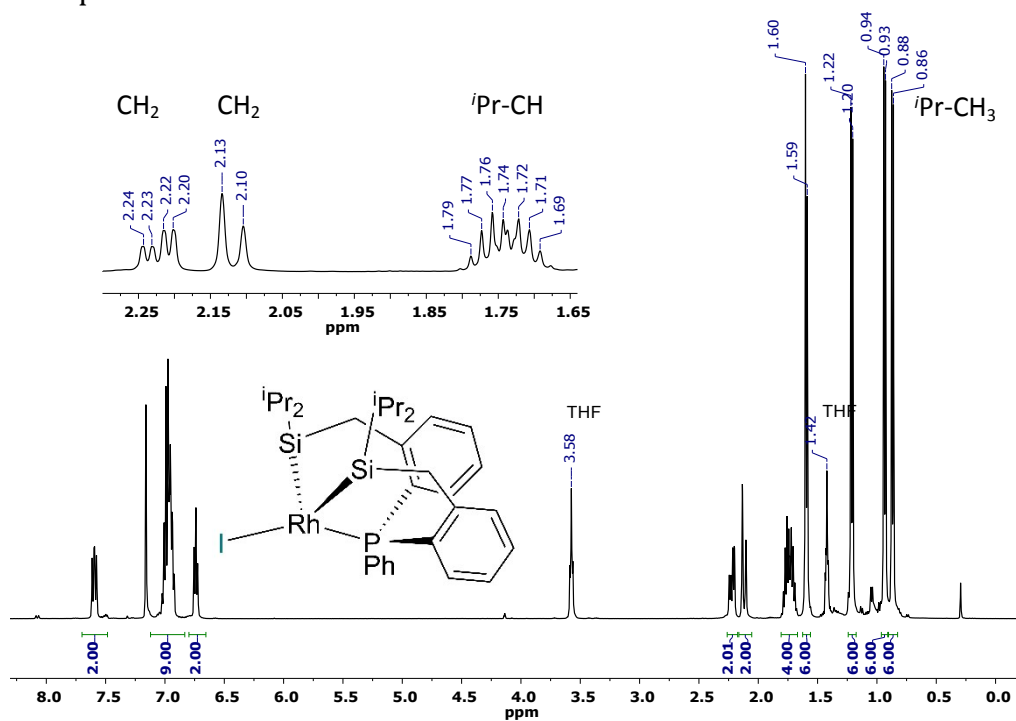


Figure S5. ^1H NMR spectrum (500 MHz, C_6D_6 , 293 K) of **Rh-3**.

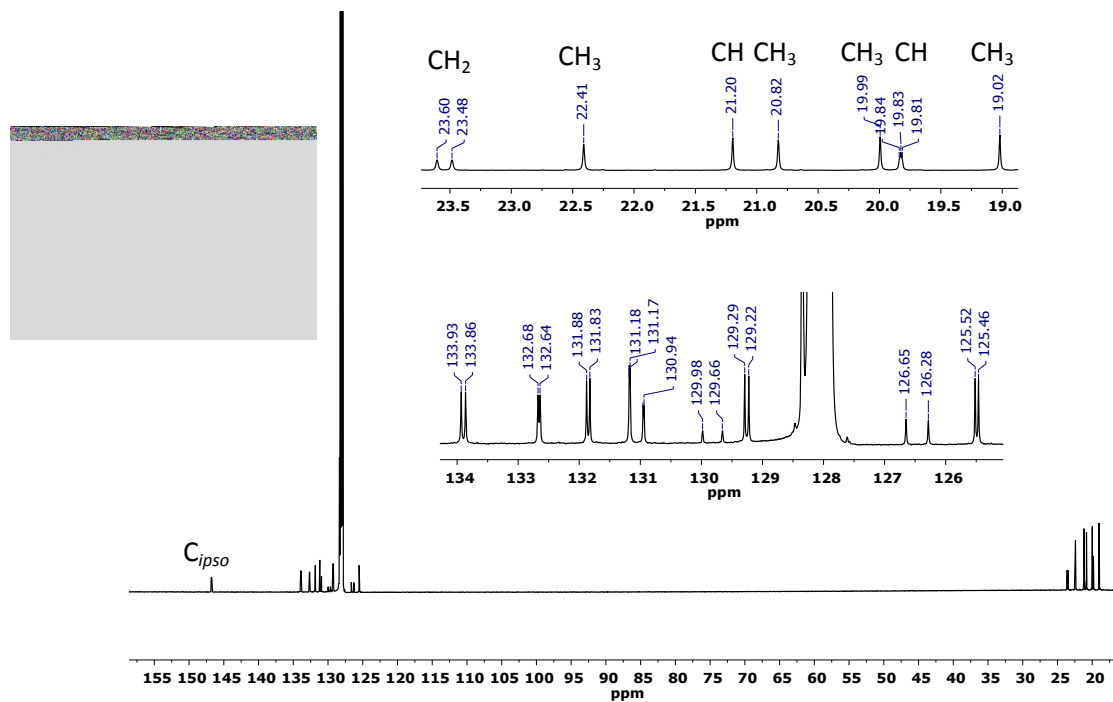


Figure S6. $^{13}\text{C}\{^1\text{H}\}$ NMR spectrum (150.9 MHz, C_6D_6 , 293 K) of Rh-3.

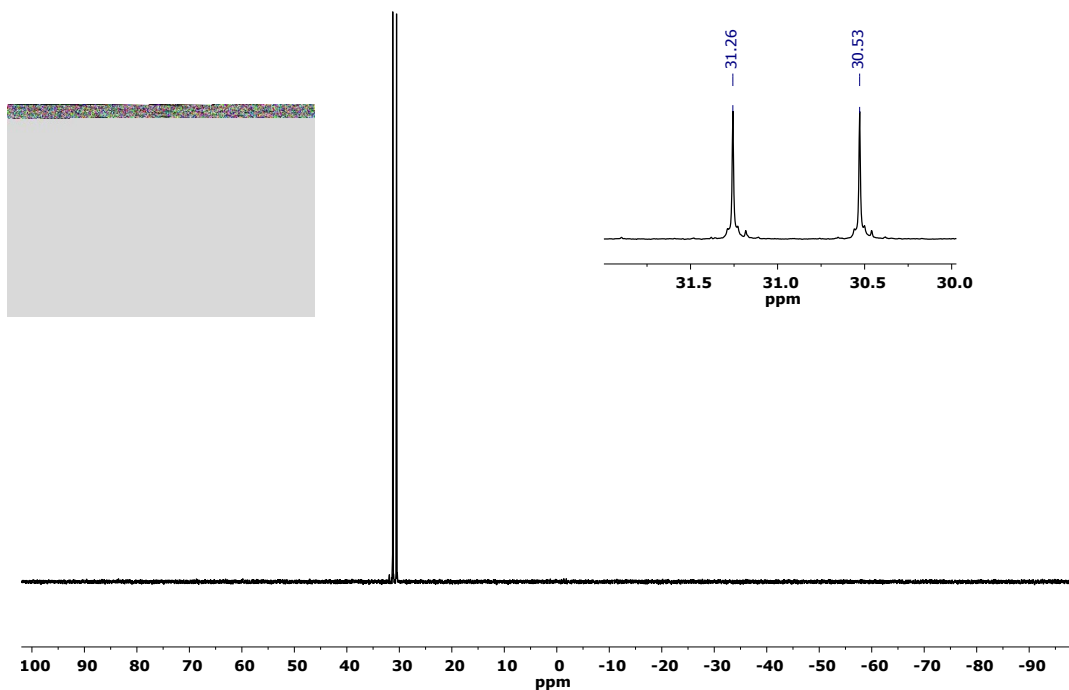


Figure S7. $^{31}\text{P}\{^1\text{H}\}$ NMR spectrum (202.46 MHz, C_6D_6 , 293 K) of Rh-3.

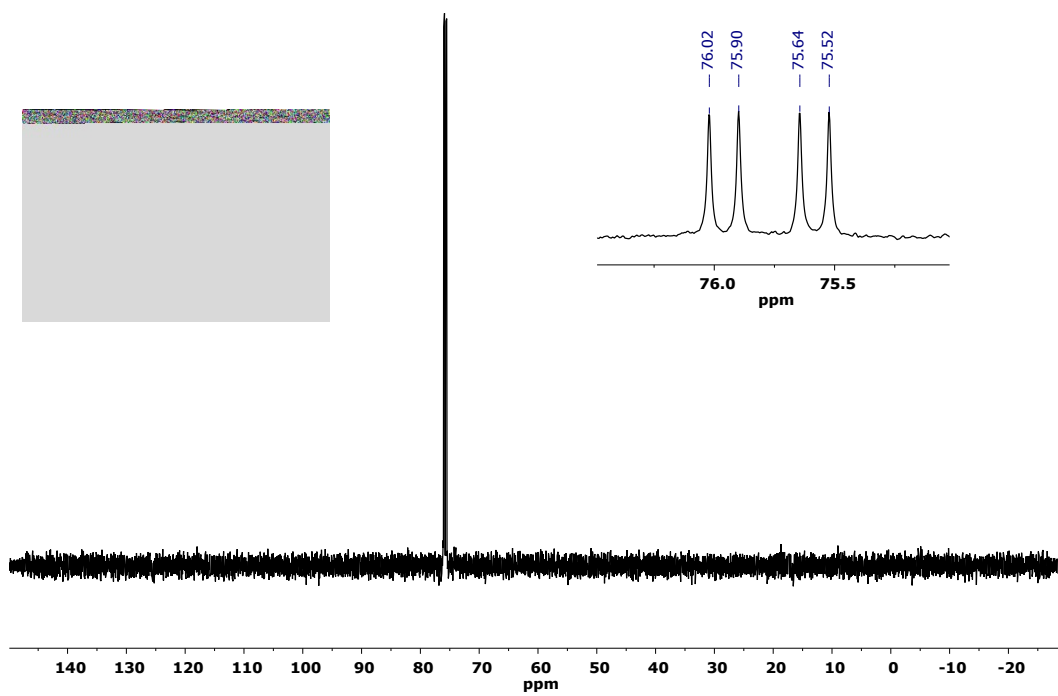
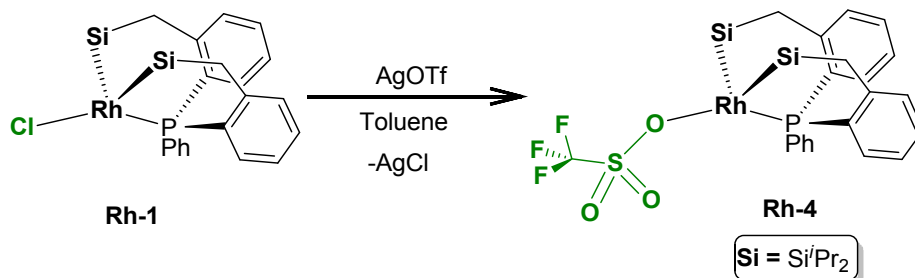


Figure S8. $^{29}\text{Si}\{^1\text{H}\}$ DEPT NMR spectrum (99.36 MHz, C_6D_6 , 293 K) of **Rh-3**.

3.3 Characterization of [RhOTf{ $\kappa^3(P,Si,Si)$ PPh(o-C₆H₄CH₂Si^{*i*}Pr₂)₂}] (**Rh-4**)



NMR spectra of Rh-4

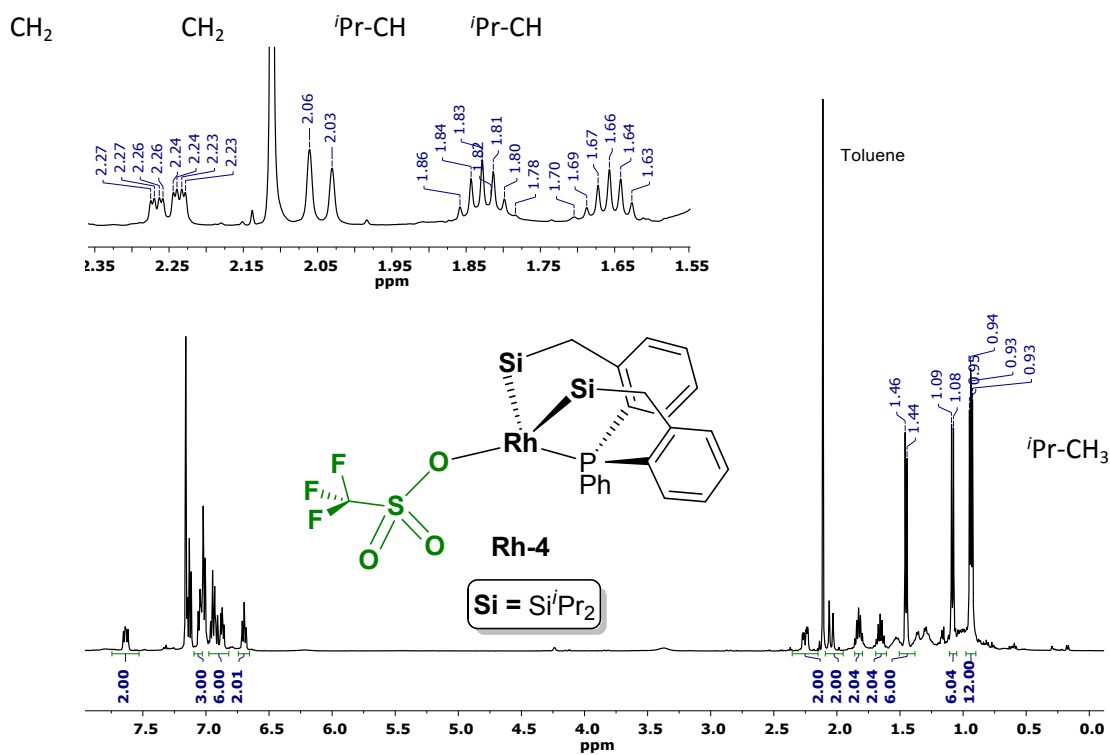


Figure S9. ¹H NMR spectrum (500 MHz, C₆D₆, 293 K) of Rh-4

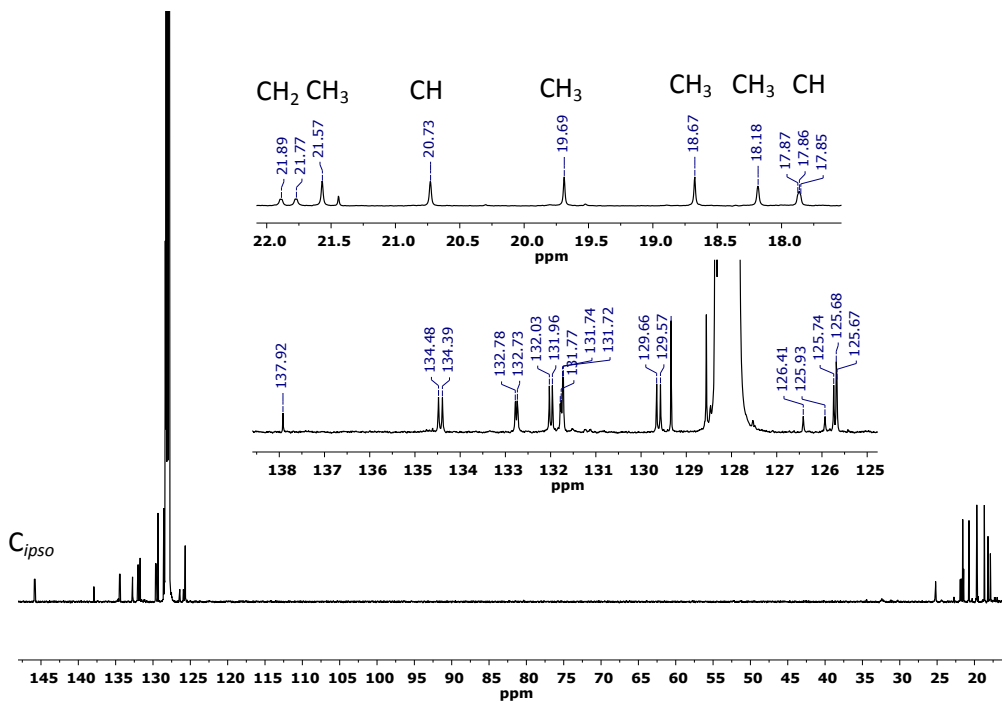


Figure S10. $^{13}\text{C}\{^1\text{H}\}$ NMR spectrum (125.76 MHz, C_6D_6 , 293 K) of Rh-4

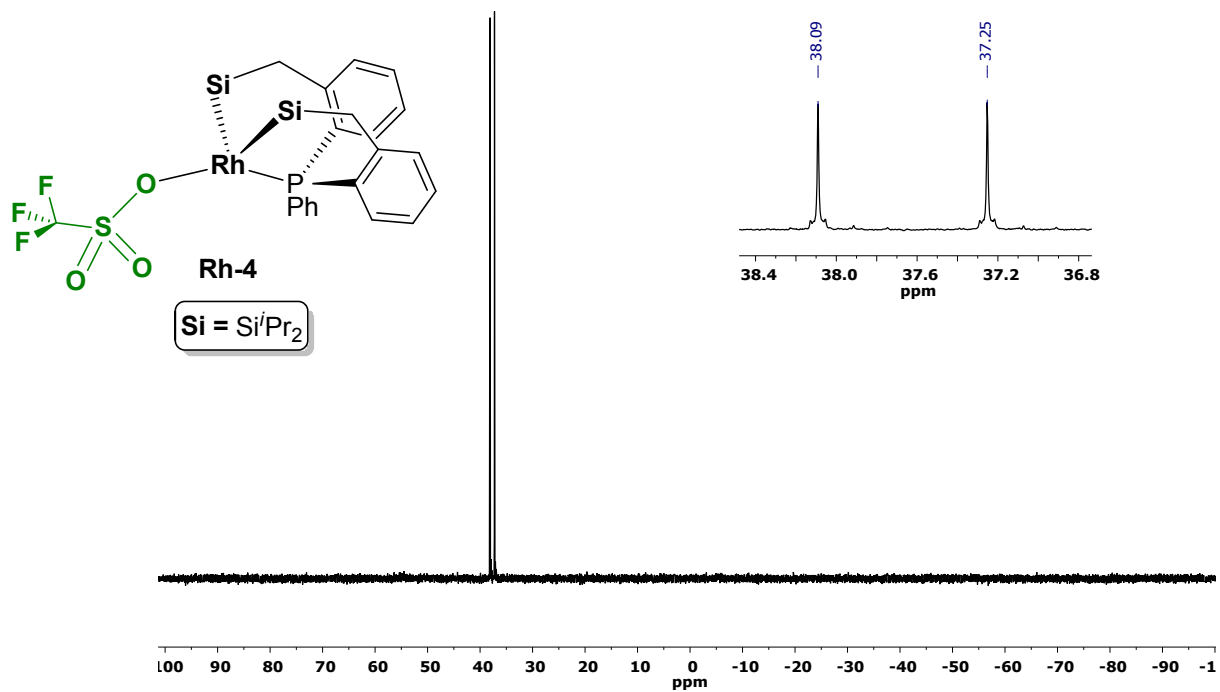


Figure S11. $^{31}\text{P}\{^1\text{H}\}$ NMR spectrum (202.46 MHz, C_6D_6 , 293 K) of Rh-4

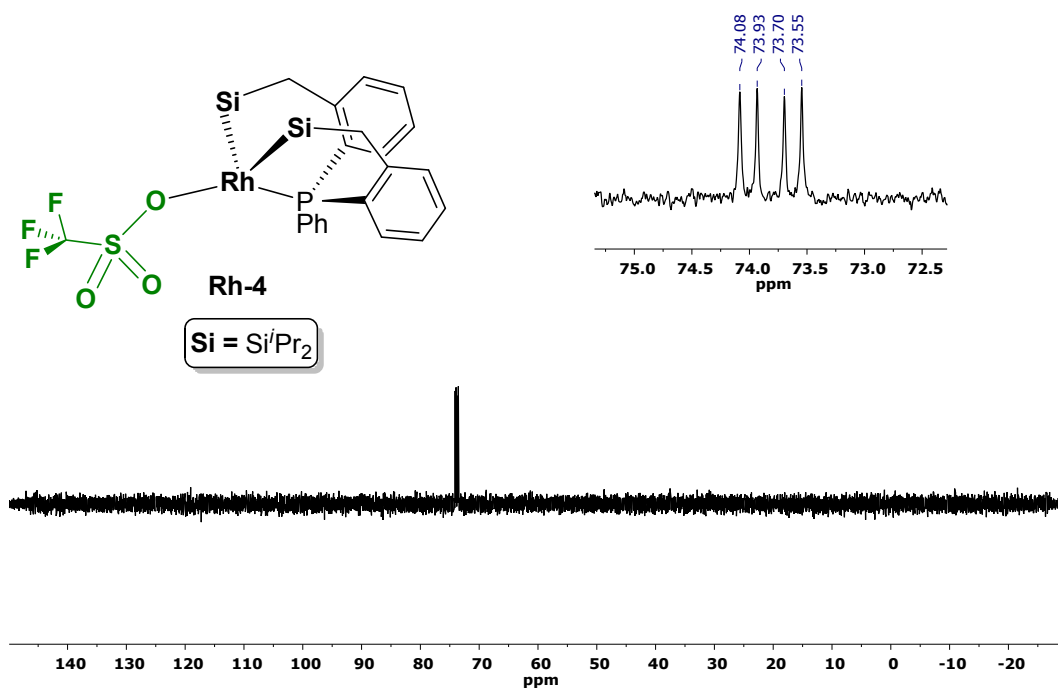
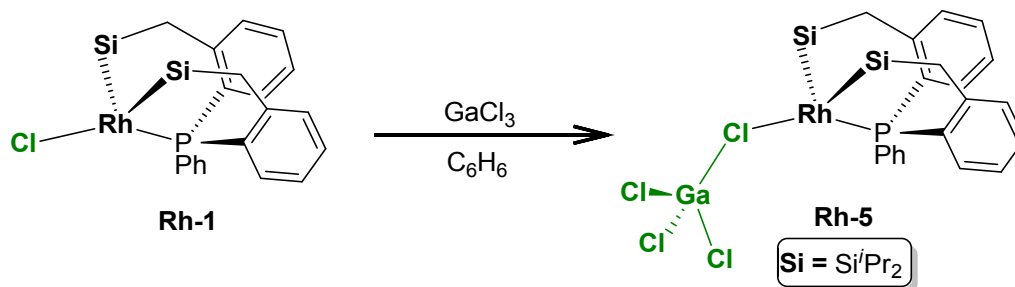


Figure S12. $^{29}\text{Si}\{^1\text{H}\}$ DEPT NMR spectrum (99.36 MHz, C_6D_6 , 293 K) of Rh-4

3.4 Synthesis of $[\text{RhCl}\{\kappa^3(\text{P},\text{Si},\text{Si})\text{PPh}(\text{o}-\text{C}_6\text{H}_4\text{CH}_2\text{Si}^i\text{Pr}_2)_2\}\text{GaCl}_3]$ (**Rh-5**)



NMR spectra of **Rh-5**

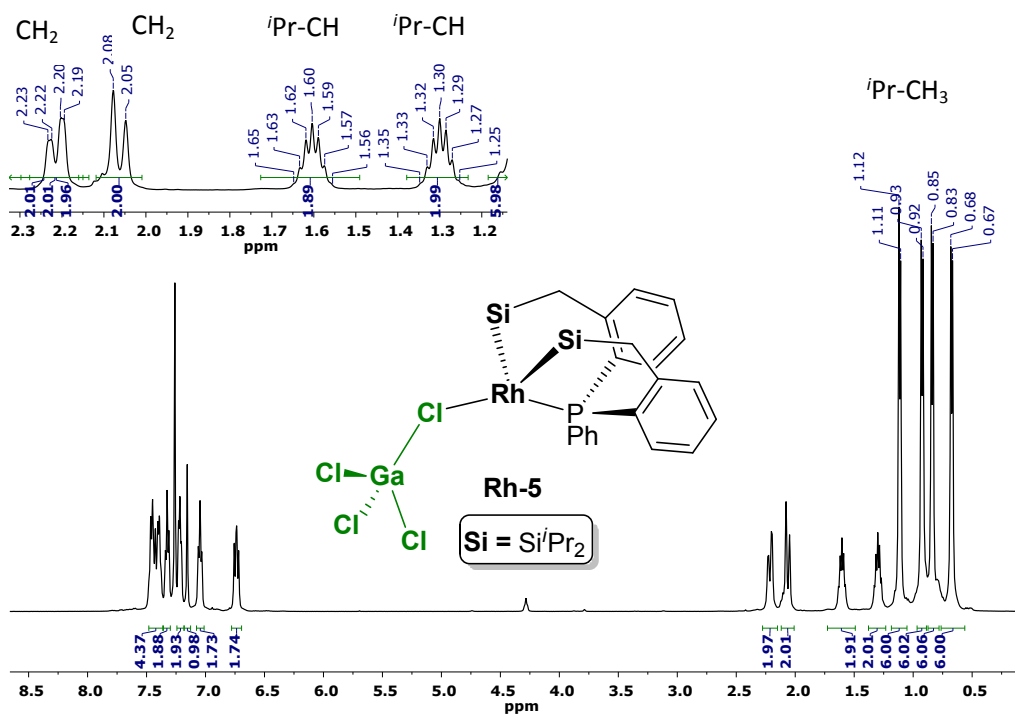


Figure S13. ^1H NMR spectrum (500 MHz, CDCl_3 , 293 K) of **Rh-5**

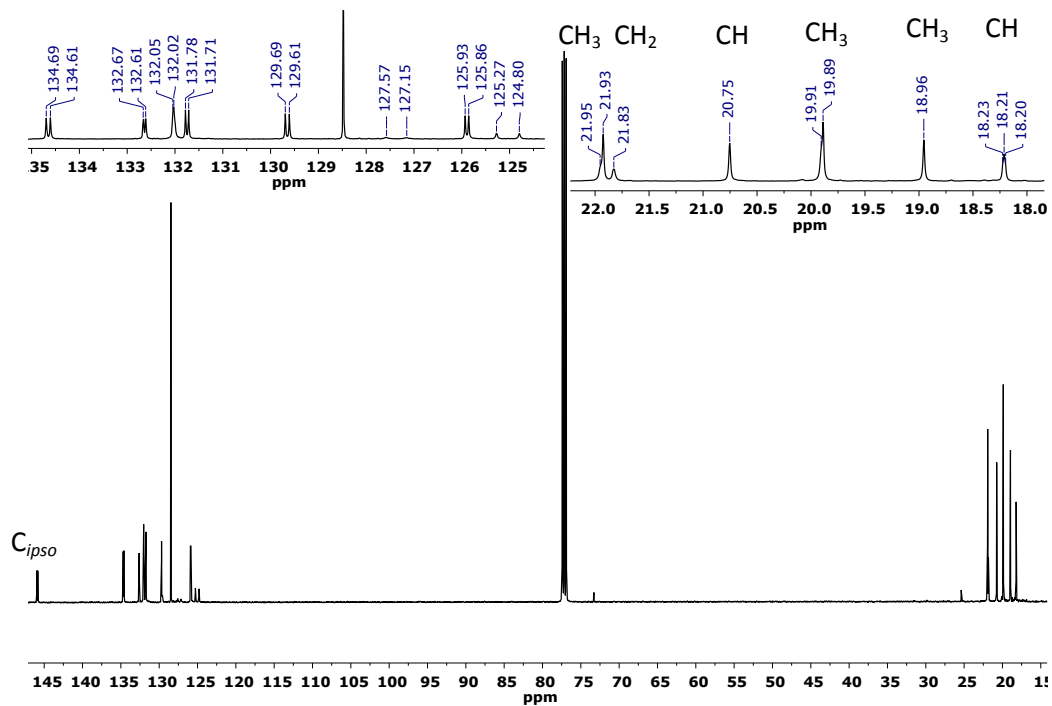


Figure S14. $^{13}\text{C}\{^1\text{H}\}$ NMR spectrum (125.76 MHz, CDCl_3 , 293 K) of Rh-5

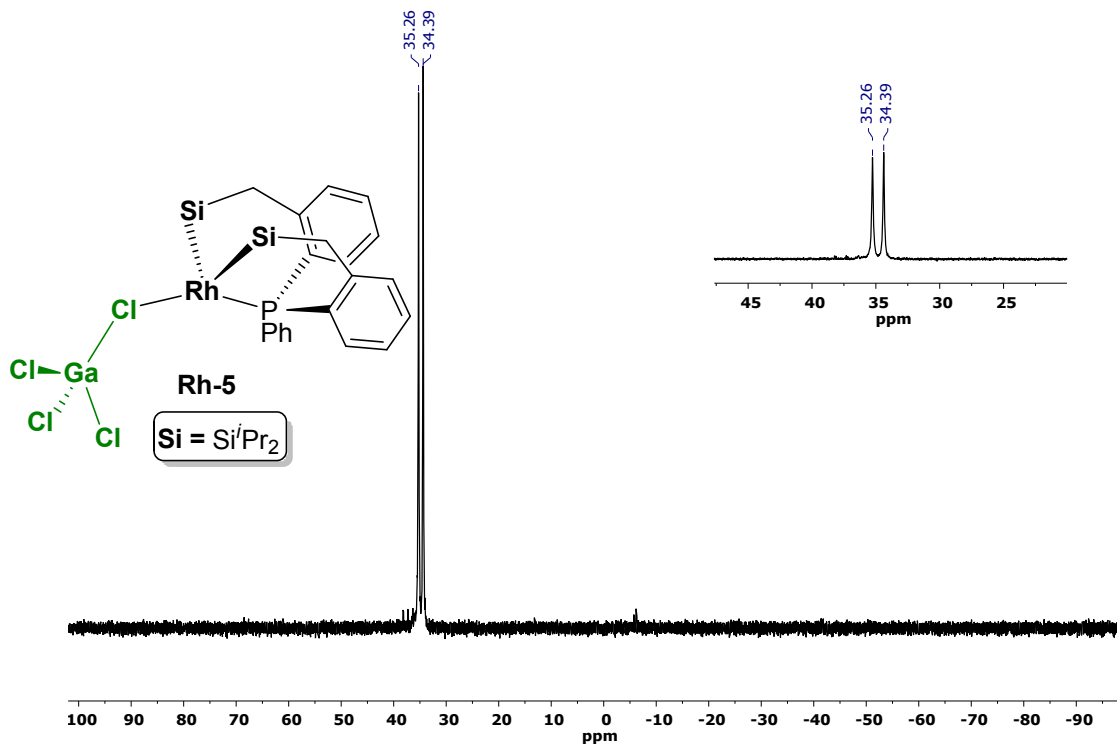


Figure S15. $^{31}\text{P}\{^1\text{H}\}$ NMR spectrum (202.46 MHz, CDCl_3 , 293 K) of Rh-5

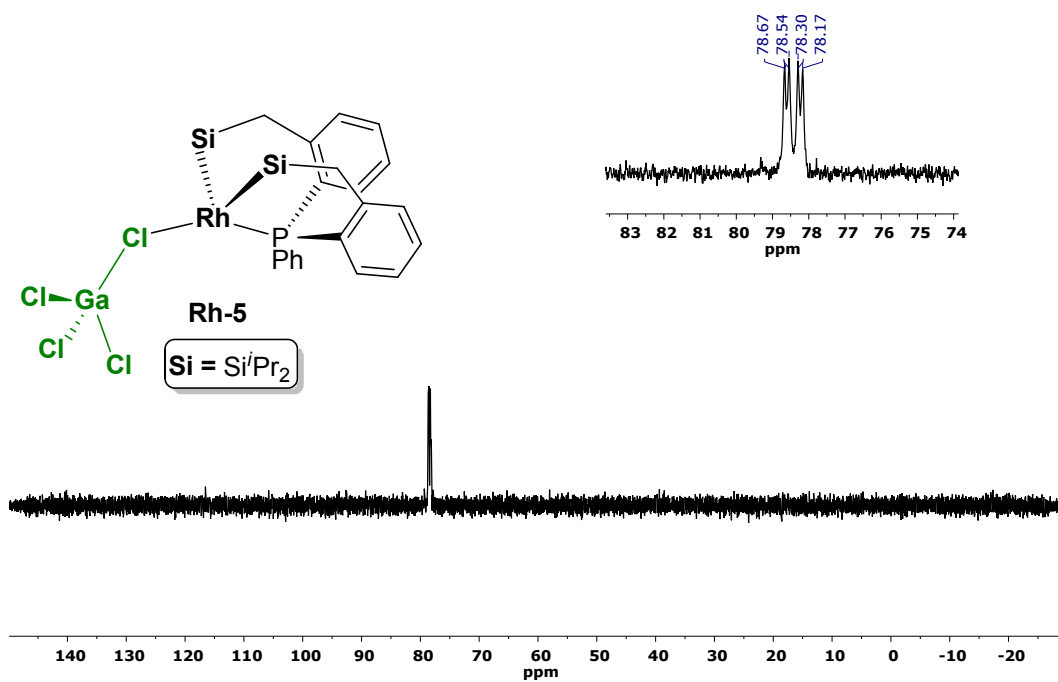


Figure S16. $^{29}\text{Si}\{^1\text{H}\}$ DEPT NMR spectrum (99.36 MHz, CDCl_3 , 293 K) of **Rh-5**

3.5 Reaction of **Rh-1** and styrene *in situ* in an NMR tube

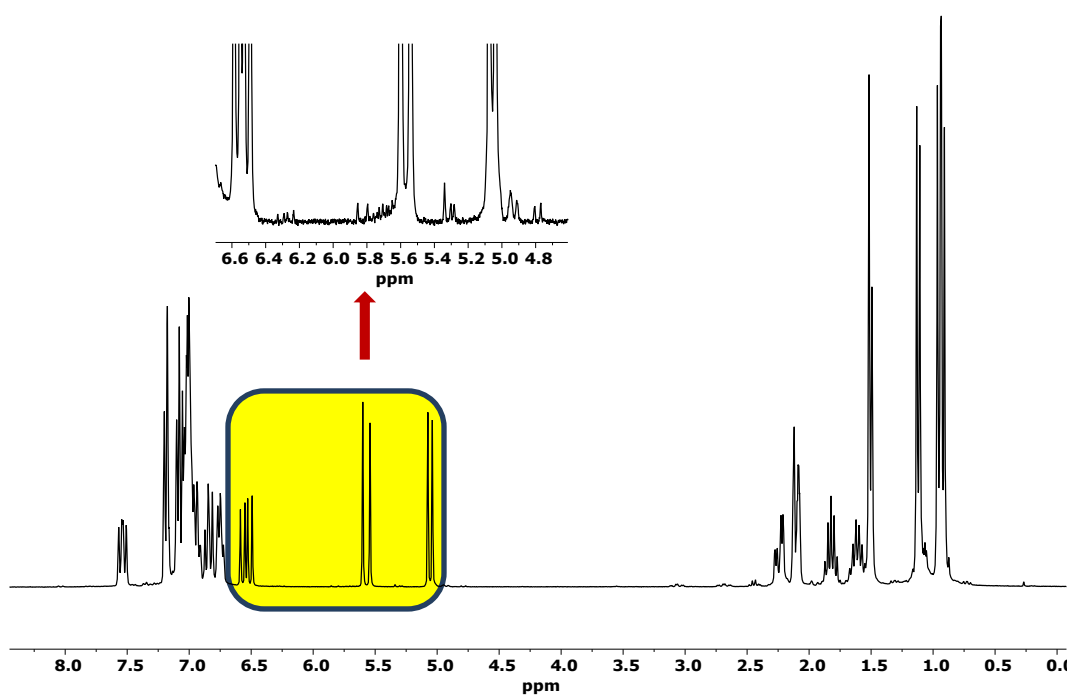
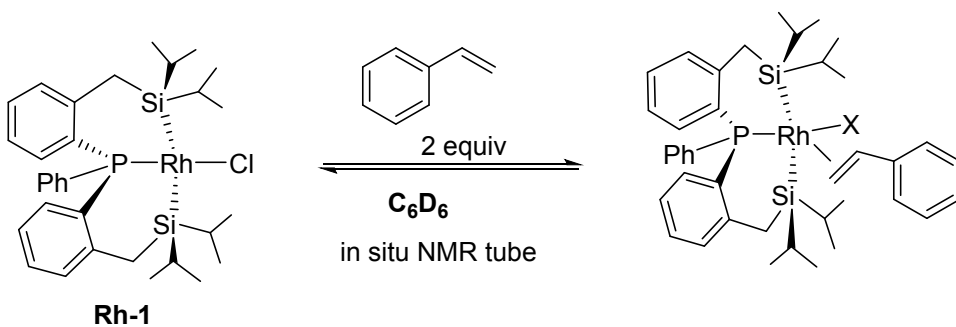


Figure S17. The *in situ* 1H NMR spectrum (300 MHz, Tol- d_8 , 298 K) of the reaction mixture of Rh-1 and 2 equivalents of styrene.

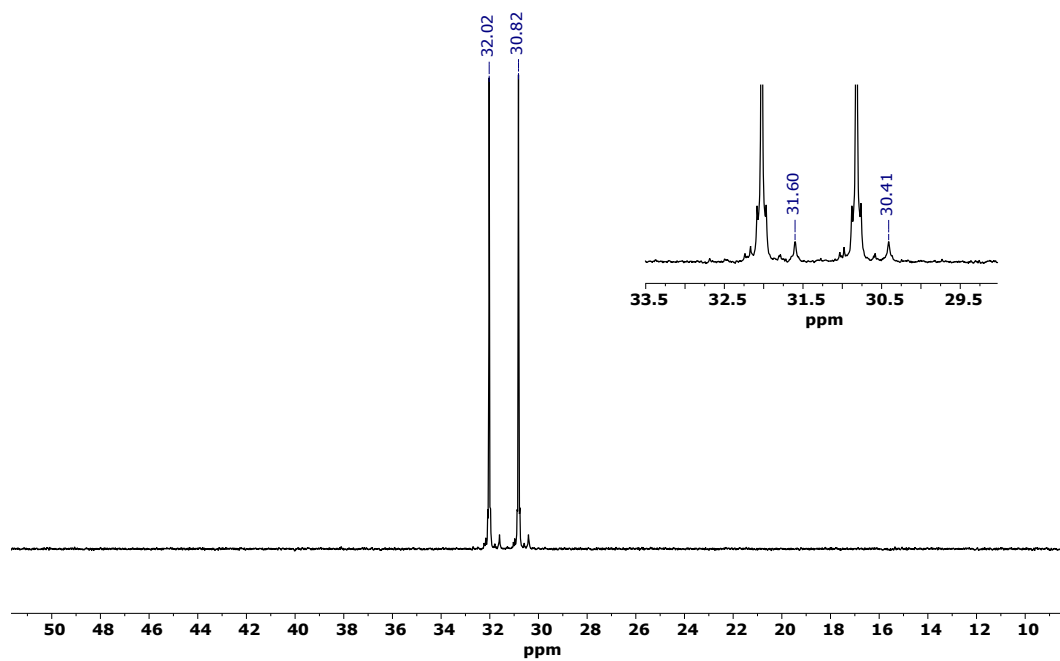


Figure S18. The *in situ* $^{31}\text{P}\{^1\text{H}\}$ NMR spectrum (121.5 MHz, Tol- d_8 , 298 K) of the reaction mixture of **Rh-1** and 2 equivalents of styrene.

3.6 Optimization of the catalytic dehydrogenative silylation conditions of styrene by Rhodium and Iridium complexes

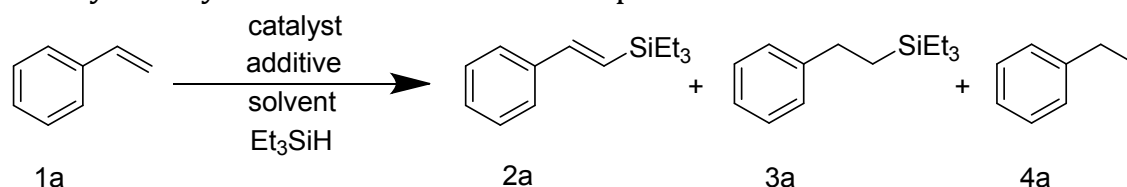
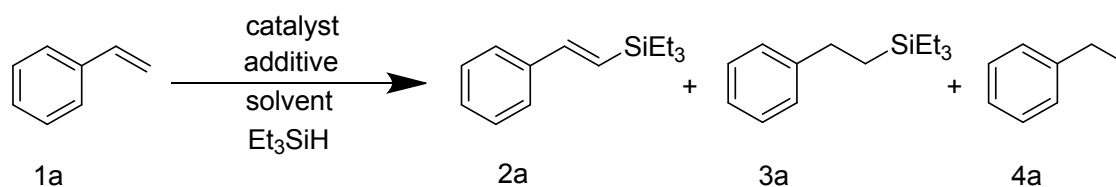


Table S3. Optimization of Dehydrogenative silylation of styrene with Et_3SiH by Rh Complexes.

Entry	Catalyst	Additive	Solvent	T(°C)	t(h)	Conversion (%)	2a	3a	4a
1	Rh-1	-	Toluene	95	24	100	40.4	39.9	19.7
2	Rh-2	-	Toluene	95	24	100	38.4	42.1	19.5
3	Rh-3	-	Toluene	95	24	100	38.4	42.7	18.9
4	Rh-4	-	Toluene	95	24	90	17.6	53.2	29.2
5	Rh-5	-	CH_2Cl_2	80	24	100	36.5	33.8	29.7
6	Rh-1	-	CH_2Cl_2	80	24	100	38.9	49.3	11.8
7	Rh-1	-	THF	80	24	100	38.9	46.6	14.5
8	Rh-1	-	neat	95	24	100	35.6	45.7	18.7
9	Rh-1 ^a	AgOTf	Toluene	95	24	100	37	45.3	17.7
10	Rh-1 ^a	KO^tBu	Toluene	95	24	100	37.5	43.2	19.3
11	Rh-1 ^b	nbe (1 eq)	Toluene	95	24	100	50.5	46.2	3.3
12	Rh-1 ^c	nbe (2 eq)	Toluene	95	24	100	50.1	46.4	3.5
13	Rh-1 ^d	nbe (3 eq)	Toluene	95	24	100	59.0	39.7	1.3
14	Rh-1 ^e	nbe (5 eq)	Toluene	95	24	100	60.6	37.1	2.3
15	Rh-1 ^f	-	Toluene	95	24	100	55.0	16.8	28.2
16	Rh-1 ^g	-	Toluene	95	5	100	62.6	6.6	30.8
17	-	-	Toluene	95	24	n.d	-	-	-

Reaction conditions: Styrene (0.2 mmol, except when explicitly mentioned), Et_3SiH (0.2 mmol), catalyst (1 mol %), solvent (0.2 mL). The conversions and selectivity were determined by GC-MS and verified by ^1H NMR. [a] 2 equiv. of additive was used. [b] 1 equiv. of additive was used. [c] 2 equiv. of additive was used. [d] 3 equiv. of styrene was used. [e] 2 equiv. of additive was used. [f] 2 equiv. of styrene was used (0.4 mmol). [g] 5 equiv. of styrene was used (1 mmol).

Table S4. Optimization of Dehydrogenative silylation of styrene with Et₃SiH by Ir-1



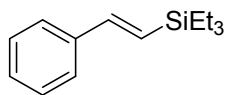
Entry	Catalyst	Additive	Solvent	T(°C)	t(h)	Conversion (%)	2a/3a	2a	3a	4a
1	Ir-1	-	THF	80	24	76	34/65	29	54	17
2	Ir-1	-	Toluene	95	24	94	49/51	35	36	29
3	Ir-1 ^b	-	Toluene	95	24	75	61/39	47	30	23
4	Ir-1 ^c	-	Toluene	95	24	85	80/20	56	14	30
5	Ir-1 ^c	-	neat	95	24	91	65/35	52	28	20
6	Ir-6 ^c	-	Toluene	95	24	98	66/34	51	26	23
7	Ir-1 ^{c, d}	Nobornene	Toluene	95	24	100	68/32	60	28	12
8	Ir-1 ^{c, e}	KO ^t Bu	Toluene	95	24	88	62/38	53	33	14
9	Ir-1 ^{c, f}	Nobornene	Toluene	95	24	64	66/34	63	33	5
10	Ir-1 ^{c, f}	Cyclohexene	Toluene	95	24	64	66/34	63	33	5

Reaction conditions: Styrene (0.2 mmol), Et₃SiH (0.2mmol), Ir-1 (1 mol%), solvent (0.2 mL). [a] The conversions and selectivity were determined by GC-MS and verified by ¹H NMR. [b] 2 equiv. of styrene was used. [c] 5 equiv. of styrene was used. [d] 1 equiv. of additive used. [e] 2 equiv. of additive used. [f] 3 equiv. of additive used.

3.7 General procedure for the catalytic dehydrogenative silylation of vinylarenes
A 4 mL screw capped high pressure bottle or vial equipped with a magnetic stir bar was charged with the catalyst (**Rh-1**, **Ir-1**, 1 mol%), vinylarenes (0.2 mmol or 1.0 mmol), and Et₃SiH (0.2 mmol) under an argon atmosphere followed by toluene (0.2 mL). The resulted solution was stirred for 5 or 24 h at 95 °C. The catalytic conversions were monitored by GC-MS and NMR. The identity of the products was ascertained by NMR of the purified products.

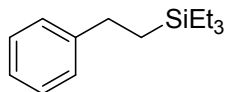
3.8 Characterization of Silane Products

3.8.1 *E*-Triethyl(styryl)silane (a)



¹H NMR (500 MHz, CDCl₃): δ 7.49 (d, *J* = 7.5 Hz 2H), 7.34 – 7.17 (m, 3H), 6.91 (d, *J* = 19.3 Hz, 1H), 6.44 (d, *J* = 19.3 Hz, 1H), 1.00 (t, *J* = 8.0 Hz, 9H), 0.68 (q, *J* = 7.9 Hz, 6H) ppm. **¹³C{¹H} NMR (125.76 MHz, CDCl₃):** 144.97 (CH), 138.65 (CH), 128.63 (C_{arom}), 128.01 (C_{arom}), 126.45 (C_{arom}), 126.04 (C_{arom}), 7.55 (Si-CH₃), 3.68 (Si-CH₂) ppm. This compound has been previously characterized.⁴

3.8.2 Triethyl(2-phenylethyl)silane (b)



¹H NMR (500 MHz, CDCl₃): δ 7.49 (d, *J* = 1.6 Hz 2H), 7.34 – 7.17 (m, 3H), 2.66 – 2.57 (m, 2H), 0.94 (t, *J* = 7.9 Hz, 9H), 0.88 (t, *J* = 9.2 Hz, 2H), 0.57 (q, *J* = 7.9 Hz, 6H) ppm. **¹³C{¹H} NMR (125.76 MHz, CDCl₃):** 145.75 (C_{arom}), 128.43 (C_{arom}), 127.84 (C_{arom}), 125.60 (C_{arom}), 30.19 (CH₂), 13.79 (CH₂), 7.60 (Si-CH₃), 3.42 (Si-CH₂) ppm. This compound has been previously characterized.⁵

3.9 Catalysis of aromatic and aliphatic alkenes under optimized conditions

Table S5. Rh-1 and Ir-1 catalyzed functionalization alkenes in toluene under optimized conditions

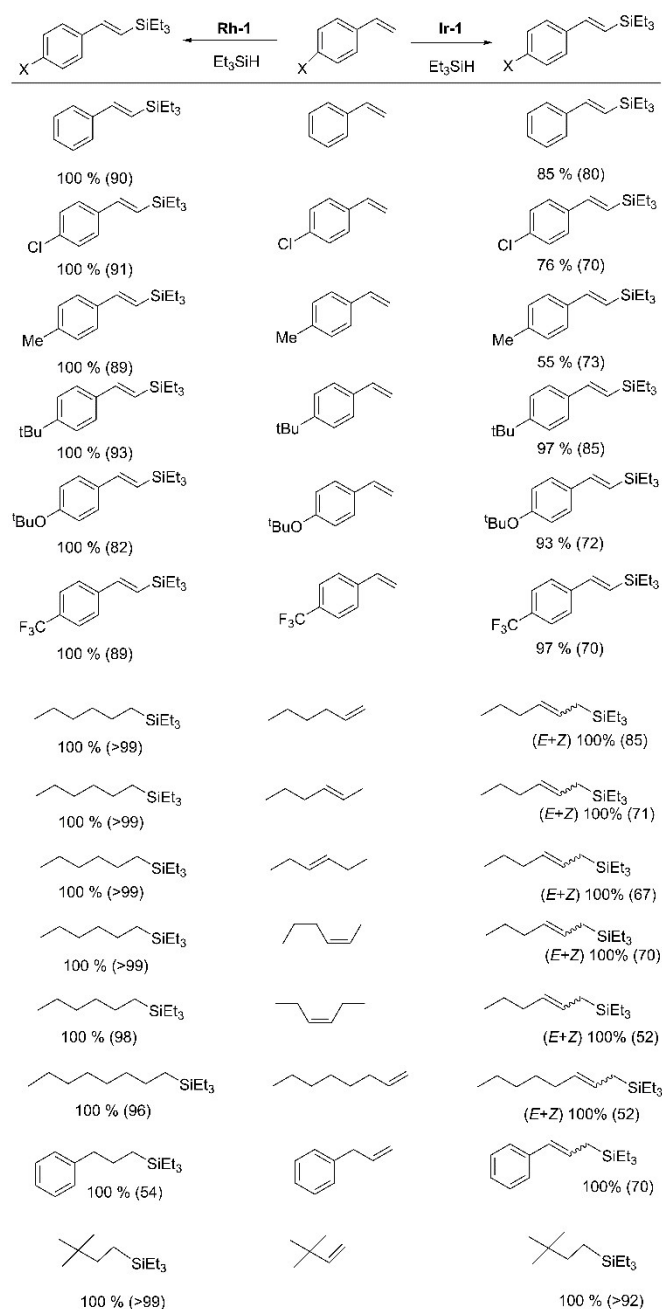
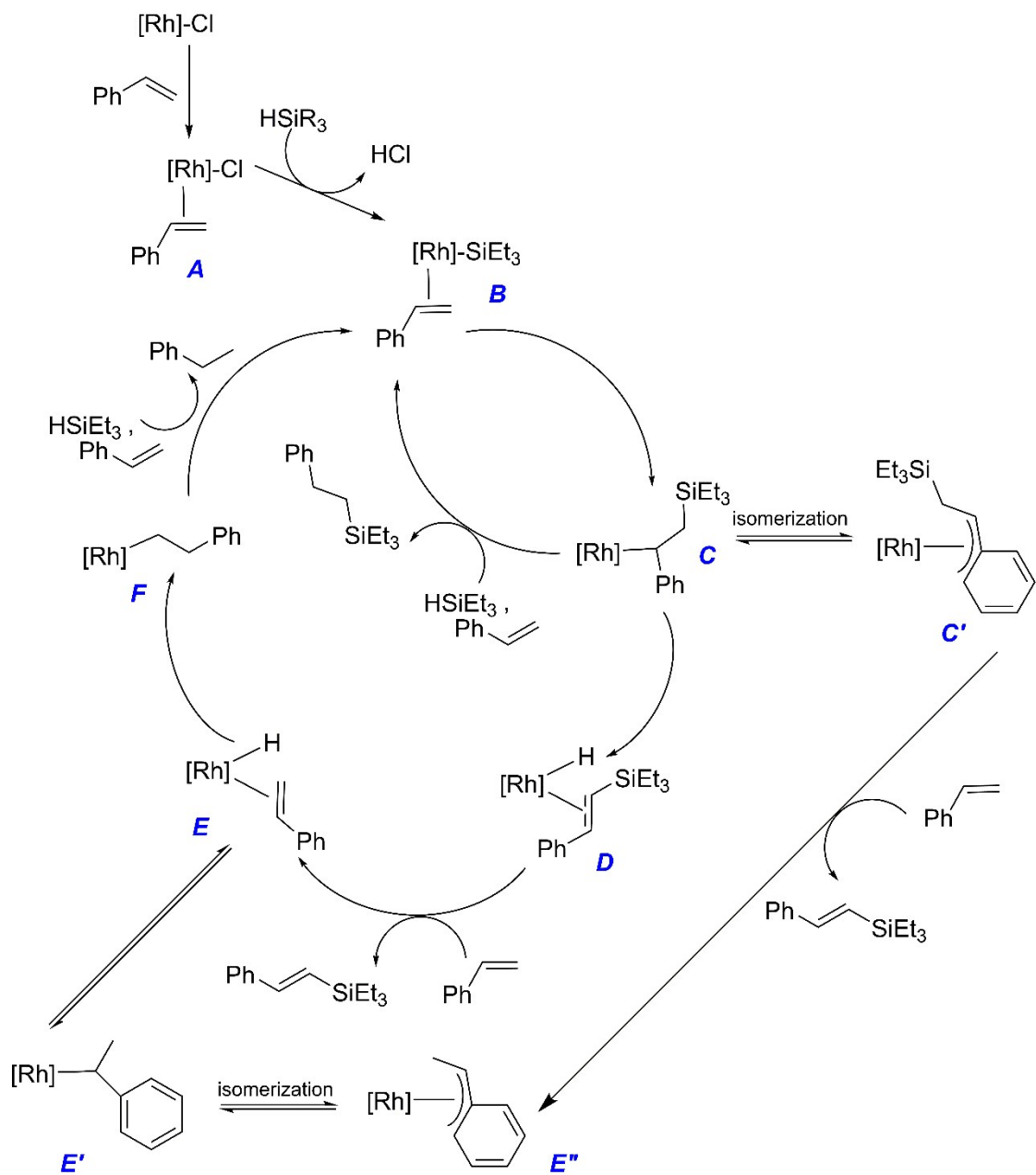


Table S5. Alkene functionalization with Et₃SiH by **Ir-1** and **Rh-1**.

Reaction conditions for styrene substrates: styrene substrates (1.0 mmol), Et₃SiH (0.2 mmol), **Rh-1** or **Ir-1** (1 mol%), toluene (0.2 mL), 95 °C for 5 h for **Rh-1**, 24 h for **Ir-1**. Reactions of aliphatic alkenes were carried out in neat conditions, alkene (0.2 mmol), Et₃SiH (0.2 mmol), **Rh-1** or **Ir-1** (1 mol%), 40 °C for 24 h.^d The conversion and selectivity were determined by GC-MS and ¹H NMR. The conversion, relative to Et₃SiH, is

shown in the table in percentages. In brackets, the selectivity to the major product is shown. In Tables 3 and 4 in the main text, the overall yield of the major products are shown.

4 A mechanistic proposal for styrene functionalization with Et₃SiH



Scheme S1. The mechanistic proposal of Scheme 2 showing also possible resting states as π-allyl intermediates.

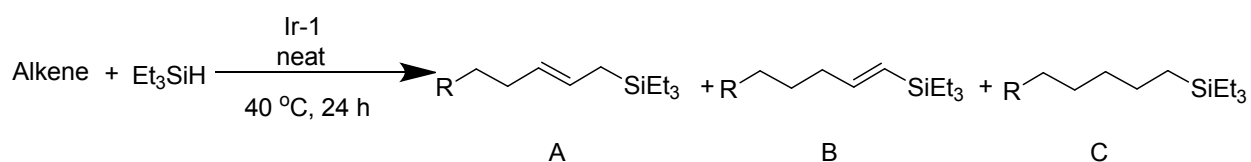
5 Catalytic studies on the reaction of Et₃SiH and aliphatic alkenes

5.1 General procedure for the hydrogenative silylation of hexene isomers

A 4 mL screw capped vial equipped with a magnetic stir bar was charged with the catalyst (**Rh-1**, **Ir-1**, 1 mol%), hexene (1-hexene, *cis*-2-, *cis*-3-, *trans*-2-, *trans*-3-, 0.2 mmol), and Et₃SiH (0.2 mmol) under an argon atmosphere without any solvent. The resulted solution was stirred for 24 h at 40 °C. The catalytic conversions were monitored by NMR and GC-MS.

5.2 Catalyzed functionalization of alkenes in toluene

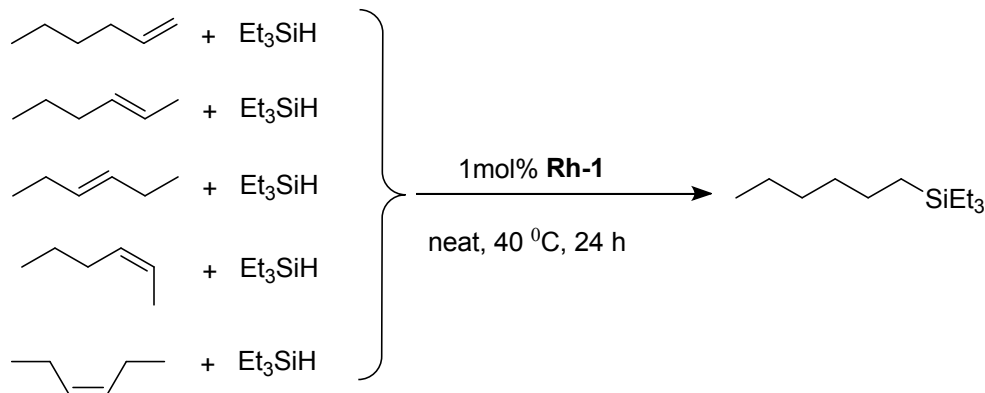
Table S6. Dehydrogenative silylation of aliphatic alkenes with Et₃SiH by using complex **Ir-1**



Entry	cat.	substrate	Solvent	T(°C)	t(h)	Conv. (%) ^a	A	B	C
1	Ir-1	1-Hexene	neat	40	24	100	85	15	-
2	Ir-1	<i>trans</i> -2-Hexene	neat	40	24	100	71	15	14
3	Ir-1	<i>trans</i> -3-Hexene	neat	40	24	100	67	16	17
4	Ir-1	<i>cis</i> -2-Hexene	neat	40	24	100	70	16	14
5	Ir-1	<i>cis</i> -3-Hexene	neat	40	24	100	52	11	37
6	Ir-1	1-Octene	neat	40	24	100	52	8	40
7	Ir-1	Allyl benzene	neat	40	24	100*	70	-	-

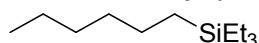
* Conversion to other unidentified products

¹H NMR spectra of the purified catalytic reactions were obtained showing conversion to the same product from the different hexene isomers.



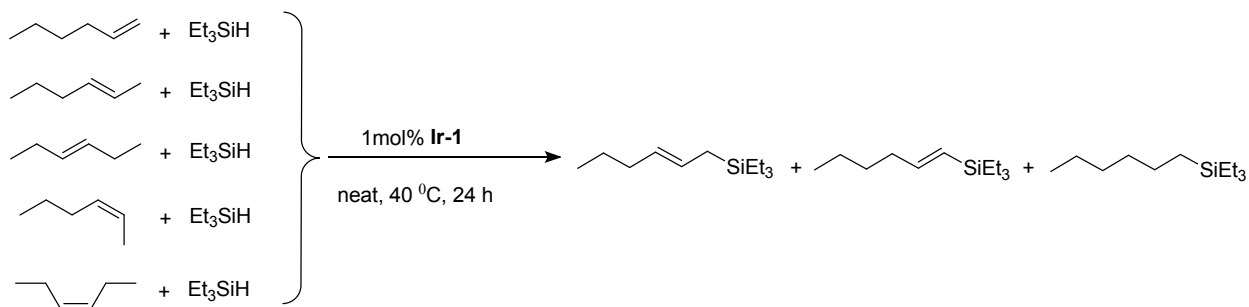
For example, from the hydrosilylation of 1-hexene in the presence of Et_3SiH using **Rh-1** as the catalyst, triethylhexylsilane (c) was obtained

5.2.1 Triethyl(hexyl)silane (c)



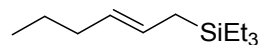
$^1\text{H NMR}$ (500 MHz, CDCl_3): δ 1.29 (m, 8H), 0.93 (t, $J = 7.9$ Hz, 9H), 0.89 (t, $J = 7.1$ Hz, 3H), 0.50 (q, $J = 8.0$ Hz, 8H) ppm. $^{13}\text{C}\{^1\text{H}\}$ NMR (125.76 MHz, CDCl_3): 33.80 (CH_2), 31.77 (CH_2), 23.99 (CH_2), 22.82 (CH_2), 14.31 (CH_3), 11.51 (CH_2), 7.63 ($\text{CH}_3\text{-SiEt}_3$), 3.52 ($\text{CH}_2\text{-SiEt}_3$) ppm. This compound has been previously characterized.⁵

5.3 Ir-1 catalysis of hexene isomers



Silane product obtained from the hydrosilylation of 1-hexene in the presence of Et₃SiH with **Ir-1** as the catalyst

5.3.1 Triethyl(hex-2-en-1-yl)silane (d)

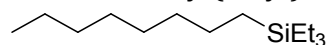


¹H NMR (500 MHz, CDCl₃): 5.38 (dt, *J* = 15.0 Hz, *J* = 7.2 Hz, 1H), 5.26 (dt, *J* = 15.0 Hz, *J* = 6.8 Hz, 1H), 1.99-1.93 (m, 2H), 1.45 (d, *J* = 7.8 Hz, 2H) 1.38-1.33 (m, 2H), 0.93 (t, *J* = 7.9 Hz, 9H), 0.88 (t, *J* = 7.3 Hz, 3H), 0.52 (q, *J* = 7.9 Hz, 6H) ppm. **¹³C{¹H} NMR (125.76 MHz, CDCl₃):** 128.6 (CH), 126.2 (CH) 34.9 (CH₂), 23.1 (CH₂), 17.3 (CH₂), 13.6 (CH₃), 7.3 (CH₃-SiEt₃), 3.1 (CH₂-SiEt₃) ppm. This compound has been previously characterized.⁵

5.3.2 General procedure for the hydrogenative silylation of other aliphatic alkenes

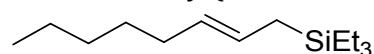
A 4 mL screw capped vial equipped with a magnetic stir bar was charged with the catalyst (**Rh-1**, **Ir-1**, 1 mol%), alkene (0.2 mmol), and Et₃SiH (0.2 mmol) under an argon atmosphere without any solvent. The resulted solution was stirred for 24 h at 40 °C. The catalytic conversions were monitored by GC-MS. ¹H NMR spectra of the purified product was obtained.

5.3.3 Triethyl(octyl)silane (e)



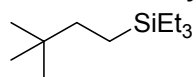
¹H NMR (500 MHz, CDCl₃): δ 1.28 (m, 12H), 0.92 (t, *J* 7.9 Hz, 9H), 0.88 (t, *J* 7.0 Hz, 3H), 0.50 (q, *J* 8.0 Hz, 8H) ppm. ¹³C{¹H} NMR (125.76 MHz, CDCl₃): 34.15 (CH₂), 32.14 (CH₂), 29.48 (CH₂), 24.03 (CH₂), 22.87 (CH₂), 14.28 (CH₃), 11.50 (CH₂), 7.63 (CH₃-SiEt₃), 3.52 (CH₂-SiEt₃) ppm. This compound has been previously characterized.⁵

5.3.4 Triethyl(oct-2-en-1-yl)silane (f)



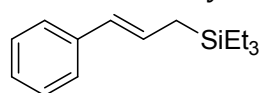
¹H NMR (500 MHz, CDCl₃): 5.37 (dt, *J* = 15.0 Hz, *J* = 7.0 Hz, 1H), 5.25 (dt, *J* = 15.0 Hz, *J* = 7.0 Hz, 1H), 1.99-1.93 (m, 2H), 1.44 (d, *J* = 7.9 Hz, 2H) 1.33-1.27 (m, 6H), 0.93 (t, *J* = 8.0 Hz, 9H), 0.88 (t, *J* = 6.8 Hz, 3H), 0.50 (q, *J* = 8.0 Hz, 6H) ppm. ¹³C{¹H} NMR (125.76 MHz, CDCl₃): 128.8 (CH), 126.0 (CH), 32.7 (CH₂), 31.3 (CH₂), 29.6 (CH₂), 22.5 (CH₂), 17.3 (CH₂), 14.1 (CH₃), 7.3 (CH₃-SiEt₃), 3.1 (CH₂-SiEt₃) ppm. This compound has been previously characterized.⁵

5.3.5 Triethyl(3,3-dimethylbutyl)silane (g)



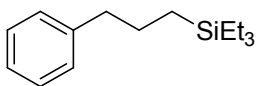
¹H NMR (500 MHz, CDCl₃): δ 1.14 (m, 2H), 0.93 (t, *J* = 7.9 Hz, 9H), 0.85 (s, 9H), 0.50 (q, *J* = 8.0 Hz, 6H), 0.44 (m, 2H) ppm. **¹³C{¹H} NMR (125.76 MHz, CDCl₃):** 37.93 (CH₂), 31.27 (C), 28.95 (CH₃), 7.62 (CH₃-SiEt₃), 5.21 (CH₂), 3.36 (CH₂-SiEt₃) ppm. This compound has been previously characterized.⁵

5.3.6 Cinnamyltriethylsilane (h)



¹H NMR (500 MHz, CDCl₃): δ 7.36 – 7.27 (m, 4H), 7.23 – 7.15 (m, 1H), 6.34 – 6.22 (m, 2H), 1.74 (dd, *J* = 4.8, 2.1 Hz, 2H), 0.94 (t, *J* = 7.9 Hz, 9H), 0.53 (q, *J* = 7.9 Hz, 6H) ppm. **¹³C{¹H} NMR (125.76 MHz, CDCl₃):** 138.69 (C_{arom}), 128.58 (C_{arom}), 128.35 (C_{arom}), 128.18 (C_{arom}), 126.28 (CH), 125.60 (CH), 18.99 (CH₂), 7.60 (CH₃), 3.45 (CH₂) ppm. This compound has been previously characterized.⁶

5.3.7 Triethyl(3-phenylpropyl)silane (i)



¹H NMR (500 MHz, CDCl₃): δ 7.36 – 7.27 (m, 2H), 7.23 – 7.15 (m, 3H), 2.65 (t, *J* = 7.7 Hz, 2H), 1.68 – 1.61 (m, 2H), 1.00 (t, *J* = 7.9 Hz, 9H), 0.61 (q, *J* = 8.0 Hz, 8H) ppm. **¹³C{¹H} NMR (125.76 MHz, CDCl₃):** 142.90 (C_{arom}), 128.59 (C_{arom}), 128.21 (C_{arom}), 125.73 (C_{arom}), 40.40 (CH₂), 26.23 (CH₂), 11.49 (CH₂), 7.52 (CH₃), 3.40 (CH₂) ppm. This compound has been previously characterized.⁷

6 Catalytic studies on the reactions of other silanes with styrene and 1-hexene

A 4 mL screw capped vial equipped with a magnetic stir bar was charged with the catalyst (**Rh-1**, **Ir-1**, 1 mol%), styrene (0.2 mmol) or 1-hexene (0.2 mmol) and silanes (0.2 mmol) under an argon atmosphere followed by toluene (0.2 mL). The resulted solution was stirred for 24 h at 95 °C. The catalytic conversions were monitored by GC-MS and ¹H NMR of the purified compounds was obtained.

Table S7. Hydrosilylation of styrene and 1-hexene with different silanes by using **Rh-1** complex

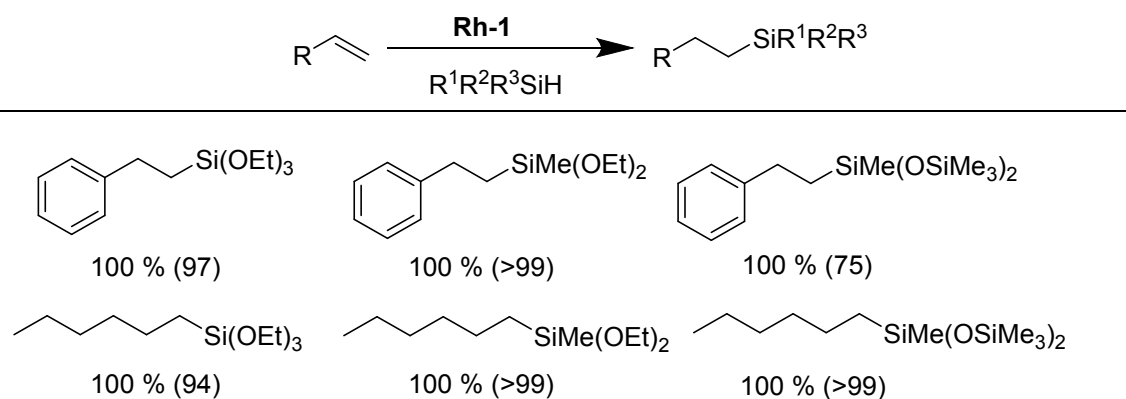
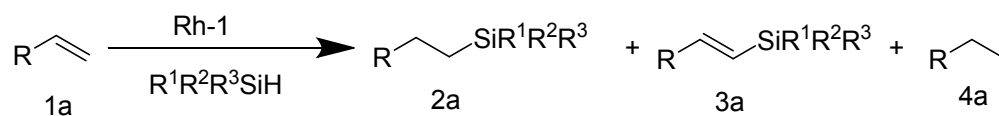


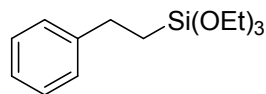
Table S8. Hydrosilylation of styrene and 1-hexene with different silanes by using **Rh-1** complex

Entry	Substrate	Silane	Solvent	T(°C)	t(h)	Conversion (%) ^a	2a/3a	2a	3a	4a
1	Styrene	(OEt) ₃ SiH	Toluene	95	24	100	97/3	93	3	4
2	1-hexene	(OEt) ₃ SiH	Toluene	95	24	100		94	-	Other hexene isomers
3	Styrene	(OEt) ₂ MeSiH	Toluene	95	24	100	99/1	97	0.9	2.1
4	1-hexene	(OEt) ₂ MeSiH	Toluene	95	24	100		>99	-	-
5	Styrene	SiMe(OTMS) ₂ H	Toluene	95	24	100	75/25	70	23	7
6	1-hexene	SiMe(OTMS) ₂ H	Toluene	95	24	100		>99	-	-

Reaction conditions: Substrate (0.2mmol), silane (0.2 mmol), **Rh-1** (1 mol %), toluene (0.2 mL), 95 °C, 24 h. ^aThe conversion and selectivity were determined by GC-MS and ¹H NMR.

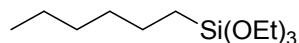
6.1 Characterization of silane products

6.1.1 Triethoxy(2-phenylethyl)silane (j)



¹H NMR (500 MHz, CDCl₃): δ 7.29 (t, *J* 7.4 Hz, 2H), 7.25 – 7.16 (m, 3H), 3.85 (q, *J* = 7.0 Hz, 6H), 2.82 – 2.69 (m, 2H), 1.26 (t, *J* = 7.0 Hz, 9H), 1.05 – 0.96 (m, 2H) ppm. ¹³C{¹H} NMR (125.76 MHz, CDCl₃): 144.73 (C_{arom}), 128.41 (2C_{arom}), 127.90 (2C_{arom}), 125.73 (C_{arom}), 58.51 (CH₂-Si(OEt)₂), 29.00 (CH₂), 18.43 (CH₃-Si(OEt)₃), 12.63 (CH₂) ppm. This compound has been previously characterized.⁸

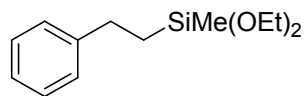
6.1.2 Triethoxy(hexyl)silane (k)



¹H NMR (500 MHz, CDCl₃): δ 3.81 (q, *J* = 7.9 Hz, 6H), 1.39 (m, 2H), 1.29 (m, 6H), 1.22 (t, *J* = 7.0 Hz, 9H), 0.89 (t, *J* = 6.7 Hz, 3H), 0.62 (m, 2H) ppm. ¹³C{¹H} NMR (125.76 MHz, CDCl₃): 58.42 (CH₂-

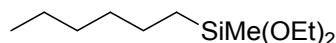
Si(OEt)₃, 33.02 (CH₂), 31.64 (CH₂), 22.87 (CH₂), 22.71 (CH₂), 18.43 (CH₃-Si(OEt)₃), 14.24 (CH₃), 10.54 (CH₂) ppm. This compound has been previously characterized.⁹

6.1.3 Diethoxy(methyl)(2-phenylethyl)silane (l)



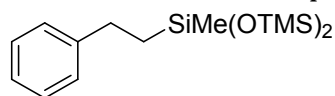
¹H NMR (500 MHz, CDCl₃): δ 7.33 – 7.29 (m, 2H), 7.27 – 7.23 (m, 2H), 7.22 – 7.18 (m, 1H), 3.82 (q, *J* = 7.0 Hz, 4H), 2.78 – 2.72 (m, 2H), 1.27 (t, *J* = 7.0 Hz, 6H), 1.07 – 1.02 (m, 2H), 0.16 (s, 3H) ppm. **¹³C{¹H} NMR (125.76 MHz, CDCl₃):** 144.76 (C_{arom}), 128.41 (2C_{arom}), 127.91 (2C_{arom}), 125.71 (C_{arom}), 58.26 (Si(OCH₂CH₃)₂), 29.07 (CH₂), 18.54 (Si(OCH₂CH₃)₂), 15.95 (CH₂), -4.68 (CH₃) ppm.

6.1.4 Diethoxy(hexyl)(methyl)silane (m)



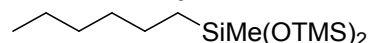
¹H NMR (500 MHz, CDCl₃): δ 3.76 (q, *J* = 7.0 Hz, 4H), 1.34 – 1.26 (m, 8H), 1.23 – 1.20 (m, 6H), 0.89 – 0.87 (m, 3H), 0.66 – 0.59 (m, 2H), 0.11 (s, 3H) ppm. **¹³C{¹H} NMR (125.76 MHz, CDCl₃):** 58.19 (CH₂-Si(OEt)₂), 33.14 (CH₂), 31.70 (CH₂), 22.73 (CH₂), 18.57 (CH₃-Si(OEt)₂), 14.28 (CH₃), 13.98 (CH₂), 2.01 (CH₂), -4.72 (CH₃) ppm.

6.1.5 1,1,1,3,5,5,5-heptamethyl-3-phenylethyltrisiloxane (n)



¹H NMR (500 MHz, CDCl₃): δ 7.33 (t, *J* = 7.6 Hz, 2H), 7.27 – 7.19 (m, 3H), 2.73 – 2.66 (m, 2H), 0.92 – 0.86 (m, 2H), 0.17 (s, 18H), 0.09 (s, 3H) ppm. **¹³C{¹H} NMR (125.76 MHz, CDCl₃):** 145.30 (C_{arom}), 128.44 (2C_{arom}), 127.94 (2C_{arom}), 125.63 (C_{arom}), 29.43 (CH₂), 19.90 (CH₂), 2.04 (CH₃-(OSi(Me)₃)₂), 0.16 (CH₃) ppm. This compound has been previously characterized.¹⁰

6.1.6 3-hexyl-1,1,1,3,5,5,5-heptamethyltrisiloxane (o)

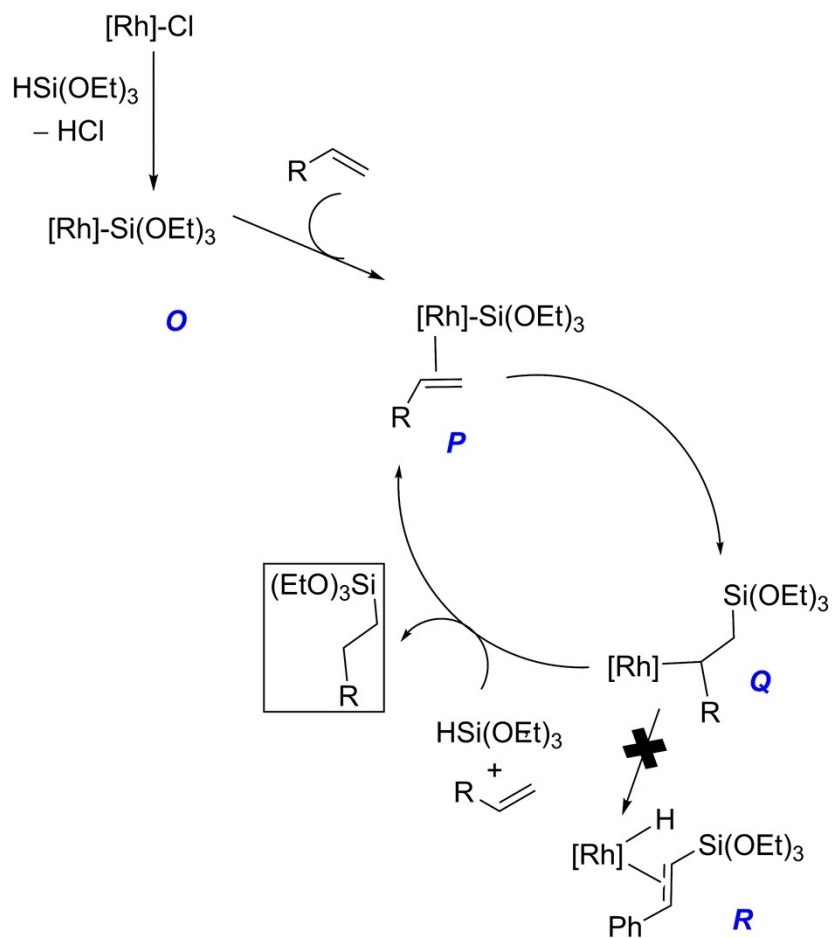


¹H NMR (500 MHz, CDCl₃): δ 1.30 (tdd, *J* = 9.6, 5.6, 3.2 Hz, 8H), 0.91 – 0.87 (m, 3H), 0.48 – 0.42 (m, 2H), 0.09 (s, 18H), 0.00 (s, 3H) ppm. **¹³C{¹H} NMR (125.76 MHz, CDCl₃):** 31.81 (CH₂), 31.73

(CH₂), 23.22 (CH₂), 22.79 (CH₂), 17.81 (CH₂), 14.30 (CH₃), 2.02 (CH₃-(OSi(Me)₃)₂), -0.10 (CH₃) ppm.

This compound has been previously characterized.¹¹

7 Mechanistic proposal for hydrosilylation/dehydrogenative silylation by Rh-1 with HSi(OEt)₃



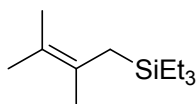
Scheme S2. The proposed mechanism for the catalysis of **Rh-1** with HSi(OEt)₃ shown in Table 6.

8 Hydrosilylation/dehydrogenative silylation of other substrates

8.1 General procedure for the catalytic reaction of 2,3-dimethyl-1,4-butadiene and Et₃SiH

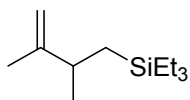
A 4 mL screw capped vial equipped with a magnetic stir bar was charged with the catalyst (**Rh-1**, **Ir-1**, 1 mol%), 2,3-dimethyl-1,4-butadiene (0.2 mmol) and Et₃SiH (0.2 mmol) under an argon atmosphere and performed the reaction under neat conditions. The resulted solution was stirred for 24 h at 60 °C. The catalytic conversions were monitored by GC-MS and ¹H NMR of the purified compounds was obtained.

8.1.1 (2,3-dimethylbut-2-en-1-yl)triethylsilane (p)



¹H NMR (500 MHz, CDCl₃): 1.63 (s, 6H), 1.61 (s, 3H), 1.53 (s, 2H), 0.94 (t, *J* = 7.9 Hz, 9H), 0.53 (q, *J* = 7.9 Hz, 9H), ppm. ¹³C{¹H} NMR (125.76 MHz, CDCl₃): 125.1 (C₂ alkene), 120.3 (C₃ alkene), 21.0 (CH₃), 20.9 (CH₃), 20.3 (CH₂), 7.3 (CH₃-SiEt₃), 4.1 (CH₂-SiEt₃) ppm. This compound has been previously characterized.¹²

8.1.2 (2,3-dimethylbut-3-en-1-yl)triethylsilane (q)



¹H NMR (300 MHz, CDCl₃): 4.74-4.73 (m, 1H), 4.63-4.62 (m, 1H), 2.41-2.34 (m, 1H), 1.72 (s, 3H), 1.07 (d, *J* = 6.8 Hz, 3H), 0.97 (t, *J* = 8.0 Hz, 9H), 0.65-0.53 (m, 8H) ppm. ¹³C{¹H} NMR (75 MHz, CDCl₃): 152.8 (C_{alkene}), 107.9 (CH₂ alkene), 37.2 (CH), 23.0 (CH₃), 18.6 (CH₃), 18.2 (CH₂), 7.4 (CH₃-SiEt₃), 3.8 (CH₂-SiEt₃) ppm. This compound has been previously characterized.¹²

9 NMR spectra

9.1 NMR spectra of a typical catalysis of styrene and Et₃SiH

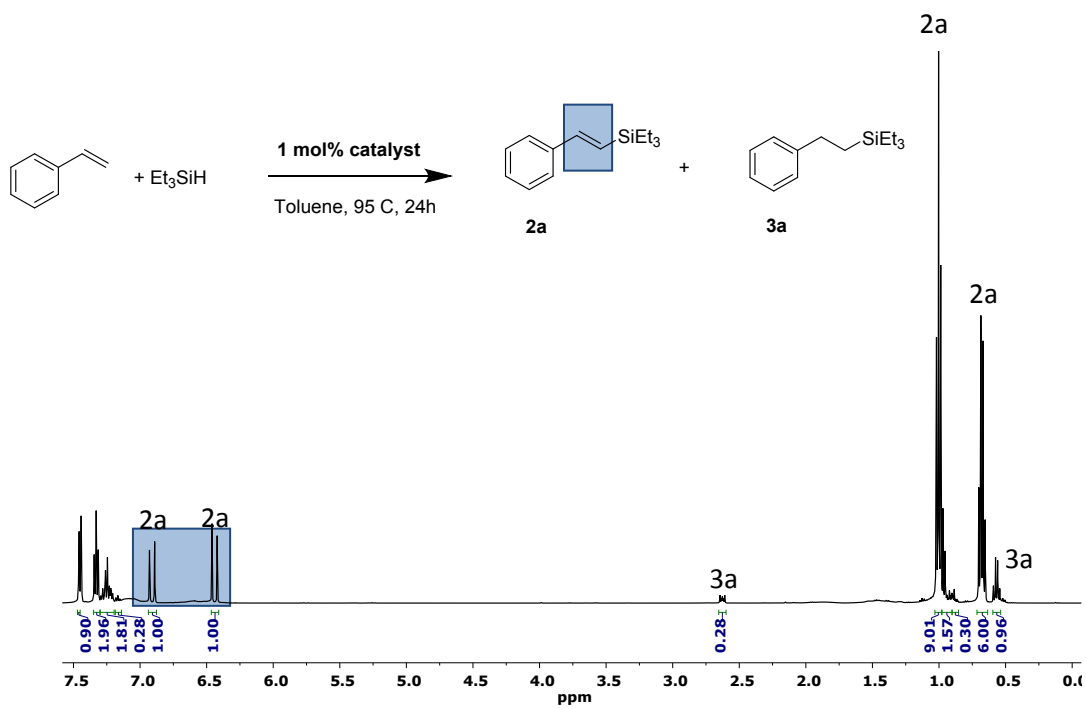


Figure S19. ¹H NMR spectrum (500 MHz, CDCl₃, 293 K) obtained for a catalysis with **Rh-1**.

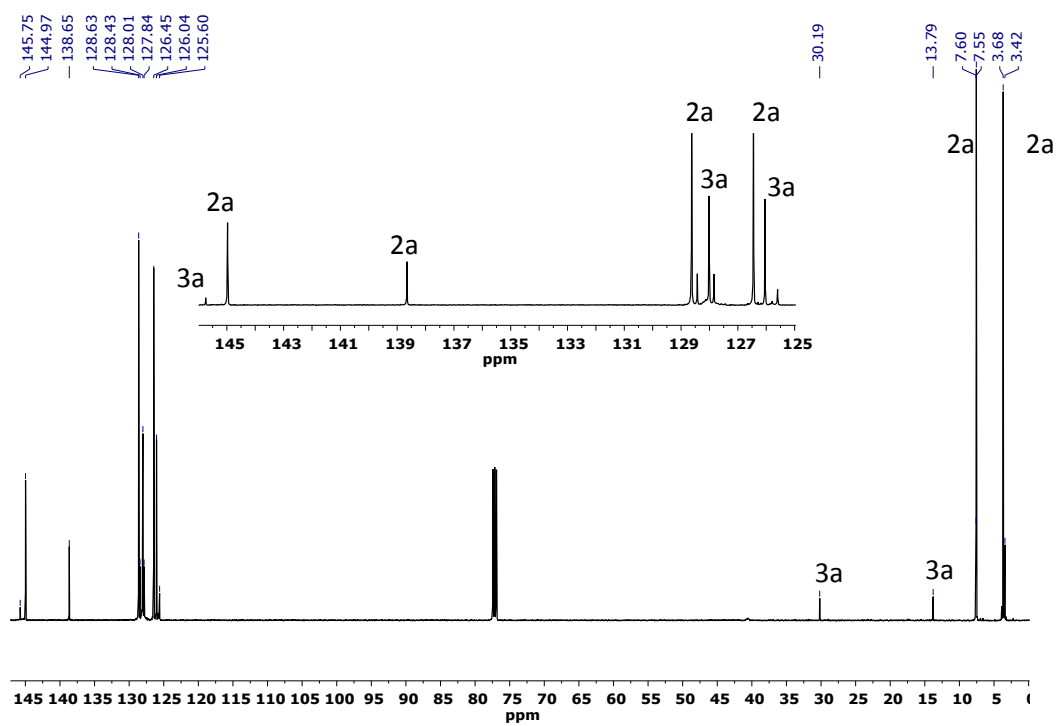


Figure S20. $^{13}\text{C}\{^1\text{H}\}$ NMR spectrum (125.76 MHz, CDCl_3 , 293 K) obtained for a catalysis with **Rh-1**.

9.2 NMR spectra of a typical hydrosilylation catalysis of 1-hexene with Et₃SiH

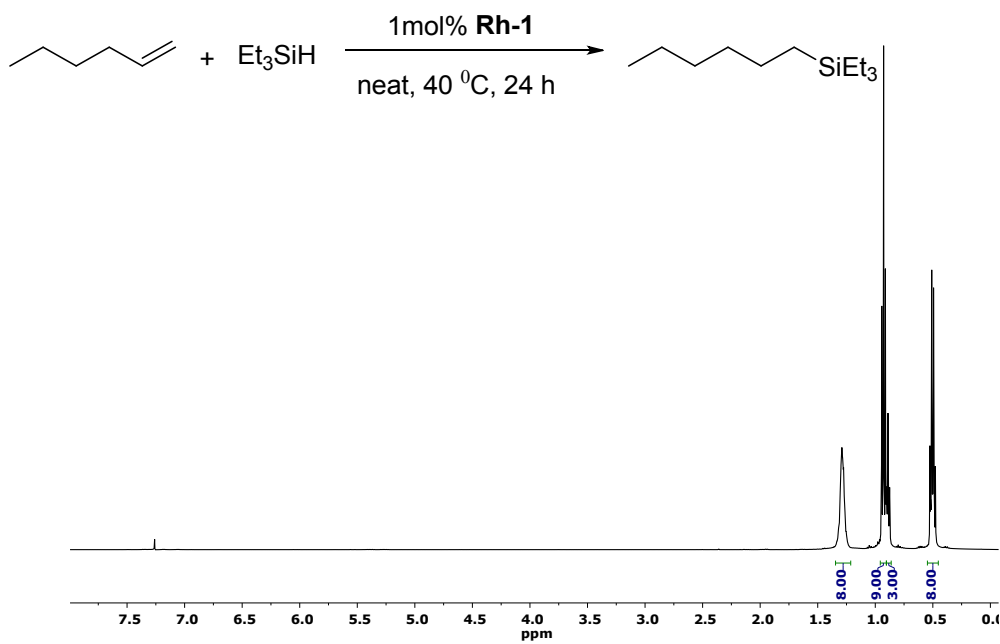


Figure S21. ¹H NMR spectrum (500 MHz, CDCl₃, 293 K) of a 1-hexene catalysis of Rh-1.

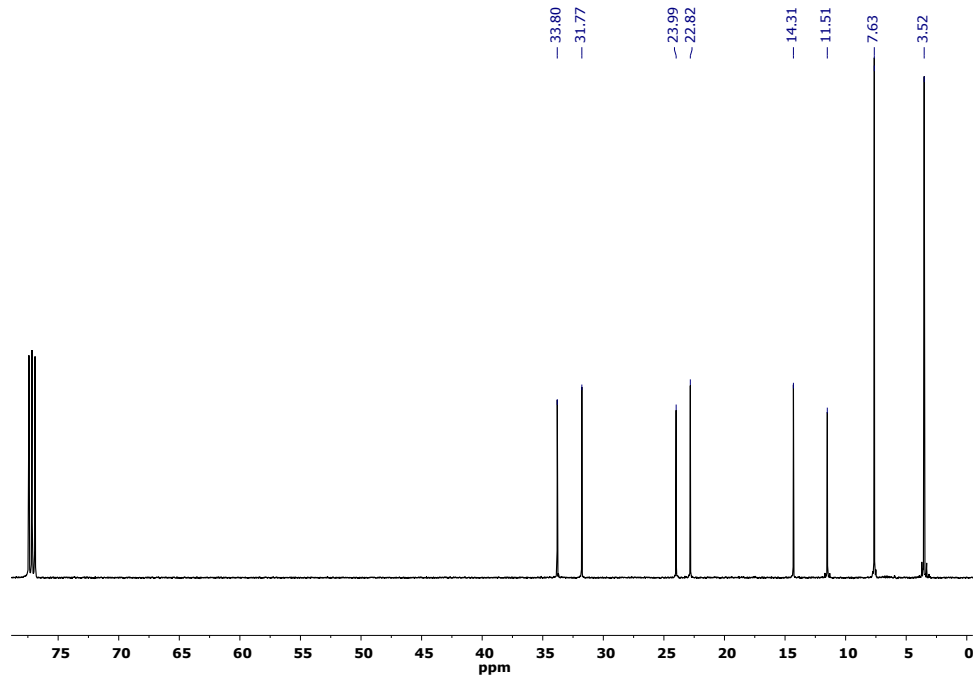
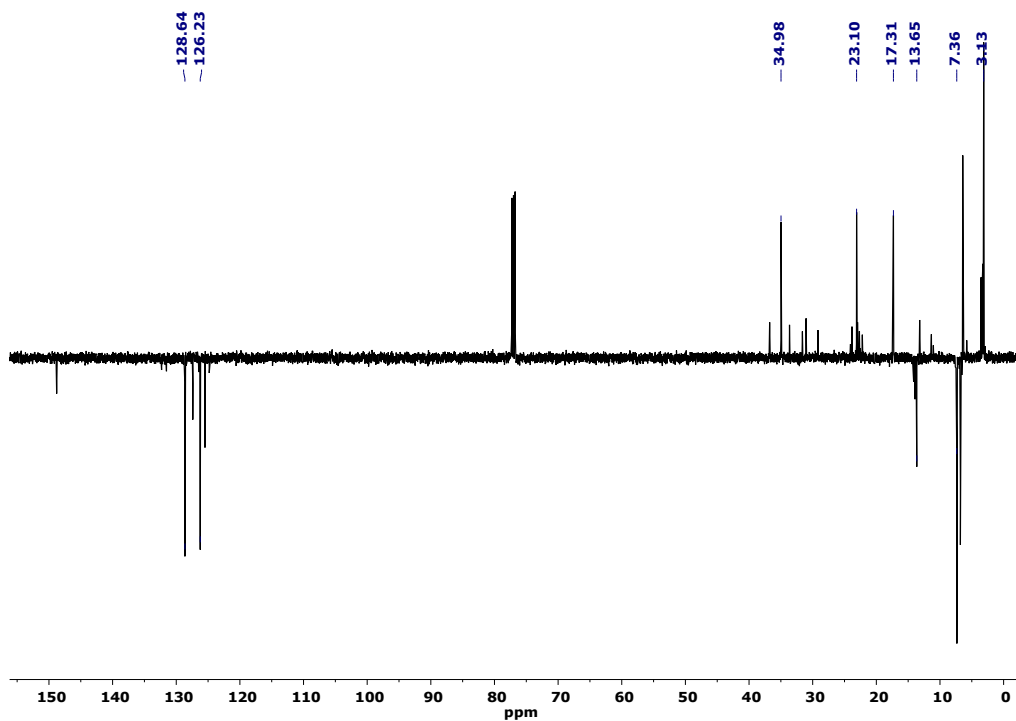
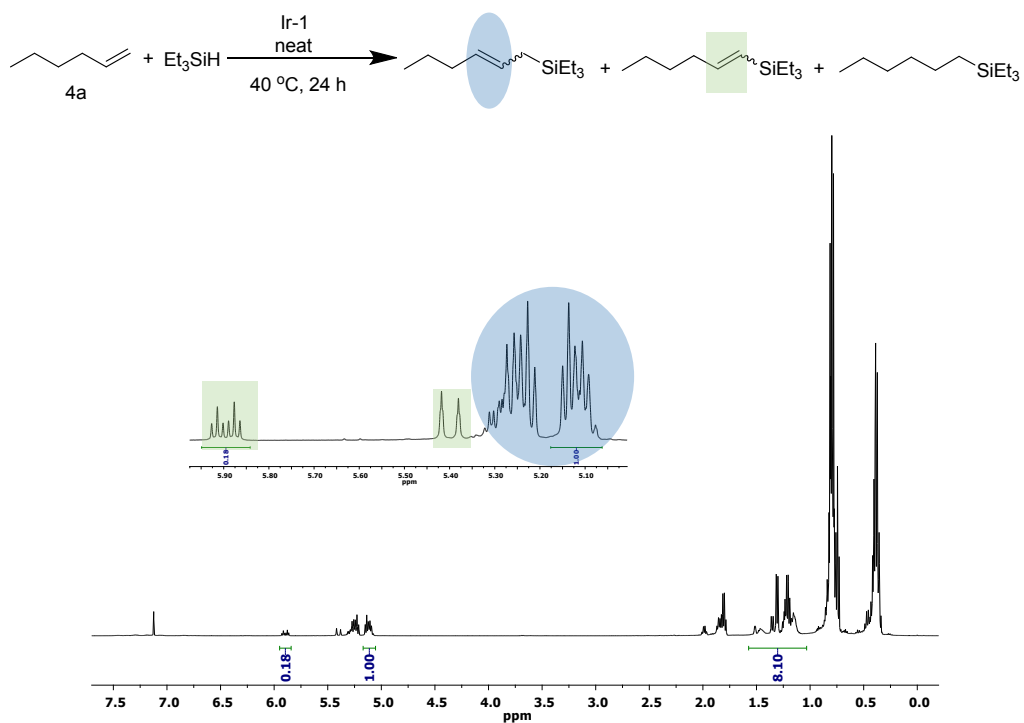


Figure S22. ¹³C{¹H} NMR spectrum (125.76 MHz, CDCl₃, 293 K).



9.3 NMR spectra of a typical hydrosilylation catalysis of t-2-hexene with Et₃SiH

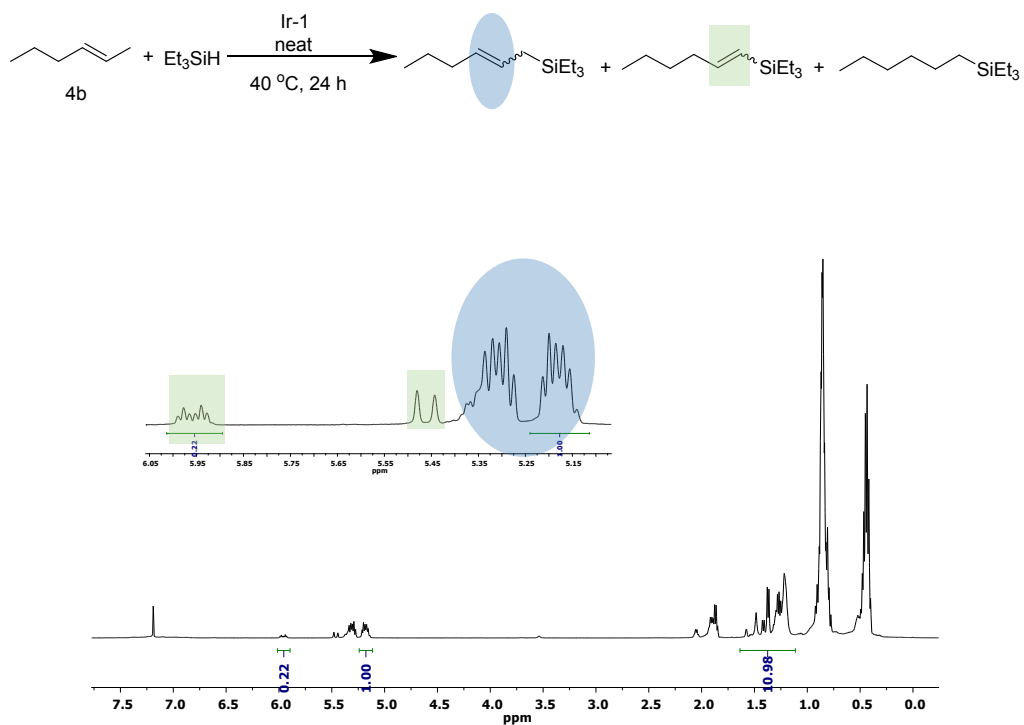


Figure S25. ¹H NMR spectrum (500 MHz, CDCl₃, 293 K).

9.4 NMR spectra of a typical hydrosilylation catalysis of t-3-hexene with Et₃SiH

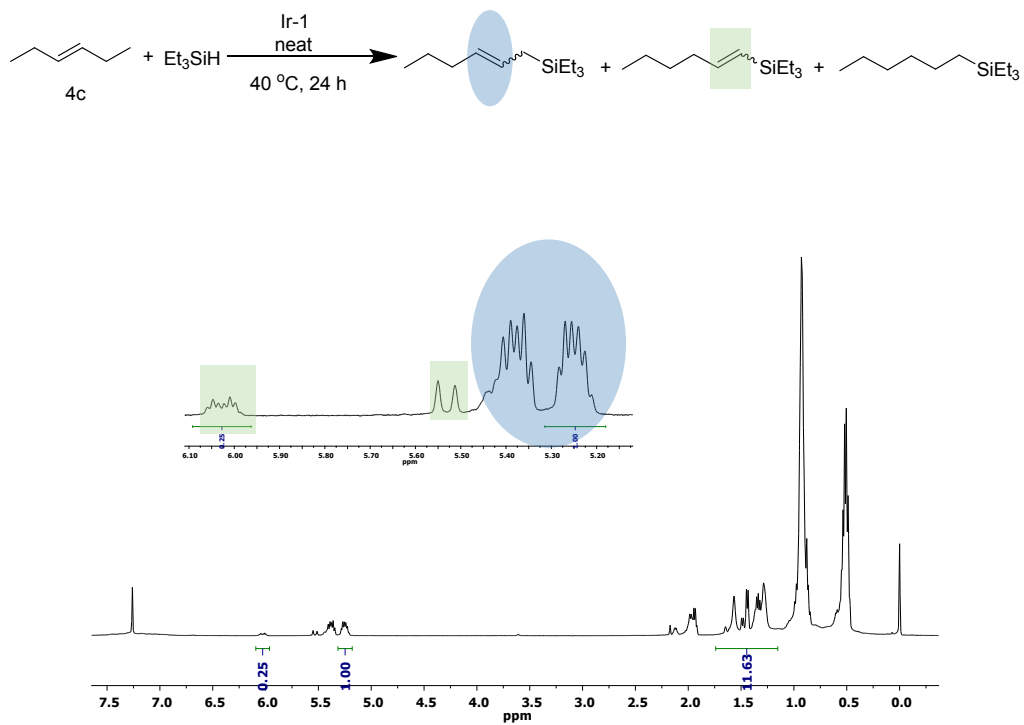


Figure S26. ¹H NMR spectrum (500 MHz, CDCl₃, 293 K).

9.5 NMR spectra of a typical hydrosilylation catalysis of c-2-hexene with Et₃SiH

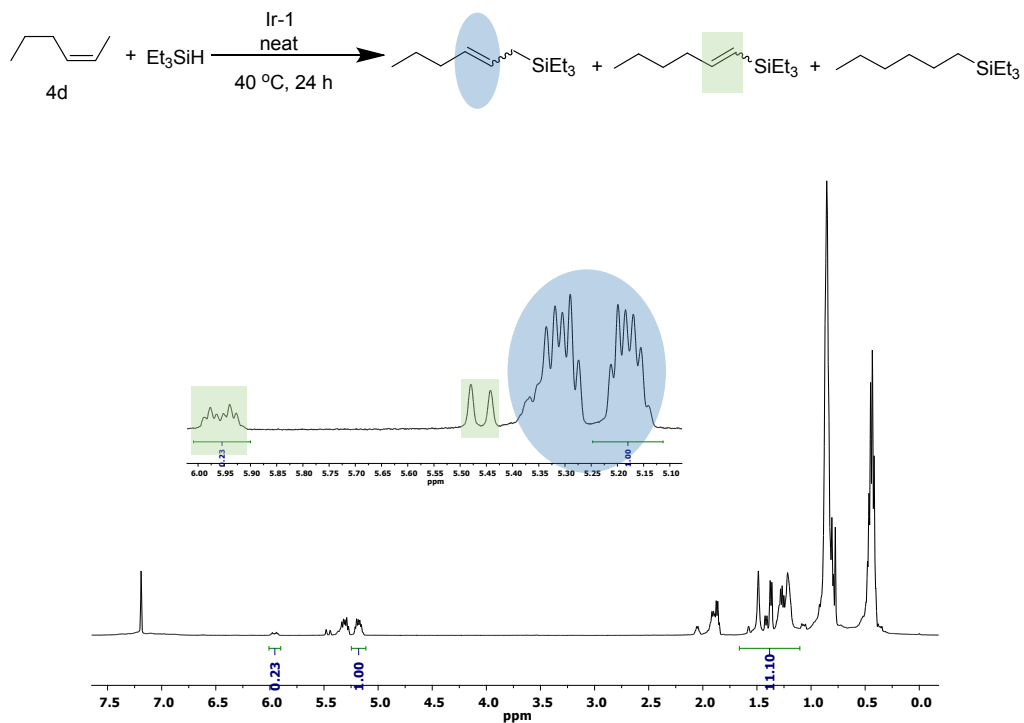


Figure S27. ¹H NMR spectrum (500 MHz, CDCl₃, 293 K).

9.6 NMR spectra of a typical hydrosilylation catalysis of c-3-hexene with Et₃SiH

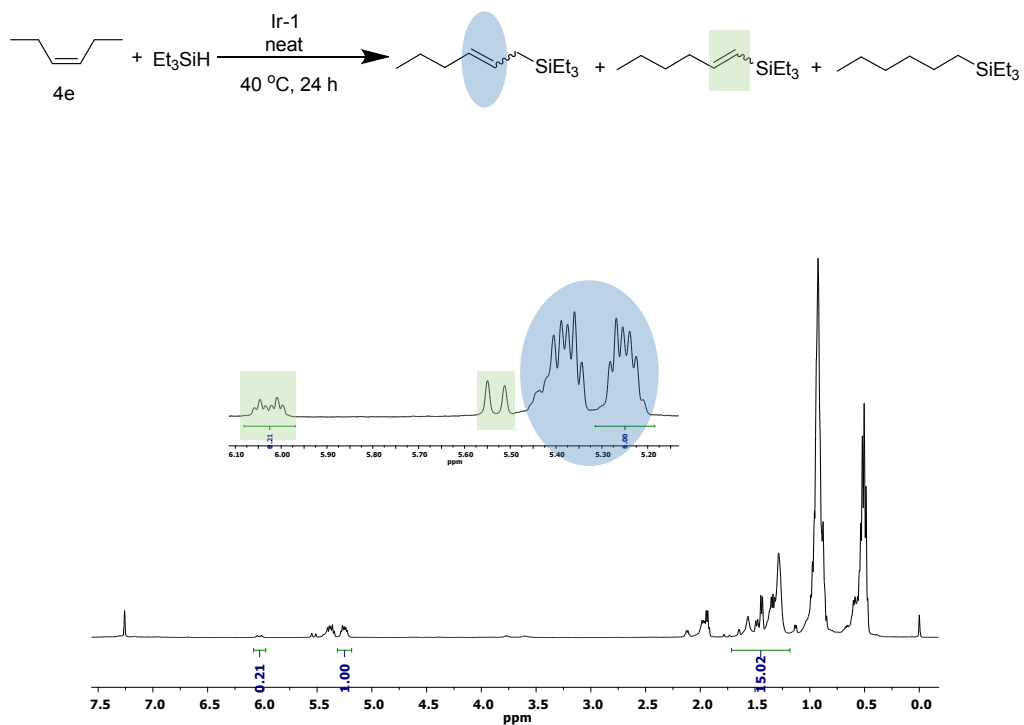


Figure S28. ¹H NMR spectrum (500 MHz, CDCl₃, 293 K).

9.7 NMR spectra of the catalytic hydrosilylation of 1-octene with Et_3SiH

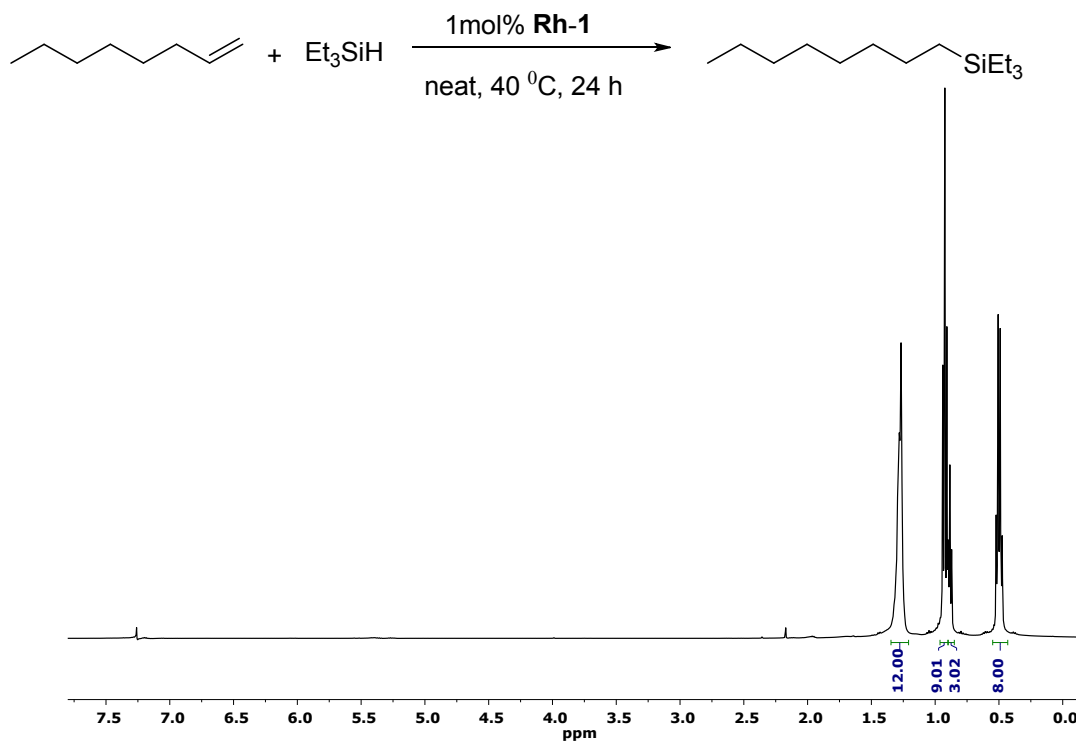


Figure S29. ^1H NMR spectrum (500 MHz, CDCl_3 , 293 K).

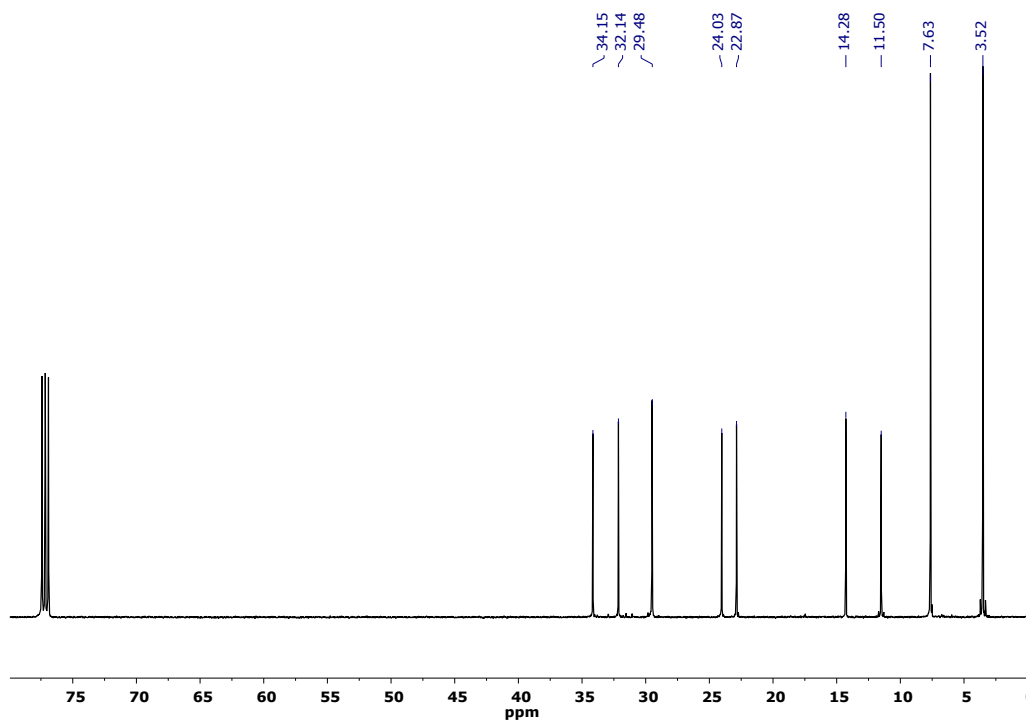


Figure S30. $^{13}\text{C}\{^1\text{H}\}$ NMR spectrum (125.76 MHz, CDCl_3 , 293 K).

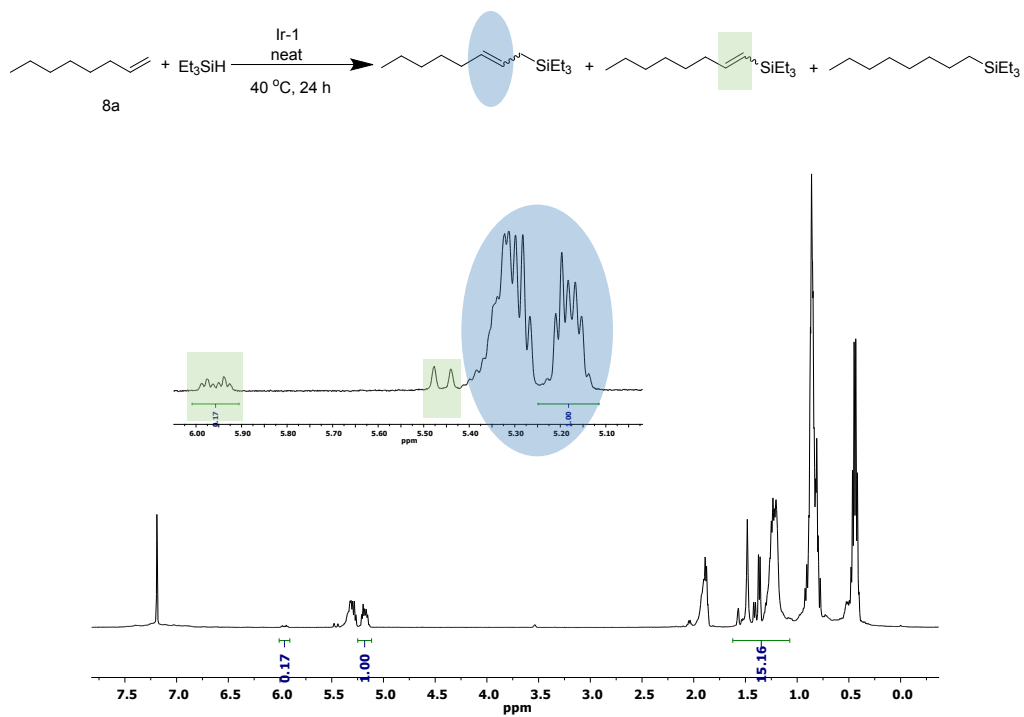


Figure S31. ^1H NMR spectrum (500 MHz, CDCl_3 , 293 K).

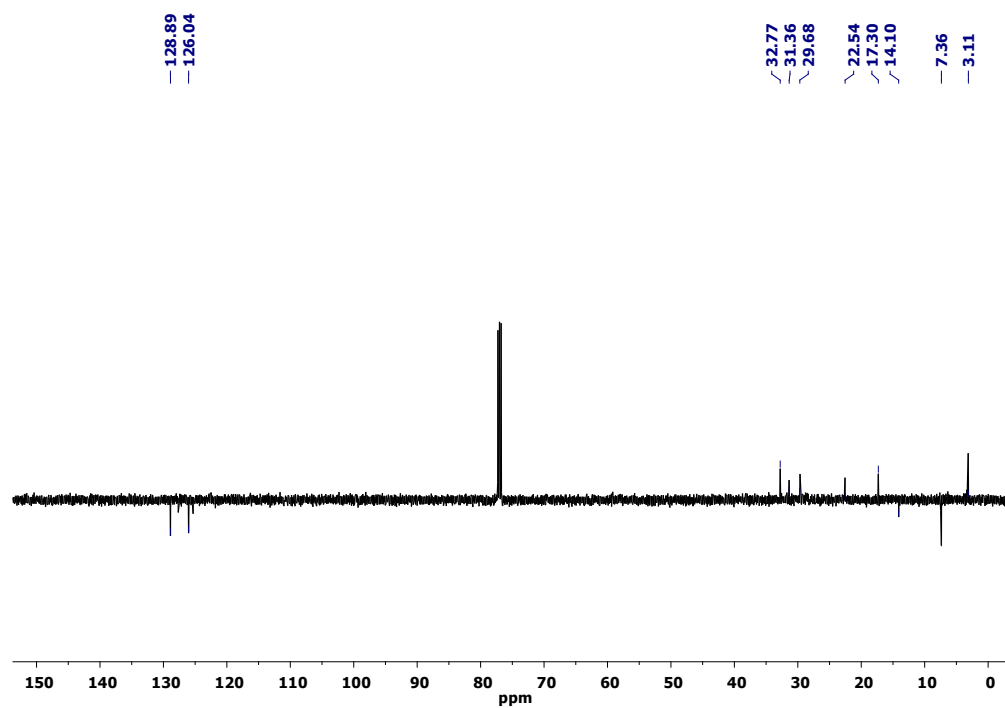


Figure S32. $^{13}\text{C}\{^1\text{H}\}$ APT NMR spectrum (125.76 MHz, CDCl_3 , 293 K).

9.8 NMR spectra of the catalytic hydrosilylation of 3,3-dimethyl-1-butene with Et_3SiH

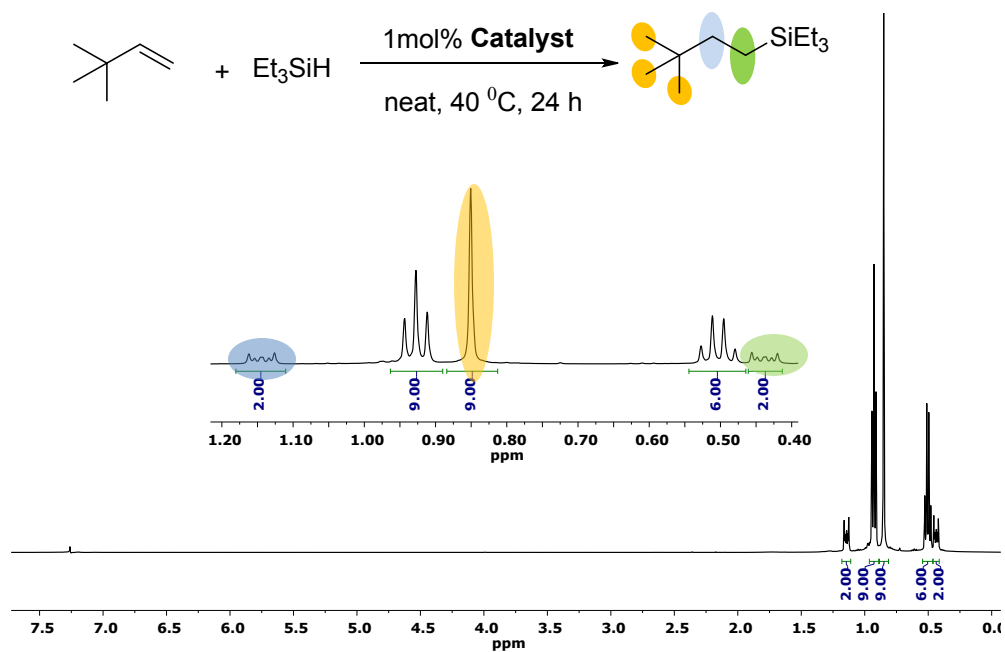


Figure S33. ^1H NMR spectrum (500 MHz, CDCl_3 , 293 K) obtained using **Rh-1** as catalyst.

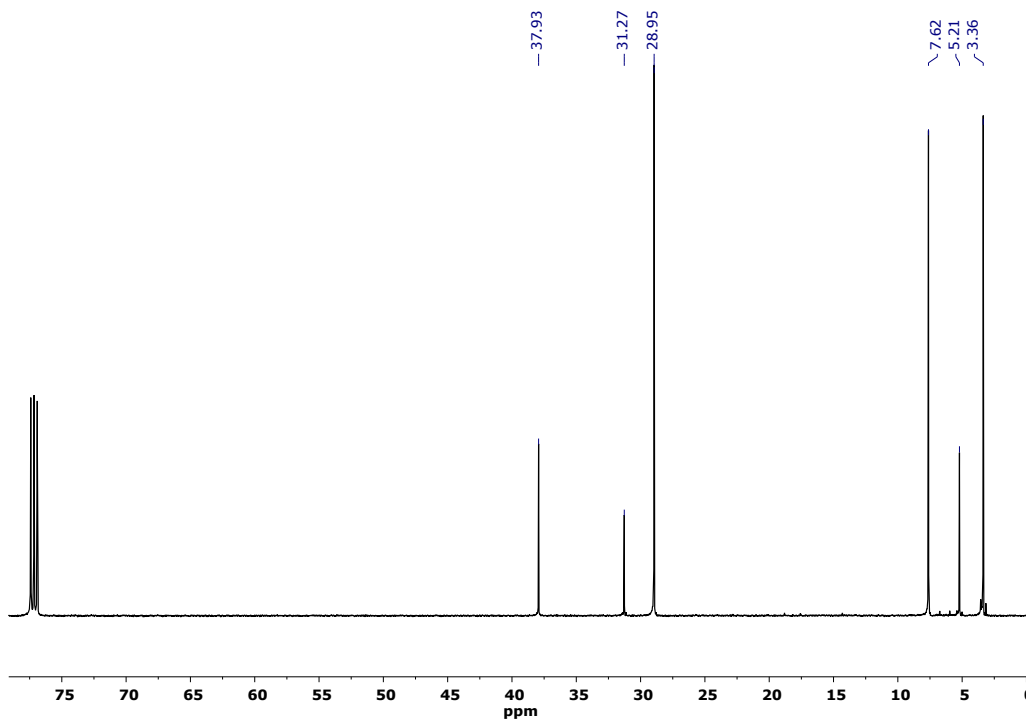


Figure S34. $^{13}\text{C}\{^1\text{H}\}$ NMR spectrum (125.76 MHz, CDCl_3 , 293 K) obtained for **Rh-1** catalyst.

9.9 NMR spectra of the catalytic hydrosilylation of allylbenzene with Et₃SiH

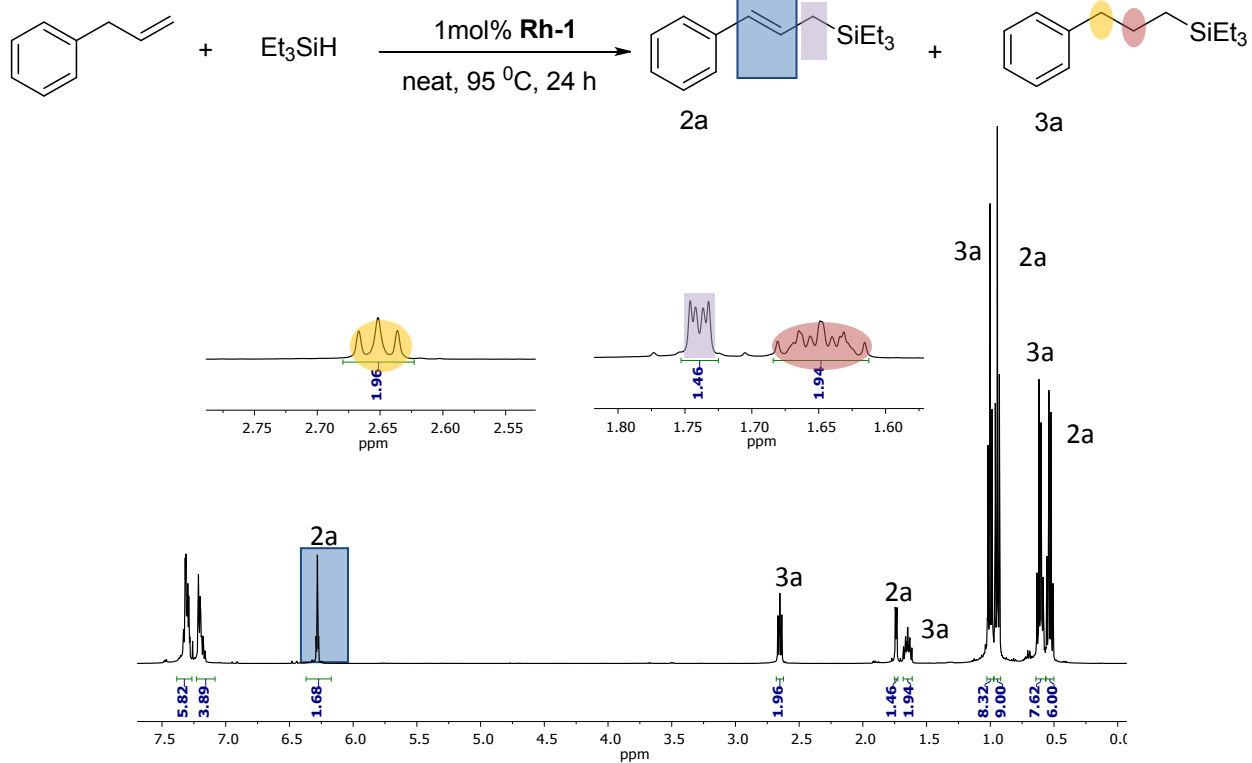


Figure S35. ¹H NMR spectrum (500 MHz, CDCl₃, 293 K).

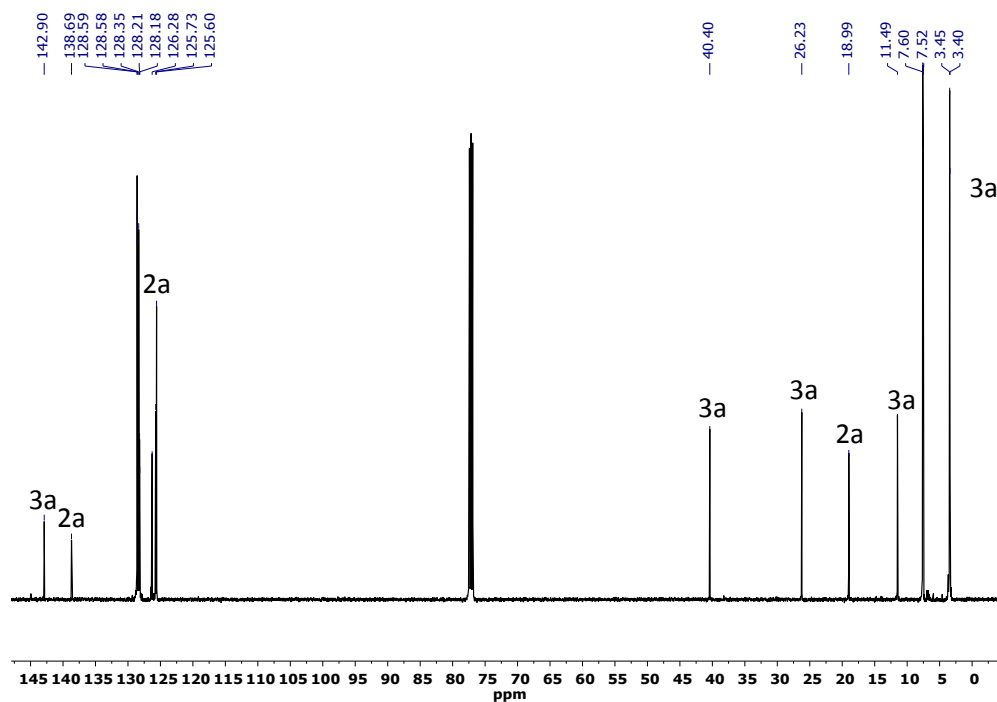


Figure S36. ¹³C{¹H} NMR spectrum (125.76 MHz, CDCl₃, 293 K).

9.10 NMR spectra of the catalytic hydrosilylation of styrene with $(\text{EtO})_3\text{SiH}$

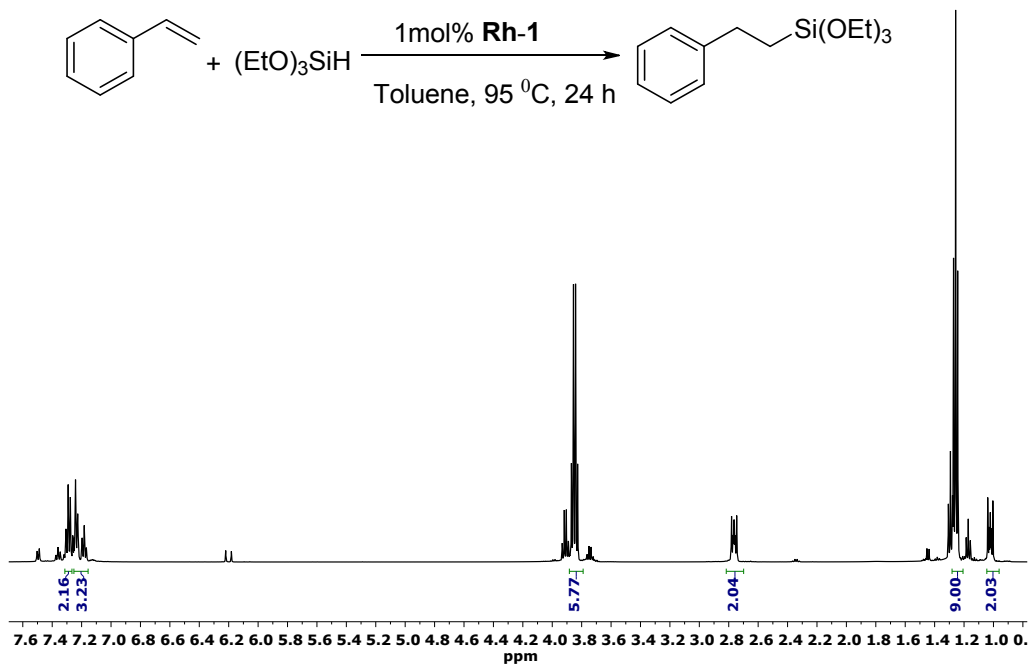
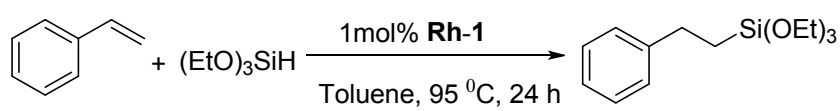


Figure S37. ^1H NMR spectrum (500 MHz, CDCl_3 , 293 K)

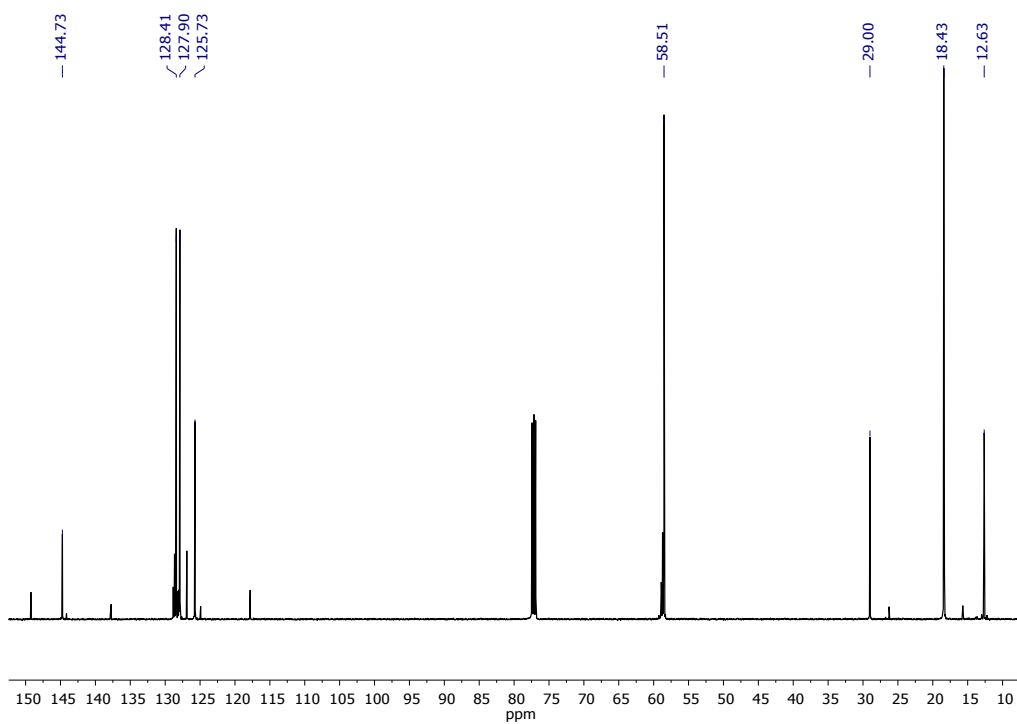


Figure S38. $^{13}\text{C}\{^1\text{H}\}$ NMR spectrum (125.76 MHz, CDCl_3 , 293 K)

9.11 NMR spectra of the catalytic hydrosilylation of 1-hexene with $(\text{EtO})_3\text{SiH}$

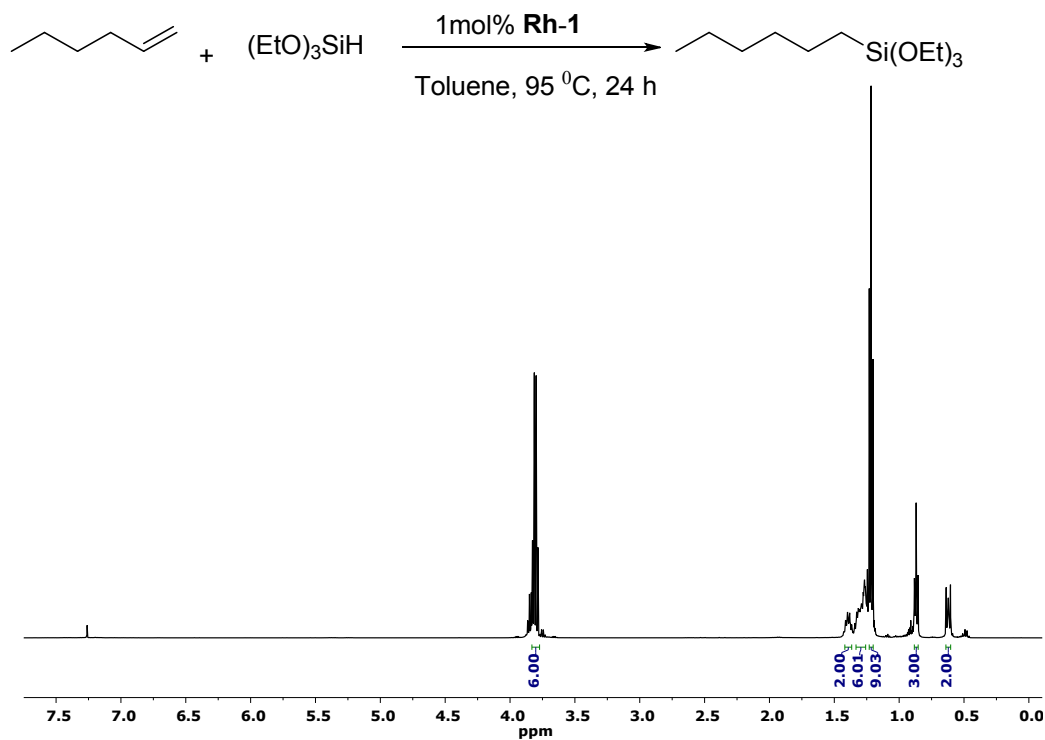


Figure S39. ^1H NMR spectrum (500 MHz, CDCl_3 , 293 K) 1-

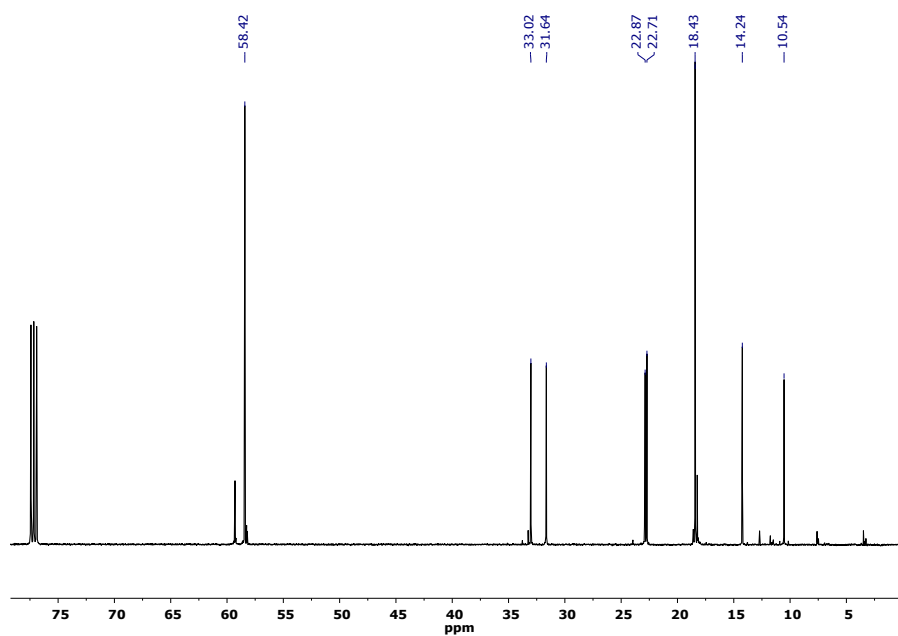


Figure S40. $^{13}\text{C}\{^1\text{H}\}$ NMR spectrum (125.76 MHz, CDCl_3 , 298 K)

9.12 NMR spectra of the catalytic hydrosilylation of styrene with $(\text{EtO})_2\text{MeSiH}$

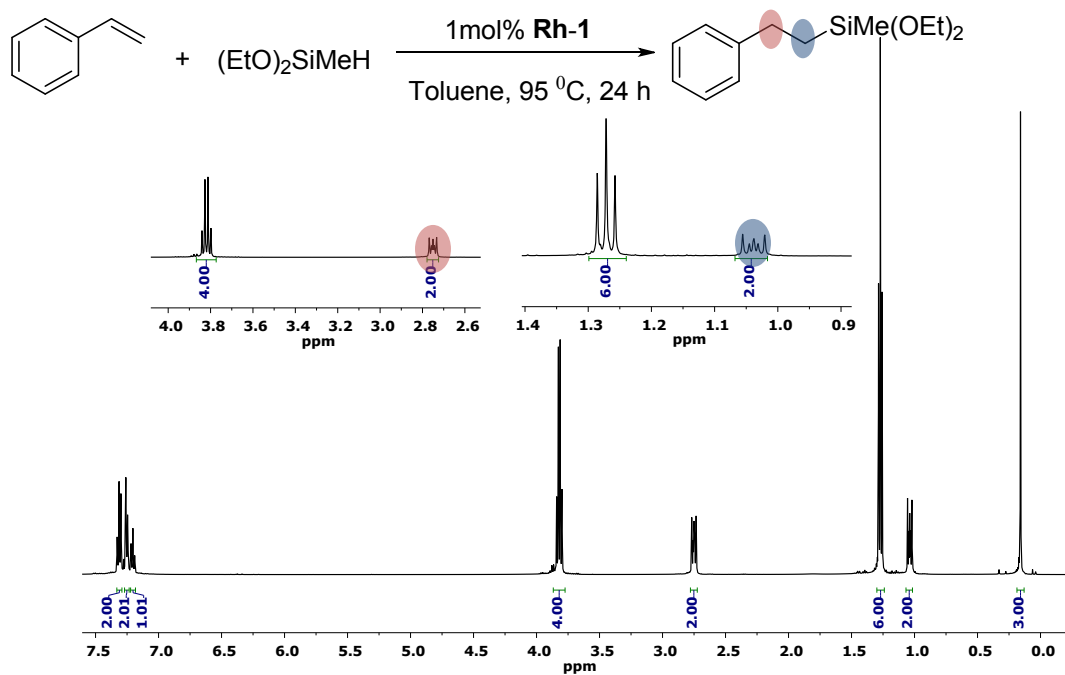


Figure S41. ^1H NMR spectrum (500 MHz, CDCl_3 , 293 K) Styrene

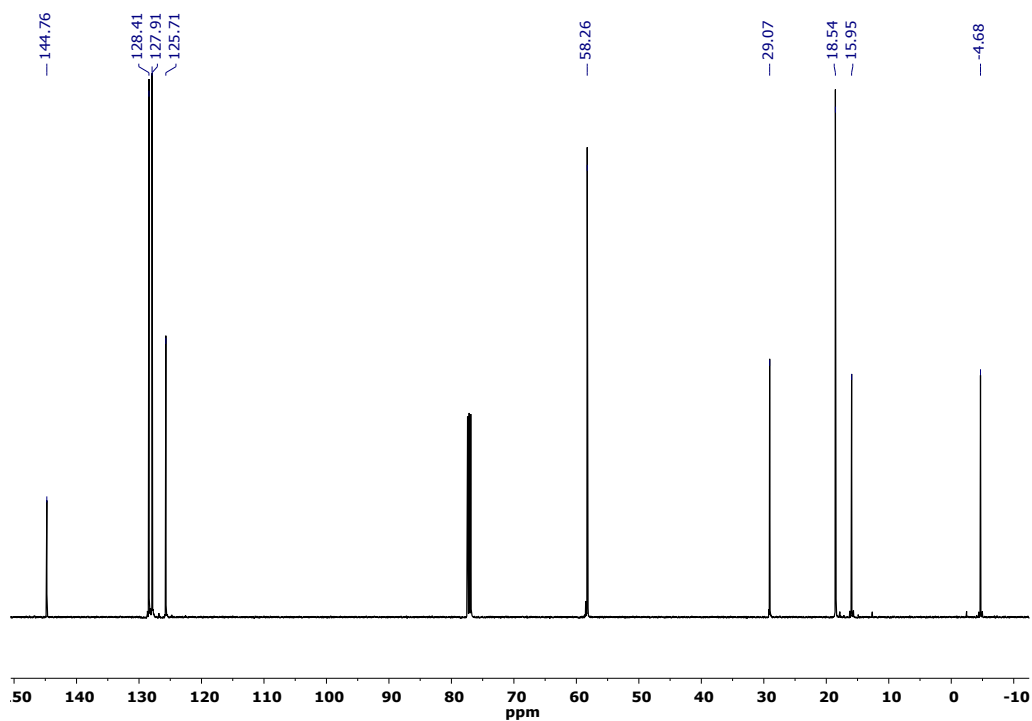


Figure S42. $^{13}\text{C}\{^1\text{H}\}$ NMR spectrum (125.76 MHz, CDCl_3 , 293 K) Styrene

9.13 NMR spectra of catalytic hydrosilylation of 1-hexene with (EtO)₂MeSiH

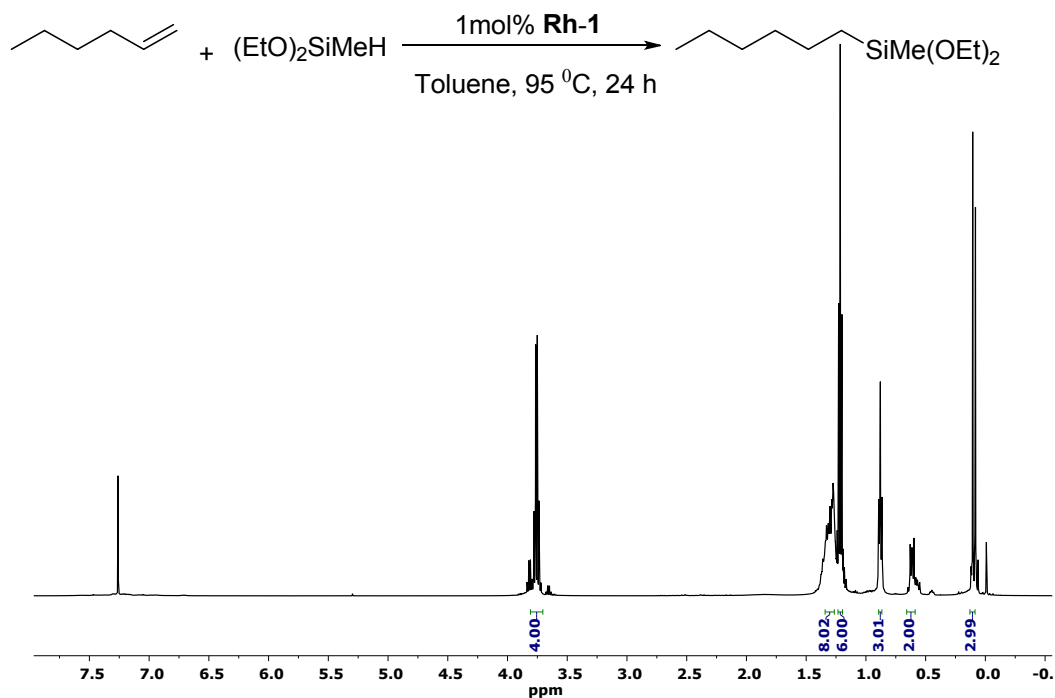


Figure S43. ¹H NMR spectrum (500 MHz, CDCl₃, 293 K)

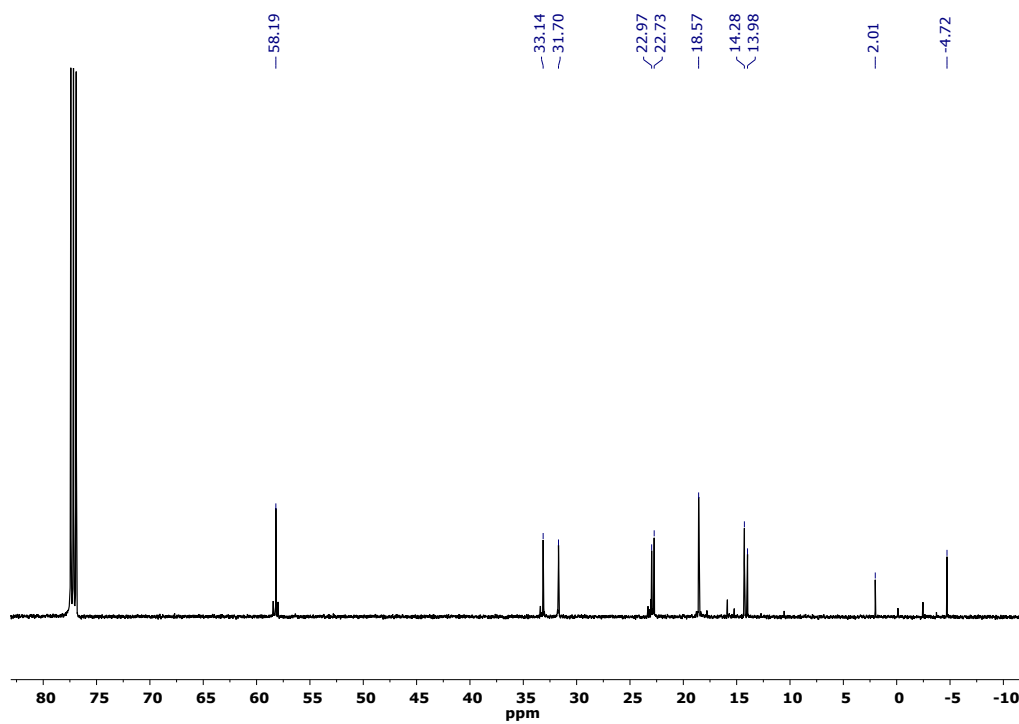


Figure S44. ¹³C{¹H} NMR spectrum (125.76 MHz, CDCl₃, 293 K)

9.14 NMR spectra of catalytic hydrosilylation of styrene with $(\text{Me}_3\text{SiO})_2\text{SiMeH}$

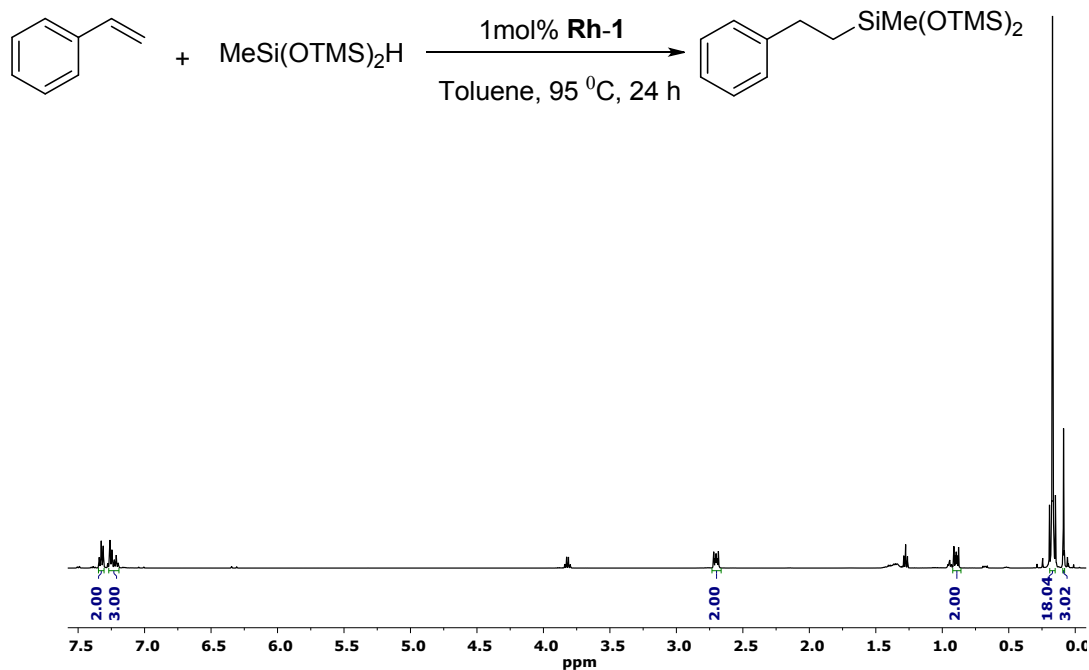


Figure S45. ^1H NMR spectrum (500 MHz, CDCl_3 , 293 K) Styrene

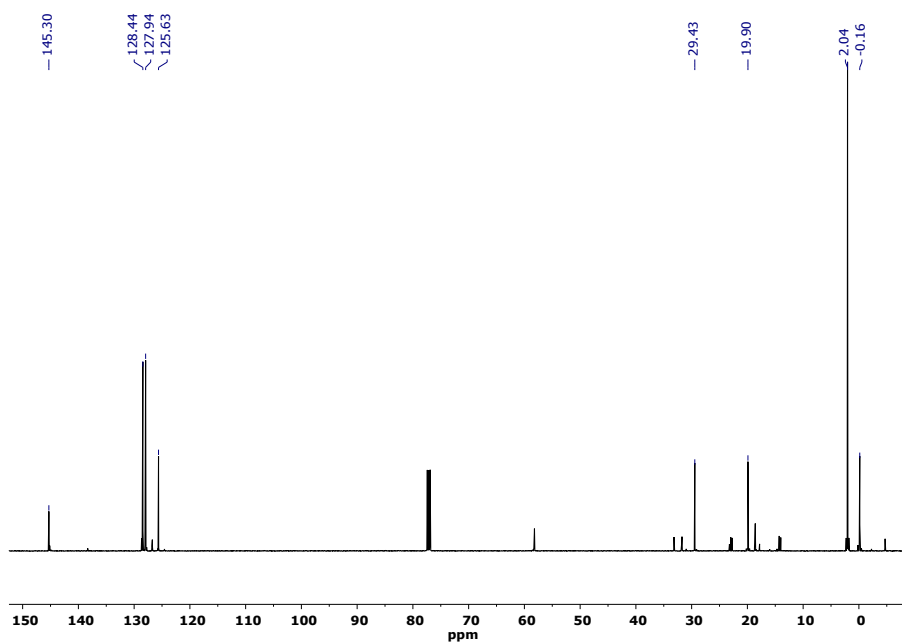


Figure S46. $^{13}\text{C}\{^1\text{H}\}$ NMR spectrum (125.76 MHz, CDCl_3 , 293 K) Styrene

9.15 NMR spectra of catalytic hydrosilylation of 1-hexene with $(\text{Me}_3\text{SiO})_2\text{SiMeH}$

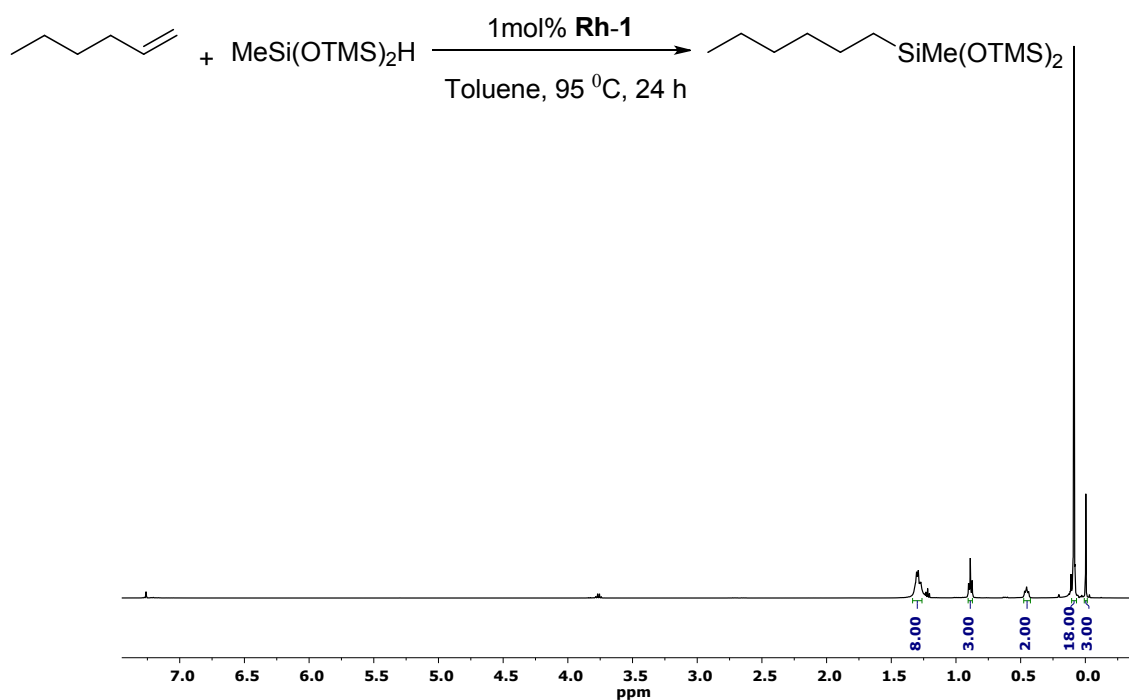


Figure S47. ^1H NMR spectrum (500 MHz, CDCl_3 , 293 K) 1-hexene

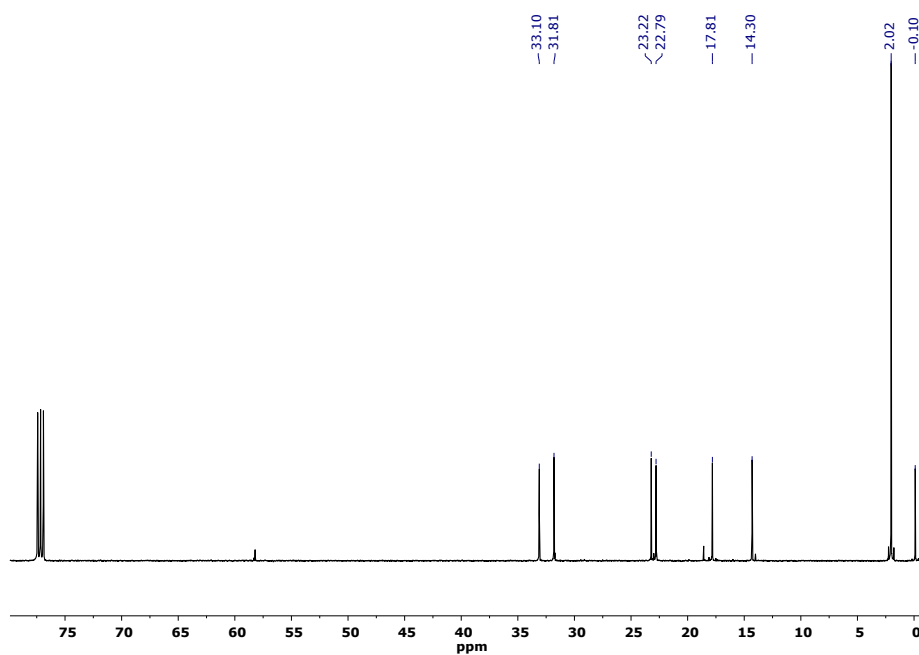


Figure S48. $^{13}\text{C}\{^1\text{H}\}$ NMR spectrum (125.76 MHz, CDCl_3 , 293 K) 1-hexene

9.16 NMR spectra of the catalysis of 2,3-dimethyl-1,4-butadiene with Et_3SiH

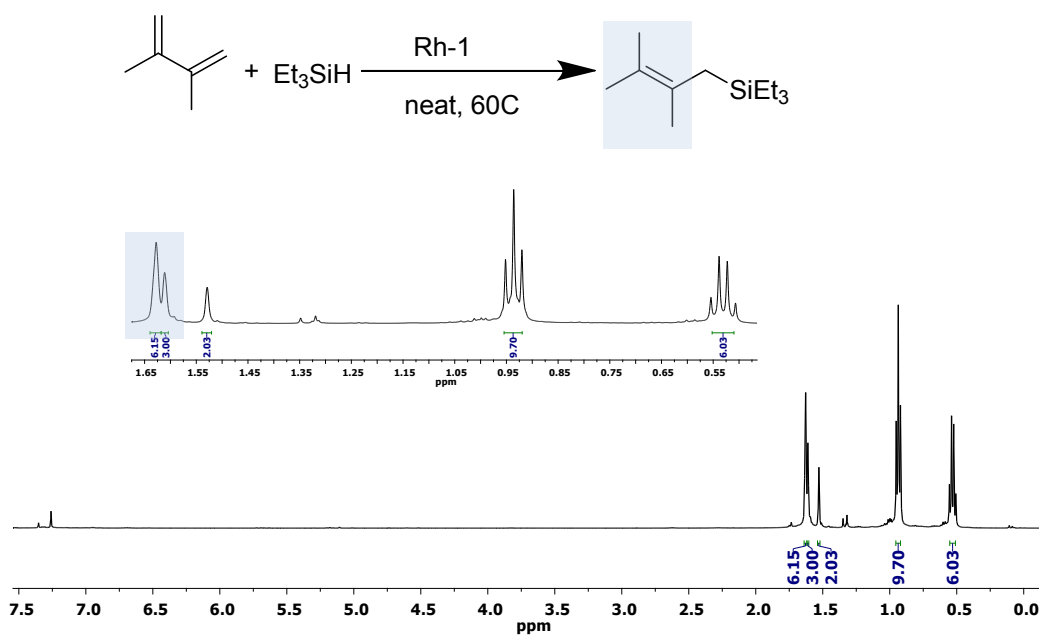


Figure S49. ^1H NMR spectrum (500 MHz, CDCl_3 , 293 K).

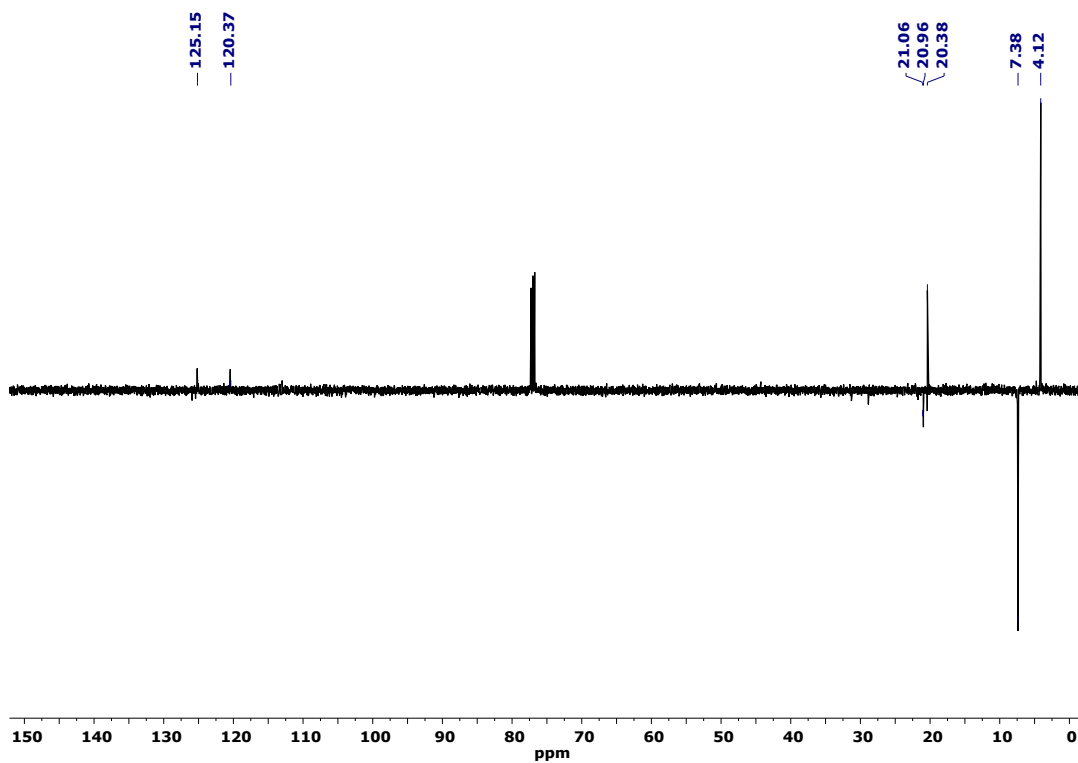


Figure S50. $^{13}\text{C}\{^1\text{H}\}$ APT NMR spectrum (125.76 MHz, CDCl_3 , 293 K).

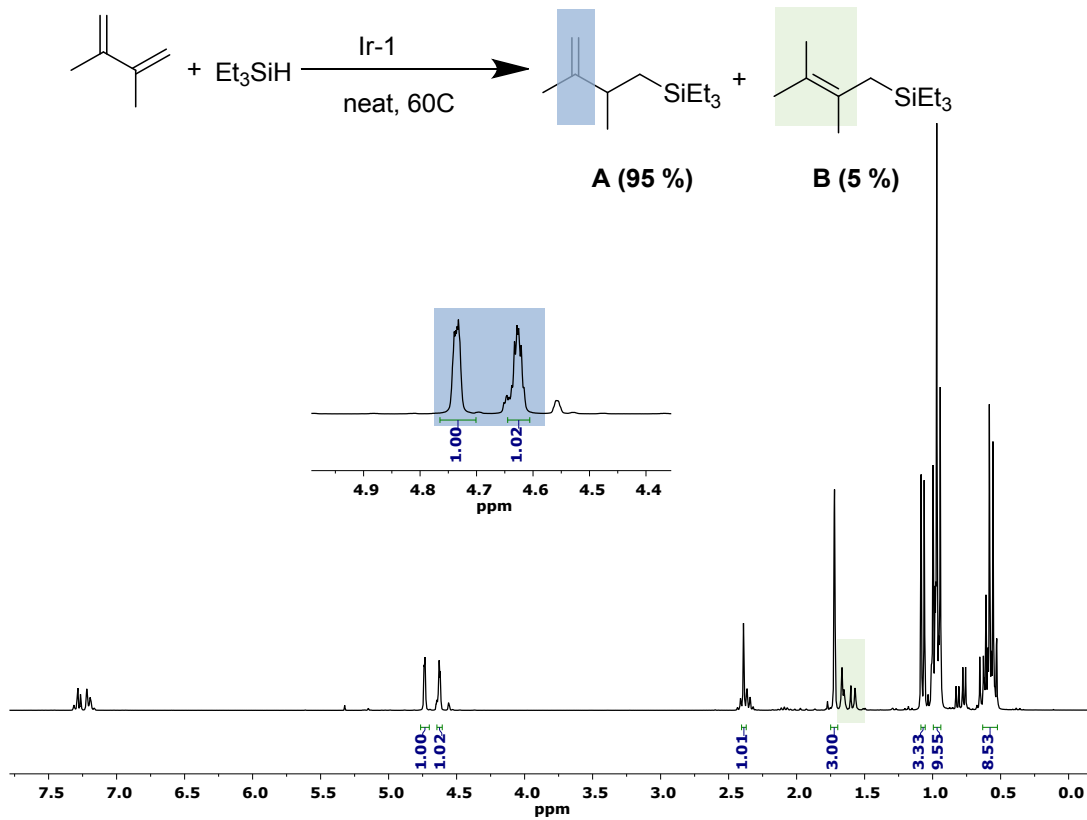


Figure S49. ^1H NMR spectrum (500 MHz, CDCl_3 , 293 K).

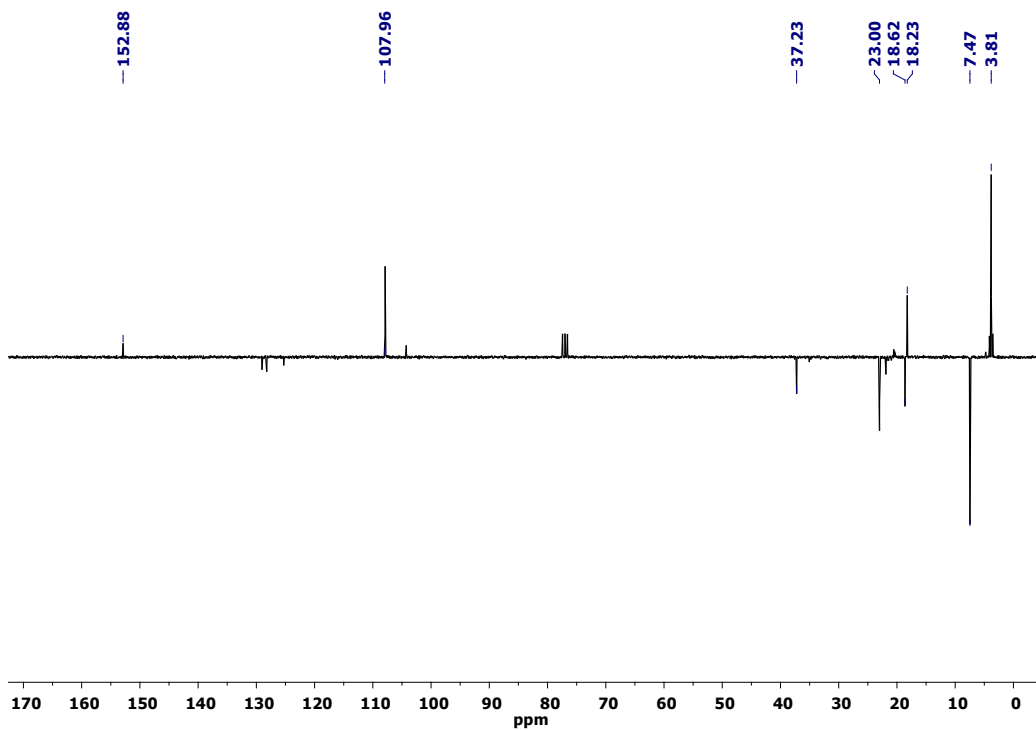


Figure S50. $^{13}\text{C}\{^1\text{H}\}$ APT NMR spectrum (125.76 MHz, CDCl_3 , 293 K).

10 X-ray diffraction analysis data for the complexes

10.1 Crystal data of Rh-2

10.1.1 Crystal Structure Report for B_VM_040

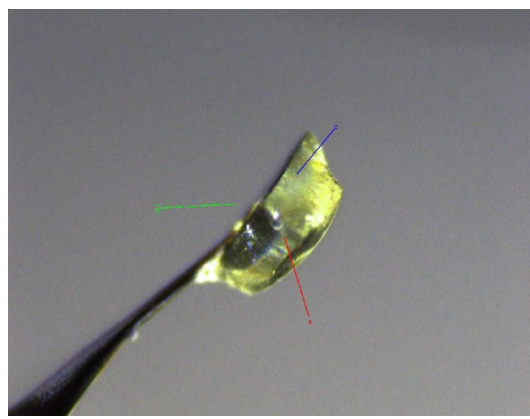
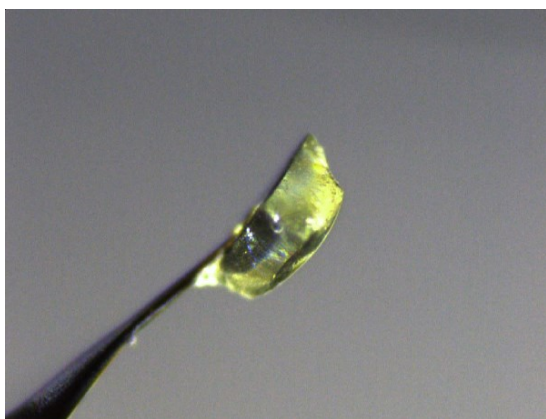
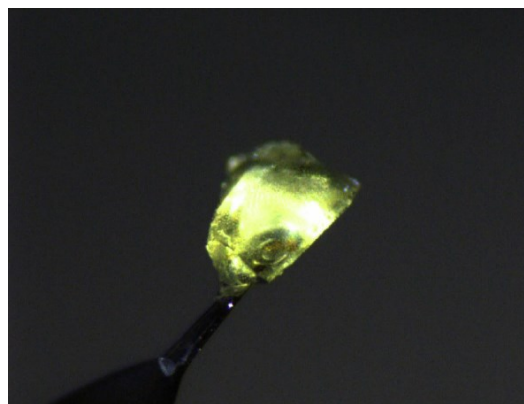
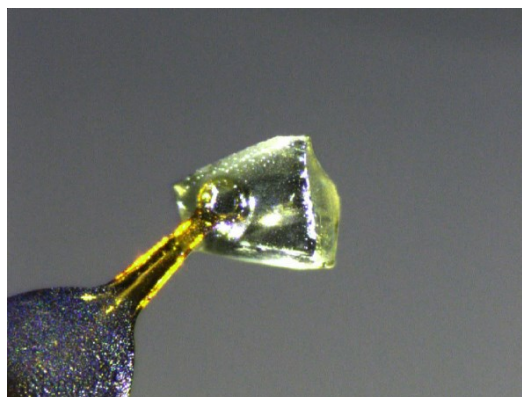
A yellow prism like single crystal of $C_{32}H_{45}BrPRhSi_2$, approximate dimensions (0.293x0.452x0.579) mm³, was selected for the X-ray crystallographic analysis and mounted on a cryoloop using an oil cryoprotectant. The X-ray intensity data was measured at low temperature (T = 100K), using a three circles goniometer Kappa geometry with a fixed Kappa angle at = 54.74 deg Bruker AXS D8 Venture, equipped with a Photon 100 CMOS active pixel sensor detector. A monochromatized Mo X-ray radiation ($\lambda = 0.71073 \text{ \AA}$) was selected for the measurement.

Frames were integrated with the Bruker SAINT software package using a narrow-frame algorithm.¹³ The integration of the data using a tetragonal unit cell yielded a total of 40461 reflections to a maximum θ angle of 27.57° (0.77 Å resolution), of which 6936 were independent (average redundancy 5.833, completeness = 99.8%, $R_{int} = 3.26\%$, $R_{sig} = 3.18\%$) and 6838 (98.59%) were greater than 2σ (F^2). The final cell constants of $a = 11.4574(11) \text{ \AA}$, $b = 11.4574(11) \text{ \AA}$, $c = 24.066(4) \text{ \AA}$, volume = 3159.2(8) Å³, are based upon the refinement of the XYZ-centroids of 1105 reflections above 20σ (I) with $4.909 < 2\theta < 55.15^\circ$. Data were corrected for absorption effects using the Multi-Scan method (SADABS).¹⁴ The ratio of minimum to maximum apparent transmission was 0.657. The calculated minimum and maximum transmission coefficients (based on crystal size) are 0.3980 and 0.5990.

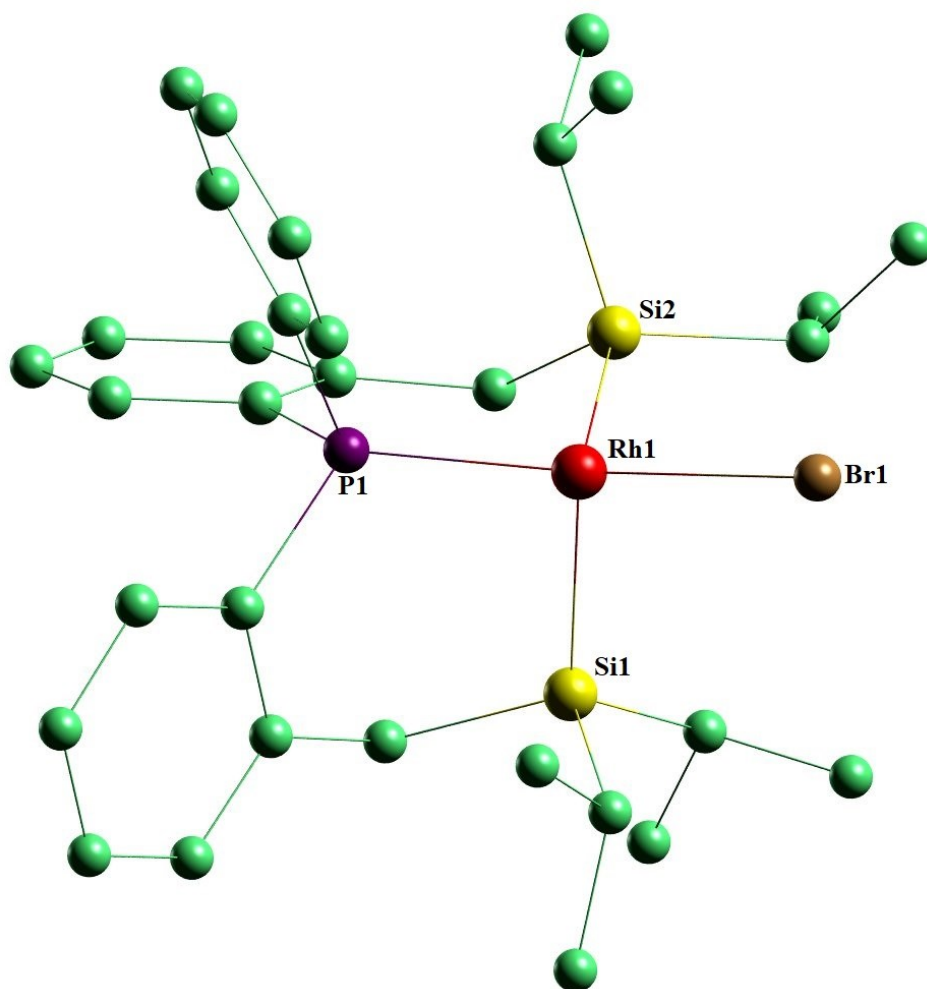
The structure was solved in an Tetragonal unit cell and refined using the Bruker SHELXTL Software Package, using the chiral space group P 4(1), with Z = 4 for the formula unit, $C_{32}H_{45}BrPRhSi_2$. Using the Bruker SHELXT Software Package¹⁵, refinement of the structure was carried out by least squares procedures on weighted F^2 values using the SHELXTL-2018/3¹⁶ included in the APEX3 v2019, 1.0, AXS Bruker program.¹⁷ Hydrogen atoms were localized on difference Fourier maps but then introduced in the refinement as fixed contributors in idealized geometry with an isotropic thermal parameters fixed at 20 % higher than those carbons atoms they were connected. The final anisotropic full-matrix least-squares refinement on F^2 with 344 variables converged at $R1 = 1.69\%$, for the observed data and $wR2 = 4.06\%$ for all data. The goodness-of-fit was 1.051. The largest peak in the final difference electron density synthesis was 0.542 e⁻

\AA^3 and the largest whole was $-0.337 \text{ e}^-/\text{\AA}^3$ with an RMS deviation of $0.052 \text{ e}^-/\text{\AA}^3$. On the basis of the final model, the calculated density was 1.471 g/cm^3 and $F(000)$, 1440 e^- . The Flack's was refined as a Racemic Twinning.¹⁸ Graphics were performed using softwares: Mercury V.4.2.0: (<https://www.ccdc.cam.ac.uk/>) and POV-Ray v 3.7: (The Persistence of Vision Raytracer, high quality, Free Software tool).

10.1.2 Crystal's view



10.1.3 Asymmetric unit's view



Asymmetric unit view of complex **Rh-2**.

Table S9. Sample and crystal data for B_VM_040.

Identification code	vm040
Chemical formula	$C_{32}H_{45}BrPRhSi_2$
Formula weight	699.65 g/mol
Temperature	100(2) K

Wavelength	0.71073 Å	
Crystal size	(0.293 x 0.452 x 0.579) mm ³	
Crystal system	tetragonal	
Space group	P 4(1)	
Unit cell dimensions	a = 11.4574(11) Å	α = 90°
	b = 11.4574(11) Å	β = 90°
	c = 24.066(4) Å	γ = 90°
Volume	3159.2(8) Å ³	
Z	4	
Density (calculated)	1.471 g/cm ³	
Absorption coefficient	1.952 mm ⁻¹	
F(000)	1440	

Table S10. Data collection and structure refinement for B_VM_040.

Theta range for data collection	1.97 to 27.57°
Index ranges	-14 ≤ h ≤ 14, -14 ≤ k ≤ 14, -31 ≤ l ≤ 31
Reflections collected	40461
Independent reflections	6936 [R(int) = 0.0326]
Max. and min. transmission	0.5990 and 0.3980
Structure solution technique	direct methods
Structure solution program	SHELXT
Refinement method	Full-matrix least-squares on F ²
Refinement program	SHELXTL-2018/3
Function minimized	$\sum w (F_o^2 - F_c^2)^2$

Data / restraints / parameters 6936 / 1 / 344

Goodness-of-fit on F^2 1.051

Δ/σ_{\max} 0.001

Final R indices 6838 data; R1 = 0.0169, wR2 = 0.0405
 $I > 2\sigma(I)$

all data R1 = 0.0172, wR2 = 0.0406

Weighting scheme $w = 1/[\sigma^2(F_o^2) + (0.0179P)^2 + 0.2739P]$

where $P = (F_o^2 + 2F_c^2)/3$

Absolute structure parameter 0.052(6)

Extinction coefficient 0.0030(2)

Largest diff. peak and hole 0.542 and -0.337 $e\text{\AA}^{-3}$

R.M.S. deviation from mean 0.052 $e\text{\AA}^{-3}$

Table S11. Bond lengths (\AA) for B_VM_040.

Rh1-P1	2.2050(7)	Rh1-Si2	2.2865(7)
Rh1-Si1	2.2882(7)	Rh1-Br1	2.4349(5)
P1-C15	1.817(2)	P1-C7	1.820(2)
P1-C8	1.824(3)	Si1-C24	1.895(3)
Si1-C1	1.904(2)	Si1-C21	1.904(2)
Si2-C14	1.888(3)	Si2-C30	1.897(2)
Si2-C27	1.914(3)	C1-C2	1.497(3)
C1-H1A	0.99	C1-H1B	0.99
C2-C3	1.394(4)	C2-C7	1.404(3)
C3-C4	1.381(4)	C3-H3	0.95
C4-C5	1.378(4)	C4-H4	0.95
C5-C6	1.386(4)	C5-H5	0.95

C6-C7	1.400(3)	C6-H6	0.95
C8-C13	1.405(3)	C8-C9	1.409(4)
C9-C10	1.378(4)	C9-H9	0.95
C10-C11	1.381(4)	C10-H10	0.95
C11-C12	1.380(4)	C11-H11	0.95
C12-C13	1.404(3)	C12-H12	0.95
C13-C14	1.506(3)	C14-H14A	0.99
C14-H14B	0.99	C15-C16	1.391(3)
C15-C20	1.405(4)	C16-C17	1.395(3)
C16-H16	0.95	C17-C18	1.377(4)
C17-H17	0.95	C18-C19	1.385(4)
C18-H18	0.95	C19-C20	1.385(4)
C19-H19	0.95	C20-H20	0.95
C21-C23	1.526(4)	C21-C22	1.537(3)
C21-H21	1.0	C22-H22A	0.98
C22-H22B	0.98	C22-H22C	0.98
C23-H23A	0.98	C23-H23B	0.98
C23-H23C	0.98	C24-C26	1.527(4)
C24-C25	1.534(4)	C24-H24	1.0
C25-H25A	0.98	C25-H25B	0.98
C25-H25C	0.98	C26-H26A	0.98
C26-H26B	0.98	C26-H26C	0.98
C27-C28	1.526(4)	C27-C29	1.536(4)
C27-H27	1.0	C28-H28A	0.98
C28-H28B	0.98	C28-H28C	0.98
C29-H29A	0.98	C29-H29B	0.98
C29-H29C	0.98	C30-C32	1.531(4)

C30-C31	1.538(4)	C30-H30	1.0
C31-H31A	0.98	C31-H31B	0.98
C31-H31C	0.98	C32-H32A	0.98
C32-H32B	0.98	C32-H32C	0.98

Table S12. Bond angles (°) for B_VM_040.

P1-Rh1-Si2	87.83(2)	P1-Rh1-Si1	89.05(2)
Si2-Rh1-Si1	100.11(2)	P1-Rh1-Br1	164.243(19)
Si2-Rh1-Br1	102.429(19)	Si1-Rh1-Br1	100.692(19)
C15-P1-C7	104.16(11)	C15-P1-C8	105.69(11)
C7-P1-C8	100.11(11)	C15-P1-Rh1	104.63(8)
C7-P1-Rh1	114.28(8)	C8-P1-Rh1	125.96(9)
C24-Si1-C1	108.43(11)	C24-Si1-C21	110.03(12)
C1-Si1-C21	107.36(11)	C24-Si1-Rh1	100.70(9)
C1-Si1-Rh1	113.00(8)	C21-Si1-Rh1	116.94(8)
C14-Si2-C30	105.95(11)	C14-Si2-C27	107.35(11)
C30-Si2-C27	112.92(11)	C14-Si2-Rh1	111.80(8)
C30-Si2-Rh1	106.59(8)	C27-Si2-Rh1	112.13(8)
C2-C1-Si1	113.11(17)	C2-C1-H1A	109.0
Si1-C1-H1A	109.0	C2-C1-H1B	109.0
Si1-C1-H1B	109.0	H1A-C1-H1B	107.8
C3-C2-C7	118.2(2)	C3-C2-C1	121.1(2)
C7-C2-C1	120.7(2)	C4-C3-C2	121.5(3)
C4-C3-H3	119.2	C2-C3-H3	119.2
C5-C4-C3	120.1(2)	C5-C4-H4	120.0

C3-C4-H4	120.0	C4-C5-C6	119.8(3)
C4-C5-H5	120.1	C6-C5-H5	120.1
C5-C6-C7	120.5(2)	C5-C6-H6	119.8
C7-C6-H6	119.8	C6-C7-C2	119.8(2)
C6-C7-P1	122.44(19)	C2-C7-P1	117.72(18)
C13-C8-C9	119.5(2)	C13-C8-P1	124.52(19)
C9-C8-P1	115.91(19)	C10-C9-C8	121.5(2)
C10-C9-H9	119.2	C8-C9-H9	119.2
C9-C10-C11	119.3(3)	C9-C10-H10	120.4
C11-C10-H10	120.4	C12-C11-C10	119.9(3)
C12-C11-H11	120.1	C10-C11-H11	120.1
C11-C12-C13	122.5(2)	C11-C12-H12	118.7
C13-C12-H12	118.7	C12-C13-C8	117.2(2)
C12-C13-C14	118.3(2)	C8-C13-C14	124.4(2)
C13-C14-Si2	118.58(17)	C13-C14-H14A	107.7
Si2-C14-H14A	107.7	C13-C14-H14B	107.7
Si2-C14-H14B	107.7	H14A-C14-H14B	107.1
C16-C15-C20	118.8(2)	C16-C15-P1	124.28(19)
C20-C15-P1	116.82(18)	C15-C16-C17	119.9(2)
C15-C16-H16	120.1	C17-C16-H16	120.1
C18-C17-C16	120.6(3)	C18-C17-H17	119.7
C16-C17-H17	119.7	C17-C18-C19	120.2(2)
C17-C18-H18	119.9	C19-C18-H18	119.9
C20-C19-C18	119.7(3)	C20-C19-H19	120.2
C18-C19-H19	120.2	C19-C20-C15	120.8(2)
C19-C20-H20	119.6	C15-C20-H20	119.6
C23-C21-C22	110.7(2)	C23-C21-Si1	112.23(18)

C22-C21-Si1	112.26(17)	C23-C21-H21	107.1
C22-C21-H21	107.1	Si1-C21-H21	107.1
C21-C22-H22A	109.5	C21-C22-H22B	109.5
H22A-C22-H22B	109.5	C21-C22-H22C	109.5
H22A-C22-H22C	109.5	H22B-C22-H22C	109.5
C21-C23-H23A	109.5	C21-C23-H23B	109.5
H23A-C23-H23B	109.5	C21-C23-H23C	109.5
H23A-C23-H23C	109.5	H23B-C23-H23C	109.5
C26-C24-C25	110.2(2)	C26-C24-Si1	114.74(19)
C25-C24-Si1	111.4(2)	C26-C24-H24	106.7
C25-C24-H24	106.7	Si1-C24-H24	106.7
C24-C25-H25A	109.5	C24-C25-H25B	109.5
H25A-C25-H25B	109.5	C24-C25-H25C	109.5
H25A-C25-H25C	109.5	H25B-C25-H25C	109.5
C24-C26-H26A	109.5	C24-C26-H26B	109.5
H26A-C26-H26B	109.5	C24-C26-H26C	109.5
H26A-C26-H26C	109.5	H26B-C26-H26C	109.5
C28-C27-C29	109.9(2)	C28-C27-Si2	114.62(18)
C29-C27-Si2	112.35(19)	C28-C27-H27	106.5
C29-C27-H27	106.5	Si2-C27-H27	106.5
C27-C28-H28A	109.5	C27-C28-H28B	109.5
H28A-C28-H28B	109.5	C27-C28-H28C	109.5
H28A-C28-H28C	109.5	H28B-C28-H28C	109.5
C27-C29-H29A	109.5	C27-C29-H29B	109.5
H29A-C29-H29B	109.5	C27-C29-H29C	109.5
H29A-C29-H29C	109.5	H29B-C29-H29C	109.5
C32-C30-C31	111.6(2)	C32-C30-Si2	112.43(18)

C31-C30-Si2	114.14(18)	C32-C30-H30	106.0
C31-C30-H30	106.0	Si2-C30-H30	106.0
C30-C31-H31A	109.5	C30-C31-H31B	109.5
H31A-C31-H31B	109.5	C30-C31-H31C	109.5
H31A-C31-H31C	109.5	H31B-C31-H31C	109.5
C30-C32-H32A	109.5	C30-C32-H32B	109.5
H32A-C32-H32B	109.5	C30-C32-H32C	109.5
H32A-C32-H32C	109.5	H32B-C32-H32C	109.5

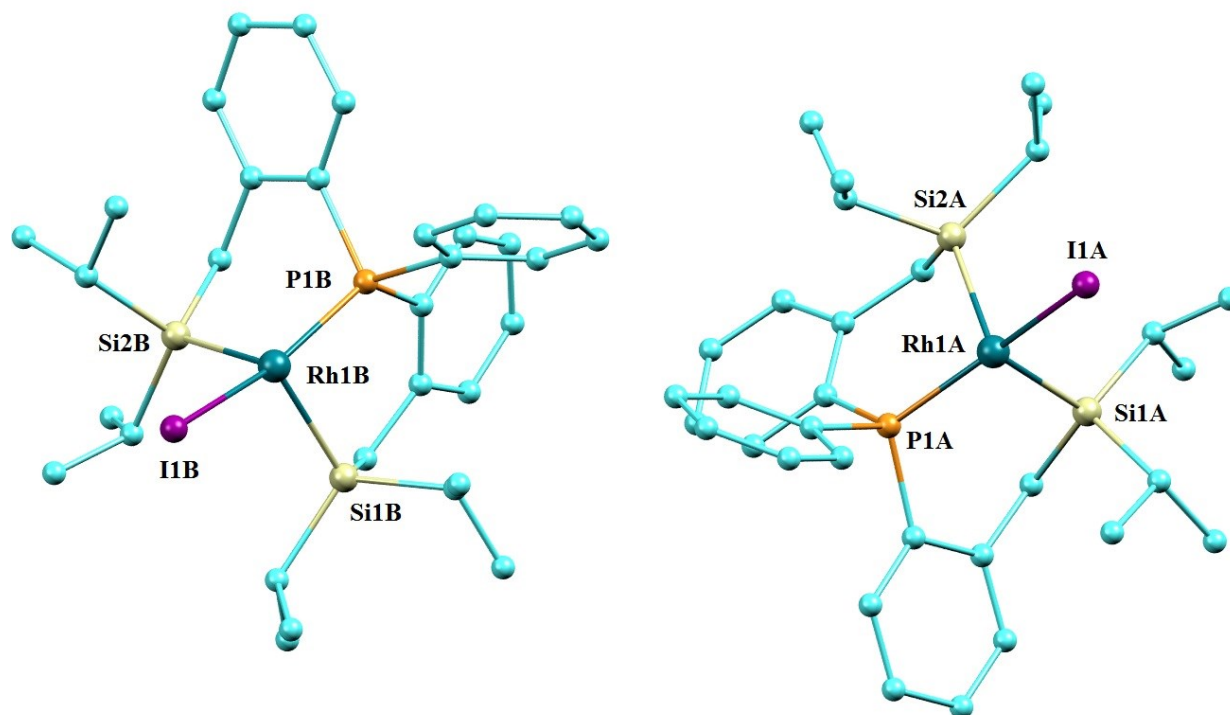
10.2 Crystal data of Rh-3

10.2.1 Crystal Structure Report for A_VM_028

An orange yellow prism single crystal of $C_{64}H_{90}I_2P_2Rh_2Si_4$, approximate dimensions (0.102 x 0.134 x 0.278) mm³, was selected for the X-ray crystallographic analysis and mounted on a cryoloop using an oil cryoprotectant. The X-ray intensity data was measured at low temperature (T = 100K), using a three circles goniometer Kappa geometry with a fixed Kappa angle at = 54.74 deg Bruker AXS D8 Venture, equipped with a Photon 100 CMOS active pixel sensor detector. A monochromatized Copper X-ray radiation ($\lambda = 1.54178 \text{ \AA}$) was selected for the measurement. All frames were integrated with the aid of the Bruker SAINT software¹³ using a narrow-frame algorithm. The integration of the data using a triclinic unit cell yielded a total of 68424 reflections to a maximum θ angle of 72.49° (0.81Å resolution), of which 12489 were independent (average redundancy 5.479, completeness = 98.5%, $R_{int} = 3.58\%$, $R_{sig} = 2.56\%$) and 11961 (95.77%) were greater than $2\sigma (F^2)$. The final cell constants of $a = 9.5705(3) \text{ \AA}$, $b = 17.6043(6) \text{ \AA}$, $c = 19.2246(7) \text{ \AA}$, $\alpha = 93.3520(10)^\circ$, $\beta = 90.1870(10)^\circ$, $\gamma = 98.870(2)^\circ$, volume = 3194.54(19) Å³, are based upon the refinement of the XYZ-centroids of 2194 reflections above $20 \sigma (I)$ with $6.653^\circ < 2\theta < 52.81^\circ$. Data were corrected for absorption effects using the Multi-Scan method implemented in the program (SADABS).¹⁴ The ratio of minimum to maximum apparent transmission was 0.479. The calculated minimum and maximum transmission coefficients (based on crystal size) are 0.1200 and 0.3450. Structure was solved in a triclinic unit cell; Space group: P -1, with Z = 2 for the formula unit, $C_{64}H_{90}I_2P_2Rh_2Si_4$. Using the Bruker SHELXT Software Package¹⁵ refinement of the structure was carried out by least squares procedures on weighted F^2 values using the SHELXTL-2018/3¹⁶ included in the APEX3 v2019, 1.0, AXS Bruker program.¹⁷ Hydrogen atoms were localized on difference Fourier maps but then introduced in the refinement as fixed contributors in idealized geometry with an isotropic thermal parameters fixed at 20 % higher than those carbons atoms they were connected. The final anisotropic full-matrix least-squares refinement on F^2 with 684 variables converged at $R1 = 2.36\%$, for the observed data and $wR2 = 5.53\%$ for all data. The goodness-of-fit: GOF was 1.105. The largest peak in the final difference electron density synthesis was $0.841e^-/\text{\AA}^3$ and the largest hole was $-0.931e^-/\text{\AA}^3$ with an RMS deviation of $0.090e^-$

\AA^3 . Based on the final model, the calculated density was 1.552 g/cm^3 and $F(000)$, 1512e⁻. Graphics were performed using softwares: Mercury V.4.2.0: (<https://www.ccdc.cam.ac.uk/>) and POV-Ray v 3.7: (The Persistence of Vision Raytracer, high quality, Free Software tool).

10.2.2 Asymmetric unit's view



Asymmetric unit view of complex **Rh-3**.

Table S13. Sample and crystal data for A_VM_028.

Identification code	A_VM_028
Chemical formula	$\text{C}_{64}\text{H}_{90}\text{I}_2\text{P}_2\text{Rh}_2\text{Si}_4$
Formula weight	1493.27 g/mol
Temperature	100(2) K
Wavelength	1.54178 Å
Crystal size	(0.102 x 0.134 x 0.278) mm ³

Crystal system	triclinic	
Space group	P -1	
Unit cell dimensions	a = 9.5705(3) Å	$\alpha = 93.3520(10)^\circ$
	b = 17.6043(6) Å	$\beta = 90.1870(10)^\circ$
	c = 19.2246(7) Å	$\gamma = 98.870(2)^\circ$
Volume	3194.54(19) Å ³	
Z	2	
Density (calculated)	1.552 g/cm ³	
Absorption coefficient	13.238 mm ⁻¹	
F(000)	1512	

Table S1. Data collection and structure refinement for A_VM_028.

Theta range for data collection	2.30 to 72.49°
Index ranges	-11<=h<=11, -21<=k<=21, -23<=l<=23
Reflections collected	68424
Independent reflections	12489 [R (int) = 0.0358]
Coverage of independent reflections	98.5%
Absorption correction	Multi-Scan
Max. and min. transmission	0.3450 and 0.1200
Structure solution technique	direct methods

Structure solution program	XT, VERSION 2014/5		
Refinement method	Full-matrix least-squares on F ²		
Refinement program	SHELXL-2018/3 (Sheldrick, 2018)		
Function minimized	$\Sigma w (F_o^2 - F_c^2)^2$		
Data / restraints / parameters	12489 / 0 / 684		
Goodness-of-fit on F²	1.105		
Δ/σ_{\max}	0.003		
Final R indices	11961		
	data; $I > 2\sigma(I)$	R1 = 0.0236, wR2 = 0.0543	
	all data	R1 = 0.0252, wR2 = 0.0553	
Weighting scheme	$w = 1/[\sigma^2(F_o^2) + (0.0126P)^2 + 5.3898P]$ where $P = (F_o^2 + 2F_c^2)/3$		
Extinction coefficient	0.0003(0)		
Largest diff. peak and hole	0.841 and -0.931 eÅ ⁻³		
R.M.S. deviation from mean	0.090 eÅ ⁻³		

Table S14. Bond lengths (Å) for A_VM_028.

Rh1A-P1A	2.2021(6)	Rh1A-Si2A	2.2960(7)
Rh1A-Si1A	2.3112(6)	Rh1A-I1A	2.6004(2)
P1A-C7A	1.820(3)	P1A-C15A	1.833(2)
P1A-C8A	1.838(2)	Si1A-C21A	1.908(3)

Si1A-C1A	1.910(3)	Si1A-C24A	1.915(3)
Si2A-C14A	1.896(3)	Si2A-C27A	1.907(3)
Si2A-C30A	1.919(3)	C1A-C2A	1.501(4)
C1A-H1A1	0.99	C1A-H1A2	0.99
C2A-C3A	1.391(4)	C2A-C7A	1.410(3)
C3A-C4A	1.385(4)	C3A-H3A	0.95
C4A-C5A	1.389(4)	C4A-H4A	0.95
C5A-C6A	1.386(4)	C5A-H5A	0.95
C6A-C7A	1.400(4)	C6A-H6A	0.95
C8A-C9A	1.399(3)	C8A-C13A	1.402(4)
C9A-C10A	1.380(4)	C9A-H9A	0.95
C10A-C11A	1.383(4)	C10A-H10A	0.95
C11A-C12A	1.383(4)	C11A-H11A	0.95
C12A-C13A	1.409(4)	C12A-H12A	0.95
C13A-C14A	1.509(3)	C14A-H14A	0.99
C14A-H14B	0.99	C15A-C20A	1.389(3)
C15A-C16A	1.400(4)	C16A-C17A	1.389(4)
C16A-H16A	0.95	C17A-C18A	1.386(4)
C17A-H17A	0.95	C18A-C19A	1.378(4)
C18A-H18A	0.95	C19A-C20A	1.396(4)
C19A-H19A	0.95	C20A-H20A	0.95
C21A-C22A	1.535(4)	C21A-C23A	1.541(4)

C21A-H21A	1.0	C22A-H22A	0.98
C22A-H22B	0.98	C22A-H22C	0.98
C23A-H23A	0.98	C23A-H23B	0.98
C23A-H23C	0.98	C24A-C26A	1.535(4)
C24A-C25A	1.538(4)	C24A-H24A	1.0
C25A-H25A	0.98	C25A-H25B	0.98
C25A-H25C	0.98	C26A-H26A	0.98
C26A-H26B	0.98	C26A-H26C	0.98
C27A-C28A	1.533(4)	C27A-C29A	1.543(4)
C27A-H27A	1.0	C28A-H28A	0.98
C28A-H28B	0.98	C28A-H28C	0.98
C29A-H29A	0.98	C29A-H29B	0.98
C29A-H29C	0.98	C30A-C32A	1.534(4)
C30A-C31A	1.534(4)	C30A-H30A	1.0
C31A-H31A	0.98	C31A-H31B	0.98
C31A-H31C	0.98	C32A-H32A	0.98
C32A-H32B	0.98	C32A-H32C	0.98
Rh1B-P1B	2.2040(6)	Rh1B-Si1B	2.2975(7)
Rh1B-Si2B	2.3039(6)	Rh1B-I1B	2.5924(2)
P1B-C8B	1.823(2)	P1B-C15B	1.828(2)
P1B-C7B	1.833(2)	Si1B-C1B	1.902(2)
Si1B-C21B	1.906(3)	Si1B-C24B	1.916(2)

Si2B-C14B	1.906(2)	Si2B-C30B	1.911(2)
Si2B-C27B	1.913(2)	C1B-C2B	1.501(3)
C1B-H1B1	0.99	C1B-H1B2	0.99
C2B-C3B	1.406(3)	C2B-C7B	1.412(3)
C3B-C4B	1.386(3)	C3B-H3B	0.95
C4B-C5B	1.387(4)	C4B-H4B	0.95
C5B-C6B	1.388(3)	C5B-H5B	0.95
C6B-C7B	1.404(3)	C6B-H6B	0.95
C8B-C9B	1.401(3)	C8B-C13B	1.406(3)
C9B-C10B	1.390(4)	C9B-H9B	0.95
C10B-C11B	1.384(4)	C10B-H10B	0.95
C11B-C12B	1.390(3)	C11B-H11B	0.95
C12B-C13B	1.393(3)	C12B-H12B	0.95
C13B-C14B	1.502(3)	C14B-H14C	0.99
C14B-H14D	0.99	C15B-C16B	1.394(3)
C15B-C20B	1.401(3)	C16B-C17B	1.397(4)
C16B-H16B	0.95	C17B-C18B	1.382(4)
C17B-H17B	0.95	C18B-C19B	1.381(4)
C18B-H18B	0.95	C19B-C20B	1.387(4)
C19B-H19B	0.95	C20B-H20B	0.95
C21B-C23B	1.531(4)	C21B-C22B	1.541(4)
C21B-H21B	1.0	C22B-H22D	0.98

C22B-H22E	0.98	C22B-H22F	0.98
C23B-H23D	0.98	C23B-H23E	0.98
C23B-H23F	0.98	C24B-C26B	1.534(4)
C24B-C25B	1.535(4)	C24B-H24B	1.0
C25B-H25D	0.98	C25B-H25E	0.98
C25B-H25F	0.98	C26B-H26D	0.98
C26B-H26E	0.98	C26B-H26F	0.98
C27B-C29B	1.535(4)	C27B-C28B	1.536(3)
C27B-H27B	1.0	C28B-H28D	0.98
C28B-H28E	0.98	C28B-H28F	0.98
C29B-H29D	0.98	C29B-H29E	0.98
C29B-H29F	0.98	C30B-C32B	1.531(3)
C30B-C31B	1.541(4)	C30B-H30B	1.0
C31B-H31D	0.98	C31B-H31E	0.98
C31B-H31F	0.98	C32B-H32D	0.98
C32B-H32E	0.98	C32B-H32F	0.98

Table S15. Bond angles (°) for A_VM_028.

P1A-Rh1A-Si2A	86.60(2)	P1A-Rh1A-Si1A	88.62(2)
Si2A-Rh1A-Si1A	98.97(2)	P1A-Rh1A-I1A	161.285(18)

Si2A-Rh1A-I1A	108.071(18)	Si1A-Rh1A-I1A	100.115(18)
C7A-P1A-C15A	104.20(11)	C7A-P1A-C8A	100.88(11)
C15A-P1A-C8A	105.00(11)	C7A-P1A-Rh1A	111.40(8)
C15A-P1A-Rh1A	107.12(8)	C8A-P1A-Rh1A	126.18(8)
C21A-Si1A-C1A	106.53(12)	C21A-Si1A-C24A	110.44(12)
C1A-Si1A-C24A	107.89(11)	C21A-Si1A-Rh1A	104.71(8)
C1A-Si1A-Rh1A	112.59(8)	C24A-Si1A-Rh1A	114.39(8)
C14A-Si2A-C27A	104.04(12)	C14A-Si2A-C30A	106.96(12)
C27A-Si2A-C30A	113.53(12)	C14A-Si2A-Rh1A	113.33(9)
C27A-Si2A-Rh1A	108.75(9)	C30A-Si2A-Rh1A	110.18(9)
C2A-C1A-Si1A	111.56(17)	C2A-C1A-H1A1	109.3
Si1A-C1A-H1A1	109.3	C2A-C1A-H1A2	109.3
Si1A-C1A-H1A2	109.3	H1A1-C1A-H1A2	108.0
C3A-C2A-C7A	117.8(2)	C3A-C2A-C1A	121.3(2)
C7A-C2A-C1A	120.8(2)	C4A-C3A-C2A	121.8(3)
C4A-C3A-H3A	119.1	C2A-C3A-H3A	119.1
C3A-C4A-C5A	120.2(3)	C3A-C4A-H4A	119.9
C5A-C4A-H4A	119.9	C6A-C5A-C4A	119.3(3)
C6A-C5A-H5A	120.4	C4A-C5A-H5A	120.4
C5A-C6A-C7A	120.7(2)	C5A-C6A-H6A	119.7
C7A-C6A-H6A	119.7	C6A-C7A-C2A	120.2(2)
C6A-C7A-P1A	122.79(19)	C2A-C7A-P1A	116.95(19)

C9A-C8A-C13A	119.7(2)	C9A-C8A-P1A	115.35(19)
C13A-C8A-P1A	124.86(18)	C10A-C9A-C8A	121.4(2)
C10A-C9A-H9A	119.3	C8A-C9A-H9A	119.3
C9A-C10A-C11A	119.5(2)	C9A-C10A-H10A	120.3
C11A-C10A-H10A	120.3	C12A-C11A-C10A	119.8(2)
C12A-C11A-H11A	120.1	C10A-C11A-H11A	120.1
C11A-C12A-C13A	121.9(2)	C11A-C12A-H12A	119.1
C13A-C12A-H12A	119.1	C8A-C13A-C12A	117.5(2)
C8A-C13A-C14A	124.5(2)	C12A-C13A-C14A	117.8(2)
C13A-C14A-Si2A	118.67(18)	C13A-C14A-H14A	107.6
Si2A-C14A-H14A	107.6	C13A-C14A-H14B	107.6
Si2A-C14A-H14B	107.6	H14A-C14A-H14B	107.1
C20A-C15A-C16A	118.7(2)	C20A-C15A-P1A	124.21(19)
C16A-C15A-P1A	117.04(19)	C17A-C16A-C15A	120.9(2)
C17A-C16A-H16A	119.6	C15A-C16A-H16A	119.6
C18A-C17A-C16A	119.7(3)	C18A-C17A-H17A	120.2
C16A-C17A-H17A	120.2	C19A-C18A-C17A	120.0(2)
C19A-C18A-H18A	120.0	C17A-C18A-H18A	120.0
C18A-C19A-C20A	120.5(2)	C18A-C19A-H19A	119.7
C20A-C19A-H19A	119.7	C15A-C20A-C19A	120.2(2)
C15A-C20A-H20A	119.9	C19A-C20A-H20A	119.9
C22A-C21A-C23A	110.1(2)	C22A-C21A-Si1A	114.94(18)

C23A-C21A-Si1A	110.62(19)	C22A-C21A-H21A	106.9
C23A-C21A-H21A	106.9	Si1A-C21A-H21A	106.9
C21A-C22A-H22A	109.5	C21A-C22A-H22B	109.5
H22A-C22A-H22B	109.5	C21A-C22A-H22C	109.5
H22A-C22A-H22C	109.5	H22B-C22A-H22C	109.5
C21A-C23A-H23A	109.5	C21A-C23A-H23B	109.5
H23A-C23A-H23B	109.5	C21A-C23A-H23C	109.5
H23A-C23A-H23C	109.5	H23B-C23A-H23C	109.5
C26A-C24A-C25A	110.9(2)	C26A-C24A-Si1A	112.64(19)
C25A-C24A-Si1A	113.03(18)	C26A-C24A-H24A	106.6
C25A-C24A-H24A	106.6	Si1A-C24A-H24A	106.6
C24A-C25A-H25A	109.5	C24A-C25A-H25B	109.5
H25A-C25A-H25B	109.5	C24A-C25A-H25C	109.5
H25A-C25A-H25C	109.5	H25B-C25A-H25C	109.5
C24A-C26A-H26A	109.5	C24A-C26A-H26B	109.5
H26A-C26A-H26B	109.5	C24A-C26A-H26C	109.5
H26A-C26A-H26C	109.5	H26B-C26A-H26C	109.5
C28A-C27A-C29A	110.9(2)	C28A-C27A-Si2A	115.49(19)
C29A-C27A-Si2A	112.1(2)	C28A-C27A-H27A	105.8
C29A-C27A-H27A	105.8	Si2A-C27A-H27A	105.8
C27A-C28A-H28A	109.5	C27A-C28A-H28B	109.5
H28A-C28A-H28B	109.5	C27A-C28A-H28C	109.5

H28A-C28A-H28C	109.5	H28B-C28A-H28C	109.5
C27A-C29A-H29A	109.5	C27A-C29A-H29B	109.5
H29A-C29A-H29B	109.5	C27A-C29A-H29C	109.5
H29A-C29A-H29C	109.5	H29B-C29A-H29C	109.5
C32A-C30A-C31A	110.6(2)	C32A-C30A-Si2A	113.61(19)
C31A-C30A-Si2A	113.20(19)	C32A-C30A-H30A	106.3
C31A-C30A-H30A	106.3	Si2A-C30A-H30A	106.3
C30A-C31A-H31A	109.5	C30A-C31A-H31B	109.5
H31A-C31A-H31B	109.5	C30A-C31A-H31C	109.5
H31A-C31A-H31C	109.5	H31B-C31A-H31C	109.5
C30A-C32A-H32A	109.5	C30A-C32A-H32B	109.5
H32A-C32A-H32B	109.5	C30A-C32A-H32C	109.5
H32A-C32A-H32C	109.5	H32B-C32A-H32C	109.5
P1B-Rh1B-Si1B	88.29(2)	P1B-Rh1B-Si2B	89.44(2)
Si1B-Rh1B-Si2B	97.92(2)	P1B-Rh1B-I1B	157.885(17)
Si1B-Rh1B-I1B	104.168(17)	Si2B-Rh1B-I1B	106.474(16)
C8B-P1B-C15B	104.91(11)	C8B-P1B-C7B	102.88(10)
C15B-P1B-C7B	104.59(11)	C8B-P1B-Rh1B	114.60(7)
C15B-P1B-Rh1B	100.95(8)	C7B-P1B-Rh1B	126.64(8)
C1B-Si1B-C21B	103.41(11)	C1B-Si1B-C24B	107.90(11)
C21B-Si1B-C24B	114.37(12)	C1B-Si1B-Rh1B	111.57(8)
C21B-Si1B-Rh1B	106.51(9)	C24B-Si1B-Rh1B	112.74(8)

C14B-Si2B-C30B	106.39(11)	C14B-Si2B-C27B	107.76(11)
C30B-Si2B-C27B	110.50(11)	C14B-Si2B-Rh1B	112.48(7)
C30B-Si2B-Rh1B	116.06(8)	C27B-Si2B-Rh1B	103.43(8)
C2B-C1B-Si1B	115.56(16)	C2B-C1B-H1B1	108.4
Si1B-C1B-H1B1	108.4	C2B-C1B-H1B2	108.4
Si1B-C1B-H1B2	108.4	H1B1-C1B-H1B2	107.5
C3B-C2B-C7B	117.6(2)	C3B-C2B-C1B	118.8(2)
C7B-C2B-C1B	123.6(2)	C4B-C3B-C2B	122.0(2)
C4B-C3B-H3B	119.0	C2B-C3B-H3B	119.0
C3B-C4B-C5B	120.0(2)	C3B-C4B-H4B	120.0
C5B-C4B-H4B	120.0	C4B-C5B-C6B	119.4(2)
C4B-C5B-H5B	120.3	C6B-C5B-H5B	120.3
C5B-C6B-C7B	121.2(2)	C5B-C6B-H6B	119.4
C7B-C6B-H6B	119.4	C6B-C7B-C2B	119.7(2)
C6B-C7B-P1B	116.53(18)	C2B-C7B-P1B	123.66(17)
C9B-C8B-C13B	119.6(2)	C9B-C8B-P1B	122.71(18)
C13B-C8B-P1B	117.60(17)	C10B-C9B-C8B	120.7(2)
C10B-C9B-H9B	119.6	C8B-C9B-H9B	119.6
C11B-C10B-C9B	119.7(2)	C11B-C10B-H10B	120.1
C9B-C10B-H10B	120.1	C10B-C11B-C12B	119.8(2)
C10B-C11B-H11B	120.1	C12B-C11B-H11B	120.1
C11B-C12B-C13B	121.6(2)	C11B-C12B-H12B	119.2

C13B-C12B-H12B	119.2	C12B-C13B-C8B	118.6(2)
C12B-C13B-C14B	120.3(2)	C8B-C13B-C14B	121.1(2)
C13B-C14B-Si2B	112.92(15)	C13B-C14B-H14C	109.0
Si2B-C14B-H14C	109.0	C13B-C14B-H14D	109.0
Si2B-C14B-H14D	109.0	H14C-C14B-H14D	107.8
C16B-C15B-C20B	119.0(2)	C16B-C15B-P1B	124.52(19)
C20B-C15B-P1B	116.35(18)	C15B-C16B-C17B	120.1(2)
C15B-C16B-H16B	120.0	C17B-C16B-H16B	120.0
C18B-C17B-C16B	120.1(2)	C18B-C17B-H17B	120.0
C16B-C17B-H17B	120.0	C19B-C18B-C17B	120.4(2)
C19B-C18B-H18B	119.8	C17B-C18B-H18B	119.8
C18B-C19B-C20B	119.9(2)	C18B-C19B-H19B	120.0
C20B-C19B-H19B	120.0	C19B-C20B-C15B	120.5(2)
C19B-C20B-H20B	119.7	C15B-C20B-H20B	119.7
C23B-C21B-C22B	112.2(2)	C23B-C21B-Si1B	117.00(19)
C22B-C21B-Si1B	110.08(19)	C23B-C21B-H21B	105.5
C22B-C21B-H21B	105.5	Si1B-C21B-H21B	105.5
C21B-C22B-H22D	109.5	C21B-C22B-H22E	109.5
H22D-C22B-H22E	109.5	C21B-C22B-H22F	109.5
H22D-C22B-H22F	109.5	H22E-C22B-H22F	109.5
C21B-C23B-H23D	109.5	C21B-C23B-H23E	109.5
H23D-C23B-H23E	109.5	C21B-C23B-H23F	109.5

H23D-C23B-H23F	109.5	H23E-C23B-H23F	109.5
C26B-C24B-C25B	109.9(2)	C26B-C24B-Si1B	113.60(18)
C25B-C24B-Si1B	113.85(17)	C26B-C24B-H24B	106.3
C25B-C24B-H24B	106.3	Si1B-C24B-H24B	106.3
C24B-C25B-H25D	109.5	C24B-C25B-H25E	109.5
H25D-C25B-H25E	109.5	C24B-C25B-H25F	109.5
H25D-C25B-H25F	109.5	H25E-C25B-H25F	109.5
C24B-C26B-H26D	109.5	C24B-C26B-H26E	109.5
H26D-C26B-H26E	109.5	C24B-C26B-H26F	109.5
H26D-C26B-H26F	109.5	H26E-C26B-H26F	109.5
C29B-C27B-C28B	109.6(2)	C29B-C27B-Si2B	111.56(17)
C28B-C27B-Si2B	114.75(17)	C29B-C27B-H27B	106.8
C28B-C27B-H27B	106.8	Si2B-C27B-H27B	106.8
C27B-C28B-H28D	109.5	C27B-C28B-H28E	109.5
H28D-C28B-H28E	109.5	C27B-C28B-H28F	109.5
H28D-C28B-H28F	109.5	H28E-C28B-H28F	109.5
C27B-C29B-H29D	109.5	C27B-C29B-H29E	109.5
H29D-C29B-H29E	109.5	C27B-C29B-H29F	109.5
H29D-C29B-H29F	109.5	H29E-C29B-H29F	109.5
C32B-C30B-C31B	110.4(2)	C32B-C30B-Si2B	111.89(17)
C31B-C30B-Si2B	114.03(17)	C32B-C30B-H30B	106.7
C31B-C30B-H30B	106.7	Si2B-C30B-H30B	106.7

C30B-C31B-H31D	109.5	C30B-C31B-H31E	109.5
H31D-C31B-H31E	109.5	C30B-C31B-H31F	109.5
H31D-C31B-H31F	109.5	H31E-C31B-H31F	109.5
C30B-C32B-H32D	109.5	C30B-C32B-H32E	109.5
H32D-C32B-H32E	109.5	C30B-C32B-H32F	109.5
H32D-C32B-H32F	109.5	H32E-C32B-H32F	109.5

10.3 Crystal data of Rh-4

10.3.1 Crystal Structure Report for CU_B_VM_020_Final

A yellow prism single crystal of $C_{39}H_{51}F_3O_3PRhSSi_2$, approximate dimensions (0.099 x 0.102 x 0.334) mm³, was selected for the X-ray crystallographic analysis and mounted on a cryoloop using an oil cryoprotectant. The X-ray intensity data was measured at low temperature (T = 100K), using a three circles goniometer Kappa geometry with a fixed Kappa angle at = 54.74 deg Bruker AXS D8 Venture, equipped with a Photon 100 CMOS active pixel sensor detector. A monochromatized Cu X-ray radiation ($\lambda = 1.54178 \text{ \AA}$) was selected for the measurement.

All frames were integrated with the aid of the Bruker SAINT software¹³ using a narrow-frame algorithm. The integration of the data using a monoclinic unit cell yielded a total of 53650 reflections to a maximum θ angle of 72.76° (0.81 Å resolution), of which 7861 were independent (average redundancy 6.825, completeness = 99.5%, $R_{\text{int}} = 5.56\%$, $R_{\text{sig}} = 3.61\%$) and 7579 (96.41%) were greater than $2\sigma (F^2)$.

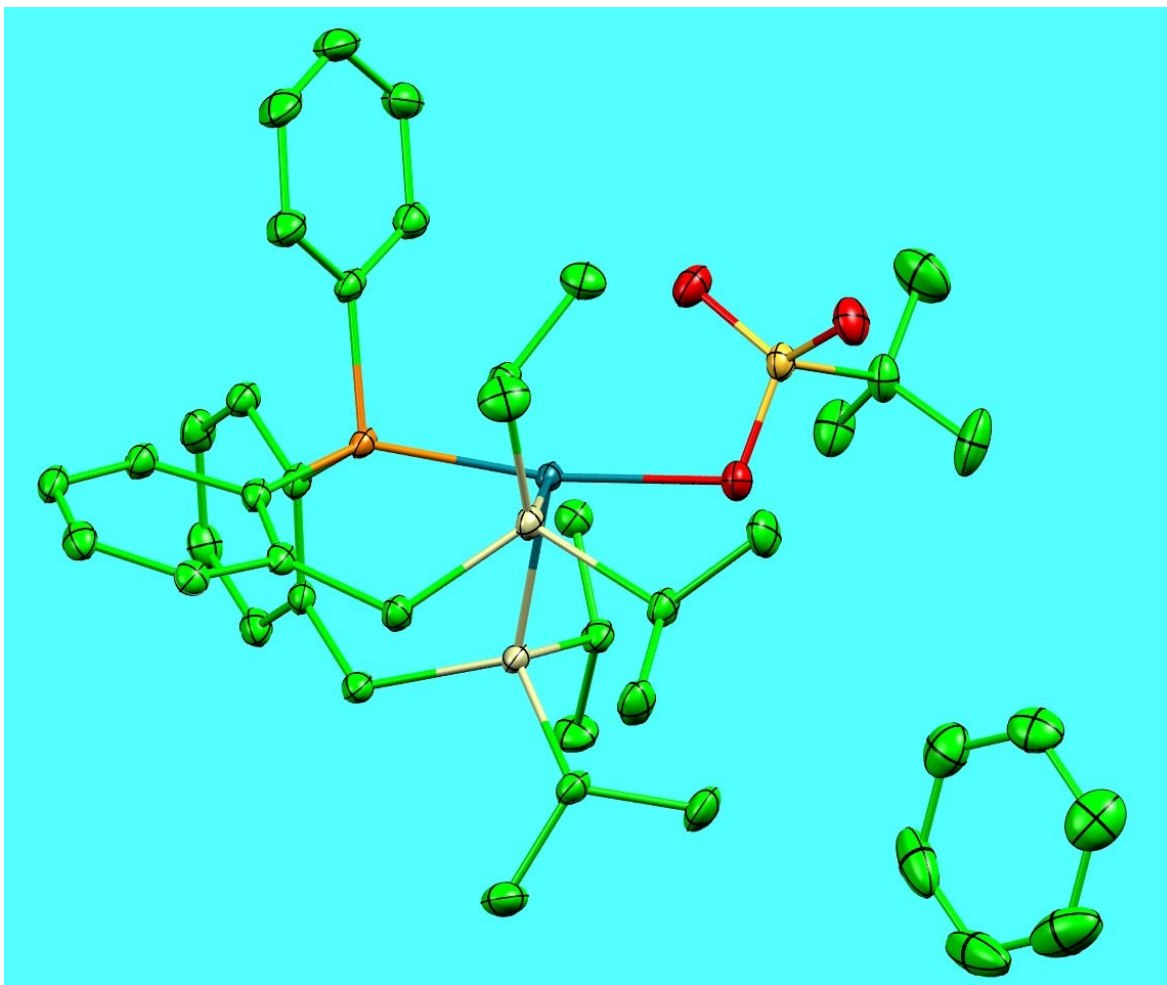
The final cell constants of $a = 11.7311(8) \text{ \AA}$, $b = 21.7488(15) \text{ \AA}$, $c = 15.5316(11) \text{ \AA}$, $\beta = 93.067(2)^\circ$, volume = 3957.0(5) Å³, are based upon the refinement of the 2178 XYZ-centroids of reflections above $20 \sigma (I)$ with $3.150^\circ < \theta < 72.160^\circ$. Data were corrected for absorption effects using the Multi-Scan method (SADABS)¹⁴ The calculated minimum and maximum transmission coefficients (based on crystalsize) are 0.2680 and 0.6200.

Structure was solved in a monoclinic unit cell; Space group: P 1 21/n 1, with Z = 4 for the formula unit, $C_{39}H_{51}F_3O_3PRhSSi_2$. Using the Bruker SHELXT Software Package,¹⁵ refinement of the structure was carried out by least squares procedures on weighted F^2 values using the SHELXTL-2018/3¹⁶ included in the APEX3 v2019, 1.0, AXS Bruker program.¹⁷ Hydrogen atoms were localized on difference Fourier maps but then introduced in the refinement as fixed contributors in idealized geometry with an isotropic thermal parameters fixed at 20 % higher than those carbons atoms they were connected. A molecule of solvent of crystallization: Benzene was also found in the unit cell.

The final anisotropic full-matrix least-squares refinement on F^2 with 460 variables converged at $R1 = 3.60\%$, for the observed data and $wR2 = 9.68\%$ for all data. The goodness-of-fit: GOF was 1.047. The largest peak in the final difference electron density synthesis was 1.453 e⁻/Å³ and

the largest hole was $-1.230 \text{ e}^-/\text{\AA}^3$ with an RMS deviation of $0.113 \text{ e}^-/\text{\AA}^3$. On the basis of the final model, the calculated density was 1.422 g/cm^3 and $F(000)$, 1760 e^- . Graphics were performed using softwares: Mercury V.4.2.0: (<https://www.ccdc.cam.ac.uk/>) and POV-Ray v 3.7: (The Persistence of Vision Raytracer, high quality, Free Software tool).

10.3.2 Asymmetric unit's view



Asymmetric unit view of complex **Rh-4**

Table S16. Sample and crystal data for CU_B_VM_020_Final.

Identification code	CU_B_VM_020_Final
Chemical formula	C ₃₉ H ₅₁ F ₃ O ₃ PRhSSi ₂
Formula weight	846.91 g/mol
Temperature	100(2) K

Wavelength	1.54178 Å
Crystal size	(0.099 x 0.102 x 0.334) mm ³
Crystal system	monoclinic
Space group	P 1 21/n 1
Unit cell dimensions	a = 11.7311(8) Å α = 90° b = 21.7488(15) Å β = 93.067(2)° c = 15.5316(11) Å γ = 90°
Volume	3957.0(5) Å ³
Z	4
Density (calculated)	1.422 g/cm ³
Absorption coefficient	5.361 mm ⁻¹
F (000)	1760

Table S17. Data collection and structure refinement for CU_B_VM_020_Final.

Theta range for data collection	3.50 to 72.76°
Index ranges	-14<=h<=14, -26<=k<=26, -19<=l<=19
Reflections collected	53650
Independent reflections	7861 [R(int) = 0.0556]
Max. and min. transmission	0.6200 and 0.2680
Refinement method	Full-matrix least-squares on F ²
Refinement program	SHELXL-2018/3 (Sheldrick, 2018)
Function minimized	Σ w (F _o ² - F _c ²) ²
Data / restraints / parameters	7861 / 0 / 460

Goodness-of-fit on F²	1.047	
Δ/σ_{\max}	0.001	
Final R indices	7579 data; $I > 2\sigma(I)$	R1 = 0.0360, wR2 = 0.0955
	all data	R1 = 0.0369, wR2 = 0.0968
Weighting scheme	$w = 1/[\sigma^2(F_o^2) + (0.0651P)^2 + 2.8680P]$ where $P = (F_o^2 + 2F_c^2)/3$	
Extinction coefficient	0.0002(0)	
Largest diff. peak and hole	1.453 and -1.230 eÅ ⁻³	
R.M.S. deviation from mean	0.113 eÅ ⁻³	

Table S18. Bond lengths (Å) for CU_B_VM_020_Final.

Rh1-O1	2.1736(14)	Rh1-P1	2.1948(5)
Rh1-Si1	2.2955(6)	Rh1-Si2	2.3036(5)
P1-C14	1.827(2)	P1-C7	1.828(2)
P1-C8	1.833(2)	Si1-C1	1.890(2)
Si1-C21	1.907(2)	Si1-C24	1.918(2)
Si2-C20	1.895(2)	Si2-C27	1.900(2)
Si2-C30	1.906(2)	C1-C2	1.509(3)
C1-H1A	0.99	C1-H1B	0.99
C2-C3	1.399(3)	C2-C7	1.406(3)
C3-C4	1.387(3)	C3-H3	0.95
C4-C5	1.388(3)	C4-H4	0.95
C5-C6	1.385(3)	C5-H5	0.95
C6-C7	1.408(3)	C6-H6	0.95
C8-C9	1.393(3)	C8-C13	1.401(3)

C9-C10	1.394(3)	C9-H9	0.95
C10-C11	1.387(4)	C10-H10	0.95
C11-C12	1.386(4)	C11-H11	0.95
C12-C13	1.389(3)	C12-H12	0.95
C13-H13	0.95	C14-C15	1.399(3)
C14-C19	1.405(3)	C15-C16	1.390(3)
C15-H15	0.95	C16-C17	1.386(3)
C16-H16	0.95	C17-C18	1.391(3)
C17-H17	0.95	C18-C19	1.397(3)
C18-H18	0.95	C19-C20	1.499(3)
C20-H20A	0.99	C20-H20B	0.99
C21-C23	1.531(3)	C21-C22	1.542(3)
C21-H21	1.0	C22-H22A	0.98
C22-H22B	0.98	C22-H22C	0.98
C23-H23A	0.98	C23-H23B	0.98
C23-H23C	0.98	C24-C26	1.532(3)
C24-C25	1.542(3)	C24-H24	1.0
C25-H25A	0.98	C25-H25B	0.98
C25-H25C	0.98	C26-H26A	0.98
C26-H26B	0.98	C26-H26C	0.98
C27-C29	1.534(3)	C27-C28	1.540(3)
C27-H27	1.0	C28-H28A	0.98
C28-H28B	0.98	C28-H28C	0.98
C29-H29A	0.98	C29-H29B	0.98
C29-H29C	0.98	C30-C32	1.536(3)
C30-C31	1.537(3)	C30-H30	1.0
C31-H31A	0.98	C31-H31B	0.98

C31-H31C	0.98	C32-H32A	0.98
C32-H32B	0.98	C32-H32C	0.98
C33-F2	1.325(3)	C33-F3	1.327(3)
C33-F1	1.333(3)	C33-S1	1.832(2)
S1-O3	1.4299(16)	S1-O2	1.4413(16)
S1-O1	1.4779(16)	C1S-C6S	1.368(4)
C1S-C2S	1.371(4)	C1S-H1S	0.95
C2S-C3S	1.390(5)	C2S-H2S	0.95
C3S-C4S	1.391(6)	C3S-H3S	0.95
C4S-C5S	1.368(6)	C4S-H4S	0.95
C5S-C6S	1.379(5)	C5S-H5S	0.95
C6S-H6S	0.95		

Table S19. Bond angles (°) for CU_B_VM_020_Final.

O1-Rh1-P1	170.27(4)	O1-Rh1-Si1	96.28(4)
P1-Rh1-Si1	88.926(19)	O1-Rh1-Si2	98.17(4)
P1-Rh1-Si2	89.220(19)	Si1-Rh1-Si2	97.82(2)
C14-P1-C7	102.23(9)	C14-P1-C8	104.37(9)
C7-P1-C8	104.21(9)	C14-P1-Rh1	113.62(7)
C7-P1-Rh1	125.53(7)	C8-P1-Rh1	104.82(7)
C1-Si1-C21	105.26(9)	C1-Si1-C24	108.49(9)
C21-Si1-C24	114.98(10)	C1-Si1-Rh1	112.60(7)
C21-Si1-Rh1	106.58(7)	C24-Si1-Rh1	109.00(7)
C20-Si2-C27	106.94(9)	C20-Si2-C30	110.05(9)

C27-Si2-C30	111.67(9)	C20-Si2-Rh1	113.12(7)
C27-Si2-Rh1	118.03(7)	C30-Si2-Rh1	96.69(6)
C2-C1-Si1	117.05(14)	C2-C1-H1A	108.0
Si1-C1-H1A	108.0	C2-C1-H1B	108.0
Si1-C1-H1B	108.0	H1A-C1-H1B	107.3
C3-C2-C7	117.77(18)	C3-C2-C1	118.07(18)
C7-C2-C1	124.06(18)	C4-C3-C2	122.0(2)
C4-C3-H3	119.0	C2-C3-H3	119.0
C3-C4-C5	120.2(2)	C3-C4-H4	119.9
C5-C4-H4	119.9	C6-C5-C4	118.7(2)
C6-C5-H5	120.7	C4-C5-H5	120.7
C5-C6-C7	121.7(2)	C5-C6-H6	119.1
C7-C6-H6	119.1	C2-C7-C6	119.41(19)
C2-C7-P1	125.11(15)	C6-C7-P1	115.36(15)
C9-C8-C13	119.1(2)	C9-C8-P1	123.24(17)
C13-C8-P1	117.59(16)	C8-C9-C10	120.3(2)
C8-C9-H9	119.9	C10-C9-H9	119.9
C11-C10-C9	120.0(2)	C11-C10-H10	120.0
C9-C10-H10	120.0	C12-C11-C10	120.1(2)
C12-C11-H11	119.9	C10-C11-H11	119.9
C11-C12-C13	120.1(2)	C11-C12-H12	119.9
C13-C12-H12	119.9	C12-C13-C8	120.2(2)
C12-C13-H13	119.9	C8-C13-H13	119.9
C15-C14-C19	119.97(19)	C15-C14-P1	122.40(16)
C19-C14-P1	117.63(15)	C16-C15-C14	120.5(2)
C16-C15-H15	119.7	C14-C15-H15	119.7
C17-C16-C15	119.9(2)	C17-C16-H16	120.0

C15-C16-H16	120.0	C16-C17-C18	119.7(2)
C16-C17-H17	120.2	C18-C17-H17	120.2
C17-C18-C19	121.5(2)	C17-C18-H18	119.3
C19-C18-H18	119.3	C18-C19-C14	118.37(19)
C18-C19-C20	120.23(18)	C14-C19-C20	121.37(18)
C19-C20-Si2	113.75(14)	C19-C20-H20A	108.8
Si2-C20-H20A	108.8	C19-C20-H20B	108.8
Si2-C20-H20B	108.8	H20A-C20-H20B	107.7
C23-C21-C22	111.14(19)	C23-C21-Si1	115.89(16)
C22-C21-Si1	111.56(16)	C23-C21-H21	105.8
C22-C21-H21	105.8	Si1-C21-H21	105.8
C21-C22-H22A	109.5	C21-C22-H22B	109.5
H22A-C22-H22B	109.5	C21-C22-H22C	109.5
H22A-C22-H22C	109.5	H22B-C22-H22C	109.5
C21-C23-H23A	109.5	C21-C23-H23B	109.5
H23A-C23-H23B	109.5	C21-C23-H23C	109.5
H23A-C23-H23C	109.5	H23B-C23-H23C	109.5
C26-C24-C25	109.26(18)	C26-C24-Si1	115.00(15)
C25-C24-Si1	113.63(15)	C26-C24-H24	106.1
C25-C24-H24	106.1	Si1-C24-H24	106.1
C24-C25-H25A	109.5	C24-C25-H25B	109.5
H25A-C25-H25B	109.5	C24-C25-H25C	109.5
H25A-C25-H25C	109.5	H25B-C25-H25C	109.5
C24-C26-H26A	109.5	C24-C26-H26B	109.5
H26A-C26-H26B	109.5	C24-C26-H26C	109.5
H26A-C26-H26C	109.5	H26B-C26-H26C	109.5
C29-C27-C28	109.72(19)	C29-C27-Si2	112.55(15)

C28-C27-Si2	113.32(15)	C29-C27-H27	107.0
C28-C27-H27	107.0	Si2-C27-H27	107.0
C27-C28-H28A	109.5	C27-C28-H28B	109.5
H28A-C28-H28B	109.5	C27-C28-H28C	109.5
H28A-C28-H28C	109.5	H28B-C28-H28C	109.5
C27-C29-H29A	109.5	C27-C29-H29B	109.5
H29A-C29-H29B	109.5	C27-C29-H29C	109.5
H29A-C29-H29C	109.5	H29B-C29-H29C	109.5
C32-C30-C31	109.89(18)	C32-C30-Si2	113.31(14)
C31-C30-Si2	112.52(15)	C32-C30-H30	106.9
C31-C30-H30	106.9	Si2-C30-H30	106.9
C30-C31-H31A	109.5	C30-C31-H31B	109.5
H31A-C31-H31B	109.5	C30-C31-H31C	109.5
H31A-C31-H31C	109.5	H31B-C31-H31C	109.5
C30-C32-H32A	109.5	C30-C32-H32B	109.5
H32A-C32-H32B	109.5	C30-C32-H32C	109.5
H32A-C32-H32C	109.5	H32B-C32-H32C	109.5
F2-C33-F3	108.47(19)	F2-C33-F1	107.82(19)
F3-C33-F1	107.82(19)	F2-C33-S1	110.18(17)
F3-C33-S1	110.81(15)	F1-C33-S1	111.63(15)
O3-S1-O2	117.75(10)	O3-S1-O1	114.57(9)
O2-S1-O1	111.23(9)	O3-S1-C33	103.55(10)
O2-S1-C33	105.19(10)	O1-S1-C33	102.49(10)
S1-O1-Rh1	109.16(8)	C6S-C1S-C2S	120.4(3)
C6S-C1S-H1S	119.8	C2S-C1S-H1S	119.8
C1S-C2S-C3S	120.2(3)	C1S-C2S-H2S	119.9
C3S-C2S-H2S	119.9	C2S-C3S-C4S	118.8(3)

C2S-C3S-H3S	120.6	C4S-C3S-H3S	120.6
C5S-C4S-C3S	120.4(3)	C5S-C4S-H4S	119.8
C3S-C4S-H4S	119.8	C4S-C5S-C6S	120.1(3)
C4S-C5S-H5S	119.9	C6S-C5S-H5S	119.9
C1S-C6S-C5S	120.1(3)	C1S-C6S-H6S	120.0
C5S-C6S-H6S	120.0		

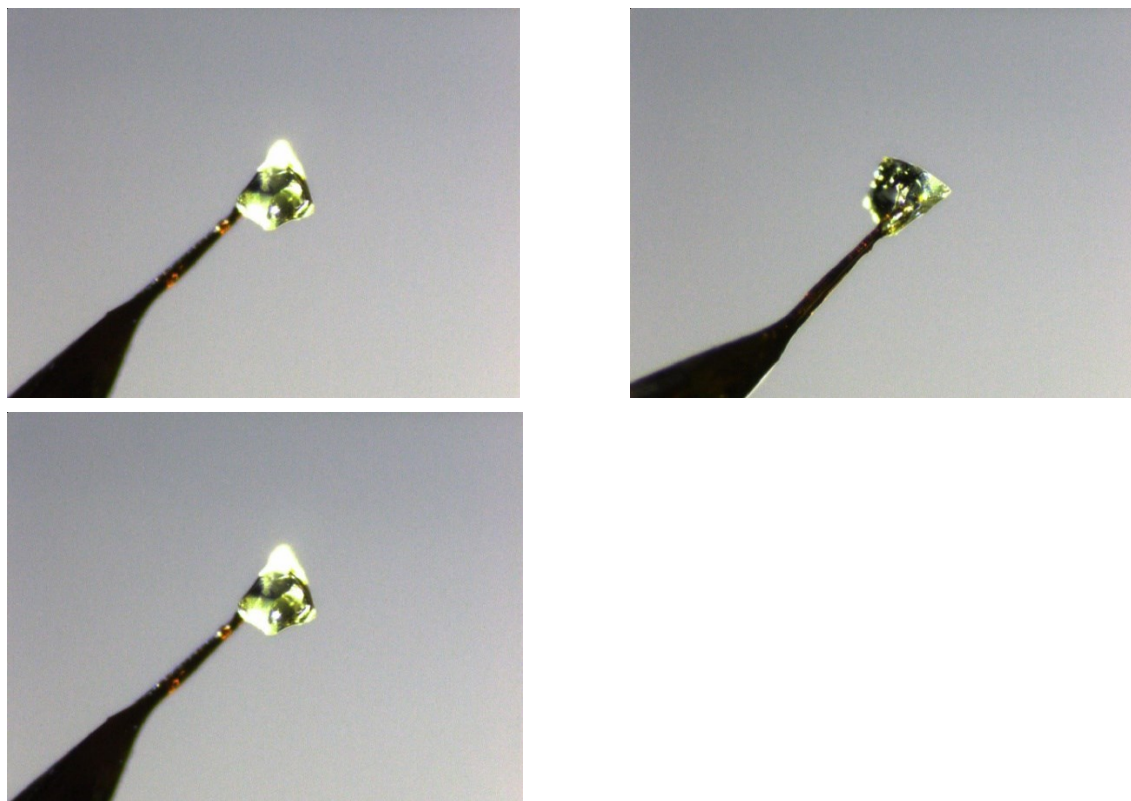
10.4 Crystal data of **Rh-5**

10.4.1 Crystal Structure Report for A_VM_013_100K

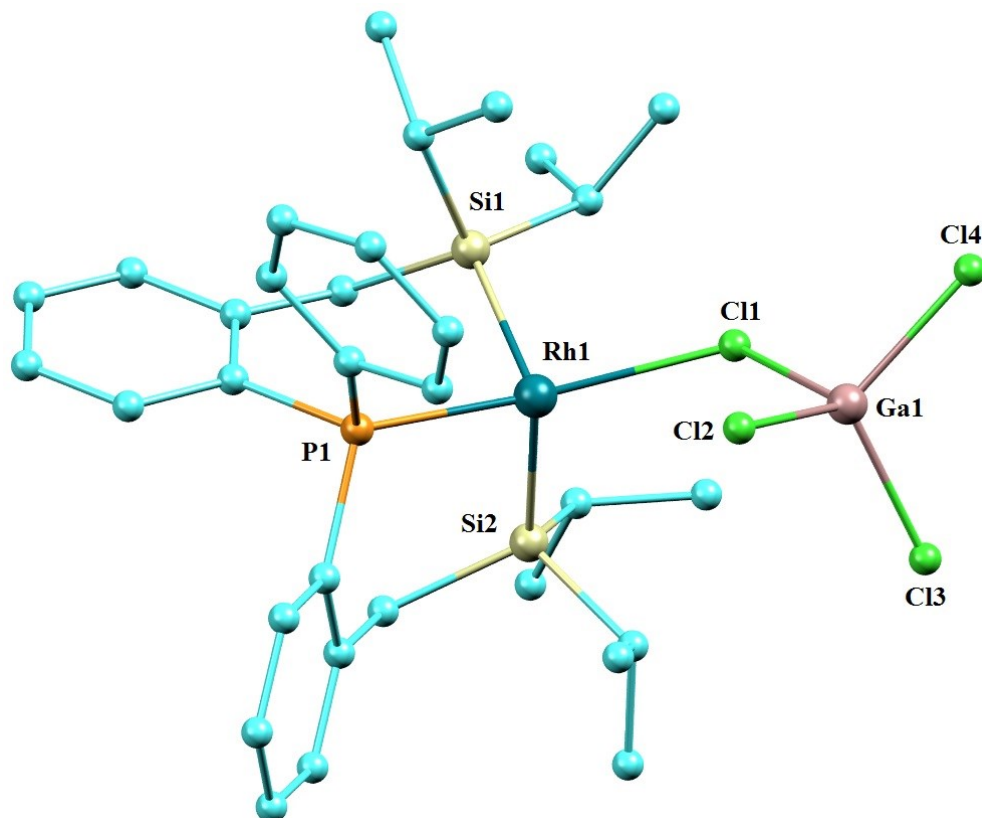
A pale yellow prism single crystal of $C_{33}H_{45}Cl_7GaPRhSi_2$, approximate dimensions (0.221 x 0.231 x 0.360) mm³, was selected for the X-ray crystallographic analysis and mounted on a cryoloop using an oil cryoprotectant. The X-ray intensity data was measured at low temperature (T = 100K), using a three circles goniometer Kappa geometry with a fixed Kappa angle at = 54.74 deg Bruker AXS D8 Venture, equipped with a Photon 100 CMOS active pixel sensor detector. A monochromatized Molybdenum X-ray radiation ($\lambda = 0.71073 \text{ \AA}$) was selected for the measurement. Frames were integrated with the Bruker SAINT software¹³ using a narrow-frame algorithm. The integration of the data using a monoclinic unit cell yielded a total of 102263 reflections to a maximum θ angle of 30.51° (0.70Å resolution), of which 12384 were independent (average redundancy 8.258, completeness = 99.8%, $R_{int} = 3.60\%$, $R_{sig} = 1.93\%$) and 11629 (93.90%) were greater than $2\sigma (F^2)$. The final cell constants of $a = 10.884(3) \text{ \AA}$, $b = 18.130(5) \text{ \AA}$, $c = 20.983(5) \text{ \AA}$, $\beta = 101.172(8)^\circ$, volume = 4062.0(18) Å³, are based upon the refinement of the XYZ-centroids of 1460 reflections above $20 \sigma (I)$ with $4.493^\circ < 2\theta < 51.17^\circ$. Data were corrected for absorption effects using the Multi-Scan method (SADABS)¹⁴. The ratio of minimum to maximum apparent transmission was 0.844. The calculated minimum and maximum transmission coefficients (based on crystal size) are 0.5880 and 0.7120. The structure was solved in a triclinic unit cell using the Bruker SHELXT Software Package,¹⁵ using the centrosymmetric space group: P 1 2(1)/c 1, with Z = 4 for the formula unit, $C_{33}H_{45}Cl_7GaPRhSi_2$. Refinement of the structure was carried out by least squares procedures on weighted F^2 values using the SHELXTL-2018/3¹⁶ included in the APEX3 v2019, 1.0,

AXS Bruker program¹⁷. Hydrogen atoms were localized on difference Fourier maps but then introduced in the refinement as fixed contributors in idealized geometry with an isotropic thermal parameters fixed at 20 % higher than those carbons atoms they were connected. A molecule of solvent: CDCl_3 was located statistically disordered on three positions and anisotropically refined with a ratio of occupancy equal to: 33%. Restraints on interatomic lengths and angles and constraints on ADP's parameters were added in order to get a chemically reasonable model. The final anisotropic full-matrix least-squares refinement on F^2 with 488 variables converged at $R1 = 2.90\%$, for the observed data and $wR2 = 7.42\%$ for all data. The goodness-of-fit: GOF was 1.052. The largest peak in the final difference electron density synthesis was $1.520 \text{ e}^-/\text{\AA}^3$ and the largest hole was $-1.791 \text{ e}^-/\text{\AA}^3$ with an RMS deviation of $0.098 \text{ e}^-/\text{\AA}^3$. On the basis of the final model, the calculated density was 1.553 g/cm^3 and $F(000)$, 1924 e^- .

10.4.2 Crystal's view



10.4.3 Asymmetric unit's view



Asymmetric unit view of complex **Rh-5**

Table S20. Sample and crystal data for A_VM_013_100K.

Identification code	A_VM_013_100K
Chemical formula	C ₃₃ H ₄₅ Cl ₇ GaPRhSi ₂

Formula weight	949.62 g/mol	
Temperature	100(2) K	
Wavelength	0.71073 Å	
Crystal size	(0.221 x 0.231 x 0.360) mm ³	
Crystal system	monoclinic	
Space group	P 1 2(1)/c 1	
Unit cell dimensions	a = 10.884(3) Å	α = 90°
	b = 18.130(5) Å	β = 101.172(8)°
	c = 20.983(5) Å	γ = 90°
Volume	4062.0(18) Å ³	
Z	4	
Density (calculated)	1.553 g/cm ³	
Absorption coefficient	1.652 mm ⁻¹	
F(000)	1924	

Table S21. Data collection and structure refinement for A_VM_013_100K.

Theta range for data collection	2.21 to 30.51°
Index ranges	-15<=h<=15, -25<=k<=25, -29<=l<=29
Reflections collected	102263

Independent reflections	12384 [R(int) = 0.0360]	
Coverage of independent reflections	99.8%	
Absorption correction	Multi-Scan	
Max. and min. transmission	0.7120 and 0.5880	
Refinement method	Full-matrix least-squares on F ²	
Refinement program	SHELXL-2018/3 (Sheldrick, 2018)	
Function minimized	$\Sigma w (F_o^2 - F_c^2)^2$	
Data / restraints / parameters	12384 / 282 / 488	
Goodness-of-fit on F²	1.052	
Δ/σ_{\max}	0.003	
Final R indices	11629 data; I > 2 σ (I)	R1 = 0.0290, wR2 = 0.0728
	all data	R1 = 0.0314, wR2 = 0.0742
Weighting scheme	w=1/[$\sigma^2(F_o^2)+(0.0295P)^2+7.0876P$] where P=(F _o ² +2F _c ²)/3	
Extinction coefficient	0.0024(1)	
Largest diff. peak and hole	1.520 and -1.791 eÅ ⁻³	
R.M.S. deviation from mean	0.098 eÅ ⁻³	

Table S22. Bond lengths (Å) for A_VM_013_100K.

Rh1-P1	2.2002(6)	Rh1-Si2	2.3116(7)
Rh1-Si1	2.3156(7)	Rh1-Cl1	2.4243(6)
P1-C8	1.8181(17)	P1-C15	1.8220(17)
P1-C7	1.8306(17)	Si1-C1	1.8964(18)
Si1-C21	1.9033(18)	Si1-C24	1.9054(19)
Si2-C27	1.9026(18)	Si2-C14	1.9047(18)
Si2-C30	1.9096(18)	Ga1-Cl3	2.1483(7)
Ga1-Cl2	2.1528(7)	Ga1-Cl4	2.1572(7)
Ga1-Cl1	2.2677(7)	C1-C2	1.506(2)
C1-H1	0.95	C2-C3	1.409(2)
C2-C7	1.410(2)	C3-C4	1.393(3)
C3-H3	0.95	C4-C5	1.389(3)
C4-H4	0.95	C5-C6	1.391(2)
C5-H5	0.95	C6-C7	1.407(2)
C6-H6	0.95	C8-C9	1.403(2)
C8-C13	1.410(2)	C9-C10	1.391(3)
C9-H9	0.95	C10-C11	1.392(3)
C10-H10	0.95	C11-C12	1.392(3)
C11-H11	0.95	C12-C13	1.399(2)
C12-H12	0.95	C13-C14	1.505(2)

C14-H14A	0.99	C14-H14B	0.99
C15-C16	1.400(2)	C15-C20	1.404(2)
C16-C17	1.392(2)	C16-H16	0.95
C17-C18	1.391(3)	C17-H17	0.95
C18-C19	1.393(3)	C18-H18	0.95
C19-C20	1.390(2)	C19-H19	0.95
C20-H20	0.95	C21-C23	1.533(2)
C21-C22	1.543(3)	C21-H21	1.0
C22-H22A	0.98	C22-H22B	0.98
C22-H22C	0.98	C23-H23A	0.98
C23-H23B	0.98	C23-H23C	0.98
C24-C26	1.538(3)	C24-C25	1.544(3)
C24-H24	1.0	C25-H25A	0.98
C25-H25B	0.98	C25-H25C	0.98
C26-H26A	0.98	C26-H26B	0.98
C26-H26C	0.98	C27-C28	1.537(3)
C27-C29	1.541(3)	C27-H27	1.0
C28-H28A	0.98	C28-H28B	0.98
C28-H28C	0.98	C29-H29A	0.98
C29-H29B	0.98	C29-H29C	0.98
C30-C31	1.538(3)	C30-C32	1.542(3)
C30-H30	1.0	C31-H31A	0.98

C31-H31B	0.98	C31-H31C	0.98
C32-H32A	0.98	C32-H32B	0.98
C32-H32C	0.98	C1S-Cl1S	1.502(8)
C1S-Cl3S	1.696(7)	C1S-Cl2S	1.810(7)
C1S-H1S	1.0	C1T-Cl1T	1.500(8)
C1T-Cl3T	1.694(7)	C1T-Cl2T	1.810(7)
C1T-H1T	1.0	C1U-Cl1U	1.507(8)
C1U-Cl3U	1.700(8)	C1U-Cl2U	1.809(7)
C1U-H1U	1.0		

Table S23. Bond angles (°) for A_VM_013_100K.

P1-Rh1-Si2	89.40(2)	P1-Rh1-Si1	87.18(2)
Si2-Rh1-Si1	99.265(18)	P1-Rh1-Cl1	167.509(17)
Si2-Rh1-Cl1	101.46(2)	Si1-Rh1-Cl1	97.01(2)
C8-P1-C15	106.10(8)	C8-P1-C7	102.42(8)
C15-P1-C7	105.76(8)	C8-P1-Rh1	114.21(6)
C15-P1-Rh1	100.26(6)	C7-P1-Rh1	126.35(6)
C1-Si1-C21	105.52(8)	C1-Si1-C24	108.56(8)
C21-Si1-C24	114.05(8)	C1-Si1-Rh1	112.72(6)
C21-Si1-Rh1	105.63(6)	C24-Si1-Rh1	110.34(6)

C27-Si2-C14	108.89(8)	C27-Si2-C30	111.17(8)
C14-Si2-C30	109.18(8)	C27-Si2-Rh1	115.02(6)
C14-Si2-Rh1	112.30(6)	C30-Si2-Rh1	99.93(6)
Cl3-Ga1-Cl2	112.86(3)	Cl3-Ga1-Cl4	111.66(3)
Cl2-Ga1-Cl4	113.86(3)	Cl3-Ga1-Cl1	106.09(3)
Cl2-Ga1-Cl1	106.77(2)	Cl4-Ga1-Cl1	104.82(2)
Ga1-Cl1-Rh1	118.35(2)	C2-C1-Si1	115.92(12)
C2-C1-H1	122.0	Si1-C1-H1	122.0
C3-C2-C7	117.63(16)	C3-C2-C1	119.03(16)
C7-C2-C1	123.32(15)	C4-C3-C2	121.84(17)
C4-C3-H3	119.1	C2-C3-H3	119.1
C5-C4-C3	120.14(17)	C5-C4-H4	119.9
C3-C4-H4	119.9	C4-C5-C6	119.08(17)
C4-C5-H5	120.5	C6-C5-H5	120.5
C5-C6-C7	121.40(17)	C5-C6-H6	119.3
C7-C6-H6	119.3	C6-C7-C2	119.79(15)
C6-C7-P1	114.68(13)	C2-C7-P1	125.47(13)
C9-C8-C13	120.60(16)	C9-C8-P1	121.95(13)
C13-C8-P1	117.44(13)	C10-C9-C8	120.32(17)
C10-C9-H9	119.8	C8-C9-H9	119.8
C9-C10-C11	119.47(18)	C9-C10-H10	120.3
C11-C10-H10	120.3	C12-C11-C10	120.31(17)

C12-C11-H11	119.8	C10-C11-H11	119.8
C11-C12-C13	121.34(17)	C11-C12-H12	119.3
C13-C12-H12	119.3	C12-C13-C8	117.94(16)
C12-C13-C14	120.93(15)	C8-C13-C14	121.12(15)
C13-C14-Si2	114.06(11)	C13-C14-H14A	108.7
Si2-C14-H14A	108.7	C13-C14-H14B	108.7
Si2-C14-H14B	108.7	H14A-C14-H14B	107.6
C16-C15-C20	119.30(15)	C16-C15-P1	124.65(13)
C20-C15-P1	115.61(12)	C17-C16-C15	119.90(16)
C17-C16-H16	120.1	C15-C16-H16	120.1
C18-C17-C16	120.43(17)	C18-C17-H17	119.8
C16-C17-H17	119.8	C17-C18-C19	120.11(17)
C17-C18-H18	119.9	C19-C18-H18	119.9
C20-C19-C18	119.75(17)	C20-C19-H19	120.1
C18-C19-H19	120.1	C19-C20-C15	120.51(16)
C19-C20-H20	119.7	C15-C20-H20	119.7
C23-C21-C22	111.43(15)	C23-C21-Si1	116.31(13)
C22-C21-Si1	111.91(12)	C23-C21-H21	105.4
C22-C21-H21	105.4	Si1-C21-H21	105.4
C21-C22-H22A	109.5	C21-C22-H22B	109.5
H22A-C22-H22B	109.5	C21-C22-H22C	109.5
H22A-C22-H22C	109.5	H22B-C22-H22C	109.5

C21-C23-H23A	109.5	C21-C23-H23B	109.5
H23A-C23-H23B	109.5	C21-C23-H23C	109.5
H23A-C23-H23C	109.5	H23B-C23-H23C	109.5
C26-C24-C25	109.84(15)	C26-C24-Si1	112.95(12)
C25-C24-Si1	112.70(13)	C26-C24-H24	107.0
C25-C24-H24	107.0	Si1-C24-H24	107.0
C24-C25-H25A	109.5	C24-C25-H25B	109.5
H25A-C25-H25B	109.5	C24-C25-H25C	109.5
H25A-C25-H25C	109.5	H25B-C25-H25C	109.5
C24-C26-H26A	109.5	C24-C26-H26B	109.5
H26A-C26-H26B	109.5	C24-C26-H26C	109.5
H26A-C26-H26C	109.5	H26B-C26-H26C	109.5
C28-C27-C29	110.03(16)	C28-C27-Si2	112.81(14)
C29-C27-Si2	111.96(13)	C28-C27-H27	107.2
C29-C27-H27	107.2	Si2-C27-H27	107.2
C27-C28-H28A	109.5	C27-C28-H28B	109.5
H28A-C28-H28B	109.5	C27-C28-H28C	109.5
H28A-C28-H28C	109.5	H28B-C28-H28C	109.5
C27-C29-H29A	109.5	C27-C29-H29B	109.5
H29A-C29-H29B	109.5	C27-C29-H29C	109.5
H29A-C29-H29C	109.5	H29B-C29-H29C	109.5
C31-C30-C32	109.64(16)	C31-C30-Si2	113.96(12)

C32-C30-Si2	112.05(13)	C31-C30-H30	106.9
C32-C30-H30	106.9	Si2-C30-H30	106.9
C30-C31-H31A	109.5	C30-C31-H31B	109.5
H31A-C31-H31B	109.5	C30-C31-H31C	109.5
H31A-C31-H31C	109.5	H31B-C31-H31C	109.5
C30-C32-H32A	109.5	C30-C32-H32B	109.5
H32A-C32-H32B	109.5	C30-C32-H32C	109.5
H32A-C32-H32C	109.5	H32B-C32-H32C	109.5
Cl1S-C1S-Cl3S	116.9(5)	Cl1S-C1S-Cl2S	112.6(4)
Cl3S-C1S-Cl2S	97.7(4)	Cl1S-C1S-H1S	109.7
Cl3S-C1S-H1S	109.7	Cl2S-C1S-H1S	109.7
Cl1T-C1T-Cl3T	128.1(7)	Cl1T-C1T-Cl2T	112.3(6)
Cl3T-C1T-Cl2T	103.4(5)	Cl1T-C1T-H1T	103.4
Cl3T-C1T-H1T	103.4	Cl2T-C1T-H1T	103.4
Cl1U-C1U-Cl3U	115.3(7)	Cl1U-C1U-Cl2U	105.5(5)
Cl3U-C1U-Cl2U	96.4(5)	Cl1U-C1U-H1U	112.8
Cl3U-C1U-H1U	112.8	Cl2U-C1U-H1U	112.8

11 References Experimental Section

1. G. Giordano and R. H. Crabtree, "Di- μ -Chloro-Bis(η^4 -1,5-Cyclooctadiene) Dirhodium(I)," *Inorganic Synthesis*, 1979, **19**, 218-220.
2. G. W. Parshall, *Inorganic Syntheses*, 1974, **15**, 18

